A Finite element approach to determine the unknown location of the heat sources within engineering structures.

Thesis Submitted to

The School of Computing and Engineering

Of

The University of Huddersfield

By

Syed Badar Shah

In Partial Fulfilment of the Requirements for the Degree of

Master of Philosophy

Abstract

The performance of many engineering structures which contain heat sources are affected by the existence of the change in temperature. In some cases, this is an absolute change in temperature, but in others it is the thermal gradients within their assembled components that influence the integrity of their overall performance. One application that is the subject of ongoing investigation into thermal behaviour is machine tools for precision manufacturing. On such machines, several internal and external heat sources introduce unwanted energy into the machine structure. The effect of temperature gradients in these elements is a reduction in the positional accuracy and repeatability, which compromises the machine's ability to produce accurate, repeatable parts. Numerous techniques are employed to compensate such errors, but if the exact spatial location of the internal heat sources within the structure remains an unknown parameter, then the modelling of the thermal displacement and compensation is fundamentally compromised. Without the original machine designs, the location of such heat sources may well be unknown.

The focus of this thesis is to devise an approach which can assist in determining the unknown spatial location of the internal heat sources in a structure, based only on observable data. This is challenging, because one must know the temperature field of the structure to know the heat source location. However, the temperature measurements of the structure can normally only be observed externally.

The approach taken requires analysis in both transient and steady state heat transfer stages. Mathematical calculations and Finite Element Analysis (FEA) on Computer-Aided Design (CAD) models are used to provide a theoretical approach that is then validated through controlled thermal experiments. A steel plate is used throughout the work to prove the concept, first as a one-dimensional (1D) problem with observation on a single boundary and then a two-dimensional (2D) problem with observation on two perpendicular boundaries.

The analytical approach applied to the FEA simulated data yielded the unknown location of the internal heat source in the 1D structure under steady state conditions with the accuracy better than 95%. Analysis in the transient phase yielded an accuracy of up to 97%, but also provided the strength of the heat source with an accuracy up to 96%. For the 2D problem, the location of the heat source was estimated using thermal experimental data, lumped capacitance techniques, and interpolation of the temperature gradient against the various locations of the heat source.

Future work should extrapolate the methods proposed in this thesis to estimating the location of heat sources in three-dimensional structures and assemblies, so it could be readily adopted by researchers when specifying temperature sensor locations and thermal compensation models for precision machine tools.

Acknowledgment

I want to extend my appreciation to my supervisors: Dr. Naeem Mian, Professor Andrew Longstaff, and Dr. Simon Fletcher. It is their constant support and supervision which enabled me to complete this research. Their guidance has led me to flourish my skills and become a better engineer and researcher; most importantly, they have instilled in me the curiosity and desire one should possess to further improve. I will be always grateful to them.

I want to extend my appreciation to Andrew Bell, whose provision and expertise enabled me to conduct my experiments in the laboratory; as well as my colleagues: Ali Iqbal, Difference Chuku, Nemwel Ariaga, Abdul Basit, Felix Olabode, Presley, Kelly, Ebube, and Kelechi – thank you for your guidance and support.

I want to unequivocally recognise the encouragement and confidence my parents and family have given me. It is most certainly their kind wishes and prayers which have been a blessing for me.

In the end, I want to thank my wife who has been there with me throughout this journey of research. It is her constant support and faith in me that has enabled me to reach the point of completion in my degree.

Table of Contents

List of Figures

List of Tables

List of Notations

BHF/$\dot{q}$ = Body Heat Flux (W/m^3)

SHF/$q^{"}$ = Surface Heat Flux (W/m^2)

h = Convective heat transfer coefficient ($W/m^2/°C$)

hc = Thermal contact conductance ($W/m^2/°C$)

Q' = Energy (W)

qconv = Energy transfer through convection (W)

qcond = Energy transfer through conduction (W)

ΔT = Temperature difference (°C)

k = Conductivity (W/m/°C)

A = Area (m2)

ΔL = Change in Length (m)

m = Mass (Kg) = density (Kg/m^3) x Volume (m^3)

Cp = Specific heat capacity (J/Kg/°C)

t = Time (s)

Tsurf = Surface temperature (°C)

Tamb = Ambient air temperature (°C)

dT/dx = temperature gradient in the x direction (°C/m)

Ts = Temperature of the surrounding (°C)

1 Introduction

In many of the engineering structures, the presence of energy or power generators collate heat into the structures. Due to the presence of such internal heat sources, the thermal gradients are accumulated within the volume of the structure, consequently influencing the efficiency and integrity of the functionality of the machine. This can be observed in the manufacturing CNC machine tools, being used to construct the high-end products require absolute precision. However, the internal heat, generated by the heat sources, flows through the structure causing thermal expansion of the structural components. Therefore, the required accuracy is compromised due to the structural displacement and deformity, and such inaccuracies are known as position dependent thermal errors. Additionally, the internal sources of heat within the structure of the machine include spindle motors and bearings, gearboxes, axis drive systems, and belt-drives, where the major contributions in the escalation of temperature are due to the frictional movements. Postlewaite *et al.* (1998) found that the positional errors in a CNC machine tool are majorly contributed by the thermal errors with up to 75 per cent of the total. In resolution, many thermal compensation models are being used to address such problems. Abdulshahed *et al.* (2015) stated that amongst many techniques to reduce thermal distortions, the use of thermally stable materials in the construction of the machine tool or obtaining symmetry and seclusion of heat sources might be an option; however, these mitigating techniques increase the expenditure on development of such machines and lead to other problems such as increased vibration or lower acceleration. Employing numerical compensation has many advantages, this process involves recalibrating the position of the axes to overcome thermal displacements. Thermal errors existing at a certain time and position are adjusted by altering the position of the axes of a machine by the amount equating to the error present at that position. This is a more desirable approach than making structural modifications and is more accommodating whenever the error sources undergo changes which would not have been adaptable with the structural change technique. Altogether, Postlewaite *et al.* (1998) reports that all the potential solution could be divided into two categories such as direct and indirect measurement way. The direct measurement approach would usually employ probing to measure thermal errors, whereas the indirect approach estimates the thermal errors from other parameters, commonly temperature data is utilised. However, the direct measurement techniques involve many disadvantages as well such as use of tool-mounted probes, frequent measurements due to rapid movements, configuration to another machine could be challenging and time consuming etc. Therefore, indirect measurements have an advantage over these obstacles, as they are carried out at the surface of the machine structure.

Although the compensation methods have their own challenges, such as whenever the precise location of the internal heat source is an unknown parameter within the structure, the process of thermal modelling and compensation becomes a difficult task. This only happens if the complete structural access, such as the internal positions of the structural components, is restricted due to confidentiality which, in turn, could be the consequence of several reasons. In such cases, the inverse approach can be employed for the approximation of the unknown parameters through the surface measurements.

Thermal modelling also includes the use of Finite Element Method (FEM) model which would fall under the category of indirect thermal error compensation technique. The use of FEM is an offline approach for finite element analysis and can model the thermal errors of the machine, and reduce the downtime required to compensate calibrate the model. Although, numerical (FEM) modelling demands an accurate establishment of boundary conditions as well as other parameters directly involved in the heat transfer. FEM offers modelling of complex geometrical and irregular shapes. Immense options of materials, accurately solves for complicated structures with variable boundary conditions and offers easement in the repeatability and alterations to the conditions, making it a suitable technique than any other. Finally, the visualization of heat transfer is a great tool that can be utilized to demonstrate a process or even for self-understanding.

When creating FEA based thermal models of machine tools, apart from the establishment of boundary conditions, the geometrical features of the assembled components are also required. However, in many circumstances, the complete engineering drawings were not provided due to confidentiality reasons and the measurements of temperature were restricted to limited number of surfaces at the machine structure. This poses a difficult task to create computer aided models to conduct Finite Element Analysis on heat transfer. All of the parameters involved in the heat transfer need to be defined as accurately as possible, including the geometrical dimensions, material properties, thermophysical properties, initial and boundary conditions, and if any assumptions are being considered, they need to be realistic and not altering the thermal behaviour of the structure. The limitations and restrictions imposed on the accessibility of complete structural dimensions and precise locations of assembled components would pose immense difficulty in creating computer aided models for the purpose of accurate thermal simulations.

1.1 Problem Statement

To investigate heat-transfer realistically in any structure, numerous parameters need to be taken into consideration, based on an extensive literature review and thermal experimentation. Girault, Videcoq and Petit (2010) have highlighted the importance of accurately defining the parameters, such as geometry, boundary conditions, and thermo-physical properties to acquire understanding of their precise relationship within the

heat transfer. On the other hand, when one of more of these parameters is an unknown value, it becomes difficult to reconstruct thermal behaviour of a structure. As aforementioned, the limitation involved in the measurements and accessibility to the structure of machine, poses a challenge. Placement of thermocouples, temperature sensors, or even thermal imaging cameras to obtain the temperature measurement of a structure of machine, is restricted to few surfaces. Consequently, the CAD models and the FEA analysis would be inconsistent given that engineering drawings of the machine structure are not provided, and the locations of internal heat sources remain an unknown parameter. Therefore, a technique to accurately estimate the location of the heat sources from the surface of a machine structure using indirect measurements would be useful. The indirect measurement will consist of transient temperature data to approximate the location of the heat source.

The proposed approach is to investigate individual components through thermal experimentation and with further help of Finite Element Analysis to model heat transfer. The experiments and simulations will serve the purpose of replicating the heat transfer in a structure. In order to recreate the restrictions and limitations, the simulations will be constructed based on the parameters estimated from experiments and the literature review, leading to building a relationship between different parameters and their influence on the thermal behaviour of the structure, all while the focusing on determining the unknown location of the internal heat source.

The literature review was carried out to investigate various approaches being employed by researchers to mitigate similar problems, while emphasising on the literature where the researchers have focused more on the heat transfer problems and estimated an unknown parameter which directly influences the thermal gradients of the structure. To establish which, of all relevant parameters, are being considered as a known or an unknown within the heat transfer investigations; this will also help in solidifying the gap. Additionally, finding out about the extent of the complexity of the geometrical structures being considered; and, most importantly, the mathematical approaches being employed to resolute and estimate the unknown parameters such as the location of the internal heat sources. Therefore, it is established that the focus and contribution of this research is to estimate the unknown spatial location of the internal heat source while taking the challenges found in the literature review.

In this thesis, Chapter 2 covers the literature findings and the gaps identified, while commentating on different approaches being employed. Subsequently, Chapter 3 discusses the aim and objectives of the current research derived through identifying the gap found in the literature review. Furthermore, Chapter 4 contains evaluation of the methodology applied in this project along with benchmark results. Subsequently, Chapter 5 presents the application of methodology and discusses results obtained for several cases investigated in one and two-dimensional structures. Finally, the conclusion and scope for further work is discussed in chapter 6.

2 Literature Review

This literature survey has reviewed various theoretical books, journal papers, and conference proceedings in the field of heat transfer. Initially, the literature review focuses on comprehending the fundamentals of heat transfer and the analytical methods used to solve problems attached to it. This is followed by studying the mathematical models being utilized for the complex heat transfer problems revolving around determination of temperature field of a surface or for the whole structure, which, in turn, leads to the challenges being faced while determining the temperature fields of the various engineering structures. Ultimately, the literature draws attention towards the mathematical approaches being applied to estimate the unknown location of the heat source within the structures. The literature review is concluded with a critical summary that identifies the gaps which is intended to be addressed by the application of this project.

2.1 Fundamentals of Heat Transfer

The existence of a temperature difference in a medium or between media imposes the occurrence of the heat transfer. This means that heat transfer is a thermal energy being transferred due to the spatial temperature difference (Incropera, Dewitt, Lavine, & Bergman, 2007).

Hagen (1999) explains the difference between the thermodynamics laws and the heat transfer such that the thermodynamics allows to study the systems that are in an equilibrium state and determine the energy needed to change the system from one equilibrium state to another. It does not enable one to determine the rate at which the change will occur, whereas heat transfer analysis allows the determination of rate of change as well. There are two types of heat transfer; firstly, *steady heat transfer* which means that the temperature does not vary with time such as water reaching the boiling temperature and heat being transferred at steady conditions. Whereas, while water reaching boiling state, the temperature of the water changes with time, making it a *transient* heat transfer or *unsteady*. Raju (2011) defines that the steady state conduction exists when the temperature at all locations in a material is constant with time meaning temperature is a function of location only and that the rate of heat transfer is constant at any point. The transient conduction varies with time as well as position.

The fundamental law of governing heat conduction was formulated by French physicist, Joseph Fourier. He defined the heat transfer rate in conduction through proportionality relationship with the surface area, temperature gradient, and distance across the temperature gradient (Hagen, 1999). The proportionality is replaced with thermal conductivity of the material and overall relationship in mathematical form is expressed as,

$$q_x = -kA\frac{\Delta T}{\Delta x} \quad \text{Eq. 1}$$

It should be noted here that $q_x = q/t$ is the heat transfer rate, that is the rate at which thermal energy is being transferred from one region to another during the time, *t*. The surface area in Eq. 1, A, is always normal to the heat transfer direction. Raju (2011) states that the *k* is a proportionality constant, defined as thermal conductivity of the material. Thermal conductivity is a measure of materials ability to conduct thermal energy. Raju (2011) explains the existence of a negative sign signifies the direction of conduction which is to indicate that thermal energy always flows from hot area to cold area. Incropera *et al* (2007) stated that for heat transfer to occur, there must be a temperature gradient and, hence, thermodynamic nonequilibrium. However, thermodynamics and heat transfer are highly complementary and that is why heat transfer is considered as an extension of thermodynamics.

Incropera *et al.* (2007) first law of thermodynamics must be satisfied at every instant of time that is the balance between all energy rates must exist. Whenever the generated thermal and mechanical energy and inflow energy exceed the outflow, there would be an increase in the stored energy in the control volume. If it is otherwise, then exists a decrease in thermal and mechanical energy storage. Additionally, a steady state must prevail whenever the inflow and generation equal the outflow, there will be no change in the stored energy in the control volume. These explanations for the conservation of energy can be written as,

$$\Delta E_{st} = E_{in} - E_{out} + E_g \quad \text{Eq. 2}$$

Using a dot over terms indicates the rate,

$$\Delta \dot{E}_{st} \equiv \frac{dE_{st}}{dt} = \dot{E}_{in} - \dot{E}_{out} + \dot{E}_g \quad \text{Eq. 3}$$

Defining the symbols in the expressions starting with the ΔE_{st} is the change in stored energy (mechanical and thermal) in control volume, E_{in} and E_{out} are for the inflow and outflow energies. Lastly, E_g is the thermal energy generation in the control volume, which is associated with conversion of other forms of internal energy (nuclear, electrical, electromagnetic, or chemical) to thermal energy and it is a volumetric phenomenon.

This emphasises that utilising first law (conservation of energy) to attain solution for heat transfer problems, one must initialise by identifying a control volume and its control surface, to which subsequently analysis will be applied. Followed by deciding the analysis conducted for a time interval basis (Eq. 2) or rate basis (Eq. 3).

Although, surface energy balance is also applicable on many occasions, this does not entertain energy generation and storage terms, even though thermal generation might be occurring in the medium. Additionally, this method is applicable to steady as well as transient heat transfer conditions,

$$\dot{E}_{in} - \dot{E}_{out} = 0 \qquad \text{Eq. 4}$$

Depending on the heat transfer terms occurring in the control volume this expression can be applied accordingly,

$$q''_{cond} - q''_{conv} - q''_{rad} = 0 \qquad \text{Eq. 5}$$

The Fourier's law of conduction is a strong tool applicable to problems involving conditions such as steady state, transient, multidimensional conduction in complex geometries even when the nature of temperature distribution is not apparent. It is evident that the full nature of Fourier's law must be fully understood to comprehend heat transfer issues. Incropera *et al.* (2007) stated that a deeper understanding of Fourier's law is essential and pivotal when dealing with heat transfer problems. Finding about what form the equation takes for different geometries and how the proportionality constant (thermal conductivity) changes or depends on the material's physical nature, enables one to develop the heat equation from the basic principles. It will be the solution to this heat equation that will provide temperature distribution, heat flux and other thermophysical properties such as material conductivity.

Dividing the heat transfer rate with the surface area gives the heat flux,

$$q''_x = \frac{q_x}{A} = -k\frac{\Delta T}{\Delta x} \qquad \text{Eq. 6}$$

This expression for heat flux validates that it is a directional quantity, a vector quantity. Therefore, a more general expression of the conduction rate equation is as follows,

$$q'' = -k\nabla T = -k\left(i\frac{dT}{dx} + j\frac{dT}{dy} + k\frac{dT}{dz}\right)$$

The ∇ is a three dimensional del operator and T (x, y, z) is the scalar temperature field. When dealing with heat transfer analysis if one can determine the temperature distribution in the medium then heat flux at any point or on its surface can be calculated. Incropera *et al.* (2007) also state that many other important quantities are determinable such as for solids, the structural integrity can be identified through the determination of the

thermal stresses, expansions, and deflections. A differential control volume must be defined along with relevant energy transfer processes and introduce appropriate rate equations for the respective heat transfer mode. A general form of conservation of energy requirement is,

$$\dot{E}_{st} = \dot{E}_{in} - \dot{E}_{out} + \dot{E}_g$$

This equation translates into heat equation for rectangular coordinates with constant thermal conductivity,

$$\frac{d^2T}{dx^2} + \frac{d^2T}{dy^2} + \frac{d^2T}{dz^2} + \frac{\dot{q}}{k} = \frac{1}{\propto}\frac{dT}{dt} \qquad \text{Eq. 7}$$

Heat transfer problems are analysed as one-dimensional, two-dimensional, or three-dimensional. Generally, heat transfer through a medium is three dimensional which means the temperature varies in all three directions.

Energy generation and energy storage are two different things; a common thermal energy generation process is converting electrical to thermal energy in a current-carrying medium. The rate at which the generation is given by,

$$\frac{d^2T}{dx^2} + \frac{d^2T}{dy^2} + \frac{d^2T}{dz^2} + \frac{\dot{q}}{k} = \frac{1}{\propto}\frac{dT}{dt} \qquad \text{Eq. 8}$$

And if this power generation (W) is uniform throughout the medium then it becomes volumetric generation (W/m^3),

$$\dot{q} = \frac{\dot{E}_g}{V} = \frac{I^2 R_e}{V} \qquad \text{Eq. 9}$$

Heat transfer occurs through various modes simultaneously, generally, conduction and convection are found together as the modes of heat transfer in a system (Kothandaraman, 2006). Furthermore, heat generation can also be involved in the process. There are various approaches to obtain a solution for a heat transfer problem. When dealing with two-dimensional heat transfer problems, one can opt for analytical method, graphical methods, or numerical methods. However, for steady state conductional problems, analytical method works on simplified geometries and when thermal properties are constant, this approach yields exact solution and is sometimes utilised as a benchmark result for numerical approaches. A detailed description of these methods is given the following section.

2.2 Heat Diffusion Equation – Derivation

The main objective of the heat diffusion equation is to enable one to determine temperature distribution *T (x, y, z, t)* in a medium by knowing the temperatures and/or the heat transfer rates on the surface. First, a control volume is needed to be defined,

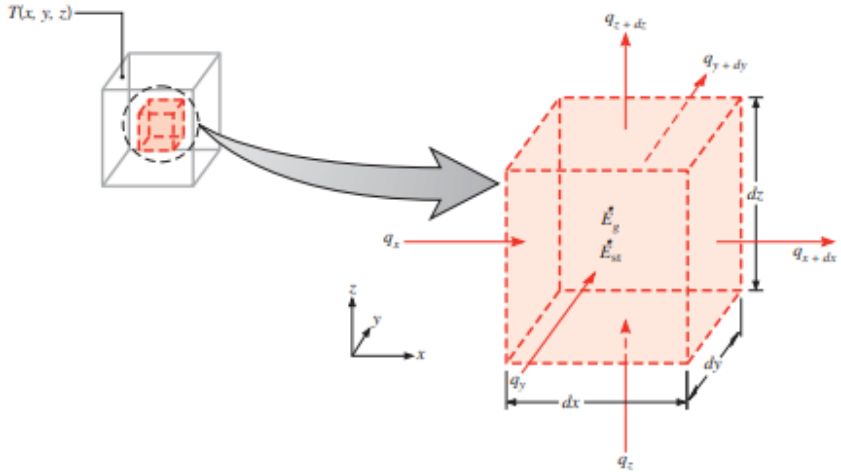

Figure 1: Differential control volume for conduction analysis in cartesian coordinates Incropera et al (2007)

Figure 1 shows the control volume and the heat fluxes coming in and leaving all the surfaces along with the internal thermal energy storage and thermal energy generation. Therefore, all these terms need to be expressed in a form on equation. Thermal energy storage by the material in the volume, can be expressed as,

$$\dot{E}_{st} = \rho c_p \frac{\partial T}{\partial t}\, dx\, dy\, dz \qquad \text{Eq. 10}$$

The internal thermal energy generation present in the volume can be expressed as,

$$\dot{E}_g = \dot{q}\, dx\, dy\, dz$$

Now all these quantities are acting in this system, therefore, a conservation of energy (first law of thermodynamics) must be applied to this volume to obtain the heat diffusion equation. Conservation of energy in rate form is,

$$\dot{E}_{in} + \dot{E}_g - \dot{E}_{out} = \dot{E}_{st}$$

Now all the mechanisms by which the energy is coming in and leaving from all the surfaces is illustrated in Figure 1 and can be substituted in the conservation of energy equation accordingly,

$$q_x + q_y + q_z + \dot{q}\, dx\, dy\, dz - q_{x+dx} - q_{y+dy} - q_{z+dz} = \rho c_p \frac{\partial T}{\partial t}\, dx\, dy\, dz \qquad \text{Eq. 11}$$

Now to simplify this equation further, Taylor series expansion will be utilised,

$$f(x+dx) = f(x) + \frac{df}{dx}(dx) + \frac{d^2 f}{dx^2}\frac{dx^2}{2} + H.O.T.$$

For q_{x+dx} (holding y and z constant),

$$q_{x+dx} = q_x + \frac{\partial q_x}{\partial x} dx \; (Eq.2)$$

Similarly,

$$q_{x+dx} = q_x + \frac{\partial q_x}{\partial x} dx$$

$$q_{z+dz} = q_z + \frac{\partial q_z}{\partial z} dz$$

Recalling the general equation of the conduction rate (*Fourier's Law*),

$$q^{"} = -k\nabla T = -k\left(i\frac{dT}{dx} + j\frac{dT}{dy} + k\frac{dT}{dz}\right)$$

$$q_x - q_{x+dx} = q_x - \left(q_x + \frac{d}{dx}\left(-kA\frac{dT}{dx}\right)dx\right)$$

$$q_x - q_{x+dx} = dy.dz\, \frac{d}{dx}\left(k\frac{dT}{dx}\right)dx$$

Substituting these into eq.1 gives,

$$\cancel{dxdydz}\left[\frac{d}{dx}\left(k\frac{dT}{dx}\right) + \frac{d}{dy}\left(k\frac{dT}{dy}\right) + \frac{d}{dz}\left(k\frac{dT}{dz}\right) + \dot{q}\right] = \rho C_p \frac{dT}{dt}\cancel{dxdydz}$$

When the thermal conductivity is constant in the substance then whole equation divided by *k* simplifies it into,

$$\frac{d^2T}{dx^2} + \frac{d^2T}{dy^2} + \frac{d^2T}{dz^2} + \frac{\dot{q}}{k} = \frac{1}{\propto}\frac{dT}{dt} \quad (Heat\ Equation)$$

$$Heat\ \ Equation \rightarrow \frac{d^2T}{dx^2} + \frac{d^2T}{dy^2} + \frac{d^2T}{dz^2} \equiv \nabla \cdot \nabla T \equiv \nabla^2 T\ (Laplacian) \qquad \text{Eq. 12}$$

2.3 Analytical Solution for Heat Diffusion Equation

Since thermal energy can be conducted in a three-dimensional medium, it makes the temperature a dependent quantity (Hagen, 1999). In a rectangular coordinate system, heat transfer has three independent components corresponding to spatial coordinates *x, y,* and *z*. Additionally, if the heat transfer is conducted through a transient state, then temperature is also a function of time. If an internal source is generating thermal energy, then it should also be accounted for. In short temperature is a function of spatial coordinates, time, and internal heat generation. All these factors are accounted for in the general differential equation for the heat conduction.

$$\frac{d^2T}{dx^2}+\frac{d^2T}{dy^2}+\frac{d^2T}{dz^2}+\frac{\dot{q}}{k}=\frac{1}{\propto}\frac{dT}{dt}$$

The heat conduction equation is modified depending on the conditions of the heat transfer such as steady or transient state or the number of dimensions under study. If the heat transfer is reduced to a steady state, then the right side of the equation becomes zero and further simplifications such as heat transfer in one direction only reduces the partial differential equation into an ordinary differential equation,

$$\frac{d^2T}{dx^2}+\frac{\dot{q}}{k}=\frac{1}{\propto}\frac{dT}{dt} \qquad \text{Eq. 13}$$

Now the dependent variable, *T*, is a function of only one independent variable, *x*. This equation is the governing differential equation for the heat transfer in 1-D steady conduction in a plane wall with internal heat generation. The general solution for this ordinary differential equation can be obtained by direct integration and the specific solution by defining boundary conditions.

The heat diffusion equation further reduces to the following expression when the system is in a steady state with uniform internal heat generation, no change in temperature with time,

$$\frac{d^2T}{dx^2}+\frac{\dot{q}}{k}=0 \qquad \text{Eq. 14}$$

The general solution by integration steps are as follows,

$$\frac{d}{dx}\left(\frac{dT}{dx}\right)+\frac{\dot{q}}{k}=0$$

$$\int d\left(\frac{dT}{dx}\right)=-\frac{\dot{q}}{k}\int dx$$

$$\frac{dT}{dx} = -\frac{\dot{q}}{k}x + C_1$$

Now multiplying both sides by dx and integrating provides the general solution,

$$\int dT = -\frac{\dot{q}}{k}\int x\, dx + \int C_1\, dx$$

$$T(x) = -\frac{\dot{q}}{2k}x^2 + C_1 x + C_2 \qquad \text{Eq. 15}$$

The constants of integration can be defined by stating the boundary conditions. When the boundary conditions are defined, the temperature distribution can be symmetrical as well as asymmetrical depending upon the conditions. This equation will be applied in various models as it will follow and the temperature distribution in the heat source will be determined through it. If the boundary condition is different temperatures at both sides then the constants are of the form,

$$C_1 = \frac{T_{s,2} - T_{s,1}}{2L} \qquad \text{Eq. 16}$$

And,

$$C_1 = \frac{\dot{q}}{2k}\mathrm{L}^2 + \frac{T_{s,1} + T_{s,2}}{2L} \qquad \text{Eq. 17}$$

Substituting in the general solution Eq. 15 gives the final expression for the temperature distribution with internal heat generation becomes,

$$T(x) = \frac{\dot{q}\mathrm{L}^2}{2k}\left(1 - \frac{x^2}{L^2}\right) + \frac{T_{s,2} - T_{s,1}}{2}\frac{x}{L} + \frac{T_{s,1} + T_{s,2}}{2} \qquad \text{Eq. 18}$$

Now the heat flux at any point is no longer independent of x.

2.4 Surface Energy Balance Technique

The generation and storage terms are irrelevant in the surface energy balance technique. This approach is often utilised and applied at the surface of a medium. Furthermore, the benefit of using surface energy balance is that its applicable in both steady-state and transient state. Figure 2 illustrates the modes of heat transfer occurring for the control surface of a medium such conduction from the medium, convection from surface to environmental fluid, and radiation exchange from surface to the surroundings. The conservation requirement becomes,

$$\dot{E}_{in} - \dot{E}_{out} = 0$$

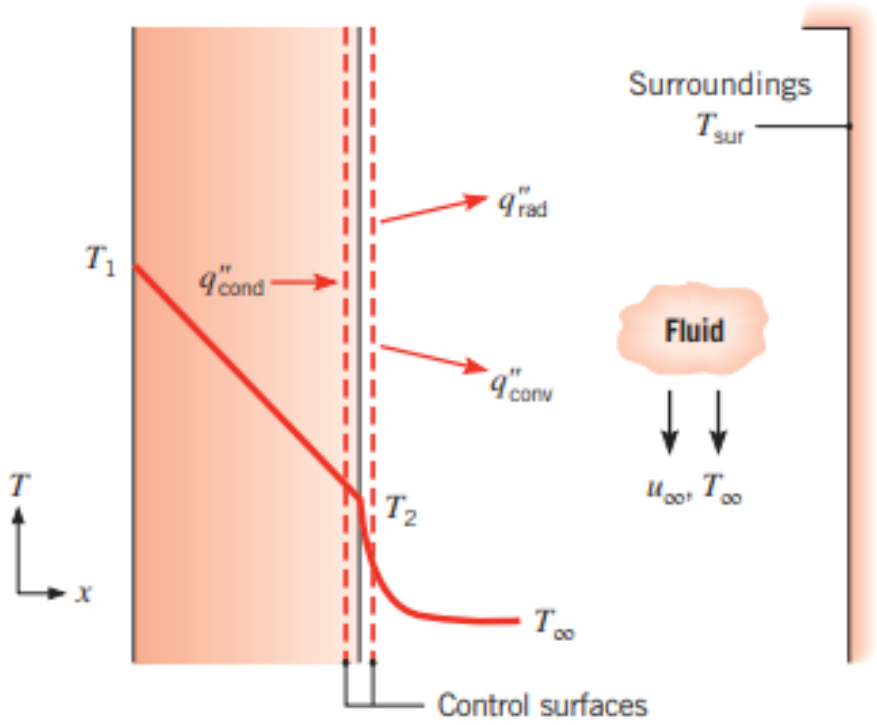

Figure 2: The energy balance for conservation of energy at the surface of a medium, Incropera et al (2007).

The surface energy balance is expressed as,

$$q''_{cond} - q''_{conv} - q''_{Rad} = 0$$

The rate of energy generated within a wall should be balanced by rate of energy leaving via convection at the boundary. When the surface temperature is not known then relating the ambient temperature and surface temperature is a necessity. This relationship can be developed by utilising surface energy balance while neglecting radiation and replacing the relevant rate equations. Considering the surface at $x = L$, the expression will take the form of,

$$-k\frac{dT}{dx}\bigg|_{x=L} = h(T_s - T_\infty)$$

The energy balance would be,

$$\dot{E}_g = \dot{E}_{out}$$

$$\dot{q}L = h(T_s - T_\infty)$$

And rearranging for T_s,

$$T_s = T_\infty + \frac{\dot{q}L}{h} \qquad \text{Eq. 19}$$

2.5 Lumped Capacitance Model by Separation of Variables

The essence of the lumped capacitance method is the assumption that the temperature of the solid is spatially uniform at any instant during the transient process (Incropera *et al.*, 2007). This method involves separating the temperature from depending on two directions, $T(x, y)$, to one direction only, $T(x)$ and $T(y)$, respectively. The resulting 2-D temperature distribution is then the product of each 1-D temperature solution, that is, $T(x, y) = T(x)\ .\ T(y)$. Four BCs are required, two in each direction to solve the 2-D heat conduction problem (Han, 2012). Key point is that only one of the four BCs can be nonhomogeneous to apply separation of variables methods. In case of more than one nonhomogeneous boundary conditions, principal of superposition is utilised.

Using the energy balance technique and lumped capacitance model to estimate the temperature profile at the boundary while optimising for the depth of the heat source from the boundary surface of the plate.

$$-\dot{E}_{out} = \dot{E}_{st}$$

$$q_o^{"} - h(T - T_\infty) = \rho L C_p \frac{dT}{dt} \qquad \text{Eq. 20}$$

Rearranging, and with $R_t^{"} = 1/h$ and $C_t^{"} = \rho L C_p$,

$$T - T_\infty - \frac{q_o^{"}}{h} = -R_t^{"} \cdot C_t^{"}\ dT/dt$$

Defining $\theta(t) \equiv T - T_\infty\ - \frac{q_o^{"}}{h}$ with $d\theta = dT$, the differential equation becomes,

$$\theta = -R_t^{"} \cdot C_t^{"} \frac{d\theta}{dt}$$

Separating the variables and integrating,

$$\int_{\theta_i}^{\theta} \frac{d\theta}{\theta} = -\int_0^t \frac{dt}{R_t^{"} C_t^{"}}$$

Which follows as,

$$\frac{\theta}{\theta_i} = exp\left(-\frac{t}{R_t^{"} C_t^{"}}\right) \qquad \text{Eq. 21}$$

where $\theta_i = \theta(0) = T_i - T_\infty\ - \frac{q_o^{"}}{h}$ or $T(\infty) = T_\infty + q_o^{"}/h$,

2.6 Mathematical Techniques Used for Heat Transfer Problems

Rao (1996) has stated that various optimisation techniques usually fall under three categories namely mathematical programming techniques, stochastic process techniques, and statistical methods. Some widely used techniques for optimisation include Genetic algorithms and neural networks which fall under mathematical programming, Ant Colony Optimisation (ACO) and Particle Swarm Optimisation (PSO) resides in stochastic processes and finally least square regression optimisation belongs statistical methods. Similarly, for ill-posed heat transfer problems, the numerical and analytical techniques include the least squares methods modified by the addition of a regularisation term, the sequential estimation approach, and conjugate gradient method (Neto & Ozisik, 1993; Beck, Blackwell, & St. Clair, 1985; Tikhonov & Arsenin, 1977).

Among many other common applications of optimisation are modelling, characterisation, design of devices, process control, approximation theory, curve fitting, and solution of systems of equations (Antoniou & Lu, 2007). The neural network and adaptive systems are an example of innovations that almost entirely rely on the optimisation theory. The authors explained that there are several approaches to the optimisation process which includes analytical methods, graphical methods, experimental methods, and numerical methods.

Hagen (1999) stated that the numerical methods are special techniques for solving multidimensional conduction problems for which analytical methods may be too difficult or impossible to apply. The numerical approach delivers an approximate solution unlike analytical methods. Powerful and widely used numerical techniques include the *finite difference and finite element* methods and both methods are offered in the shape of softwares, where the more popular ones include Abaqus, Ansys, Solidworks, and Siemens Nx.

In order to determine either heat flux at any location of the structure or calculating thermal stresses, thermal expansion, design insulation thickness, all of these have a prerequisite of knowing the temperature field within the structure under investigation. And the temperature distribution in any structure depends on the initial conditions, boundary conditions, any specified internal constraint to the region, along with material properties, dimensional features of the structure, thermal contact conductance between assembled component and so on but all these transfer parameters are of high importance in the obtaining accuracy in the study of heat transfer.

Amongst many other applications of partial differential equations, they are a highly utilized mathematical model to represent the heat transfer. Hence, differential equations bear fundamental significance and therefore it is essential to investigate how they entail the physical laws and relations to heat transfer in such manner. Esfandiari (2013) explains that when an equation involves an unknown function and one or more of its derivatives is known as a differential equation, and it would have two categories: ordinary differential equations

(ODEs) and partial differential equations (PDEs). When the unknown function is a function of only one independent variable or a function of several independent variables then the equation is either ODE or PDE, respectively. The heat equation in the form of differential equation can be solved through various methods such as analytical and numerical approach. For the complex engineering heat transfer problems, Han (2012) incorporates well-known methods of analytical solutions such as Bessel functions, separation of variables, similarity method, integral method, and matrix-inversion to equip professionals with essential knowledge and capability to understand and solve such problems.

Heat conduction can be modelled as one-dimensional, two-dimensional, or even three-dimensional depending on the nature of the problem involved, which also demands defining the steady or transient mode of the heat transfer. Han (2012) emphasizes that to determine the temperature profile of the structure, one must acquire initial and boundary conditions along with material properties which would include thermal conductivity, density, specific heat, and thermal diffusivity. The author highlights that regardless of the nature of the problem such 1-D, 2-D, 3-D, steady or unsteady, could be solved analytically given that the thermal conductivity is a constant parameter, and the thermal boundary conditions are not changing with time. Whereas, in real-life applications, thermal conductivities vary with temperature and heat equation becomes nonlinear which is difficult to solve and represent analytically.

Furthermore, in one dimensional heat conduction Keshavarz & Taheri (2007) have investigated the unsteady heat conduction in a slab by utilising polynomial approximation method. In their research, an improved lumped model is applied for a slab, cylinder, and sphere. They have made a comparison between finite difference solution and improved model; the latter approach is capable to determine the average temperature as a function of time for higher value of Biot numbers. Su (2001) also studies the transient cooling in a long slab by asymmetric heat convection within the framework of lumped parameter model. The investigation also employs the improved lumped model where heat conduction can be studied with Biot number having larger values, since the classical lumped models are restricted to values of Biot numbers below 0.1. Su's (2001) proposed lumped model was driven through two-point Hermite approximation for integrals. Based on the comparison with finite difference method, the proposed upgraded lumped model produces considerable improvement of average temperature calculation over the classical lumped model. Whenever simplified formulation of the unsteady heat conduction is required, the lumped parameter approach has been widely utilised in the thermohydraulic analysis of nuclear reactors. With the aims to improve the safe operation of nuclear power plants of pressurised water plant (PWR) and to accurately predict the reactor core behaviour, lumped parameter approach with neutron points kinetics model is utilised. To do so, Su & Cotta (2001) modelled time dependent heat transfer in a nuclear

fuel rod by using improved lumped parameter approach. Using ordinary differential equation and solving them through numerical means of initial value problem. The authors investigated the transient response of the fuel, cladding, and coolant. The high order lumped parameter approach is applied, and they concluded with it being applicable to provide a simplified formulation that can be utilised in stability analysis of PWRs or real-time simulators of nuclear power plants. Correa & Cotta (1998) have also examined the simplicity and improvement by utilising integration strategies to deduce mathematical formulation which otherwise is better than classical lumping procedures. Furthermore, solutions to heat transfer problem by the means of analytical methods include Ostrogorsky (2008) who used Laplace transforms to obtain solution for transient heat conduction in spheres exposed to surroundings at a uniform temperature and finite Bi numbers. The author stated that the methodology returned an explicit, and valid solution during early transients, for Fourier numbers $F_o < 0.3$.

Monteiro, Macêdo, Quaresma, & Cotta (2009) also utilised analytical integral transformation of the thermal wave propagation in a slab through the generalised integral transform technique. Their investigation states that the system of ODE is numerically solved by Gear's method for stiff initial value problems. The employed approach provided authors with reliable results for the temperature field. They investigated and determined temperature distribution for square and triangular wave pulses and illustrated the major features of hyperbolic heat transfer as a function of the two governing parameters, Biot number and dimensionless relaxation time.

Monte (2000) used analytic technique to solve one-dimensional unsteady heat conduction in a composite slab, perfect thermal contact between layers is considered. The research was investigated only for two material composite slabs which was conducting heat due to sudden variations of the temperature of the surrounding fluid. The author employed separation of variables to further the steps in obtaining solution for the problem under study. However, the focus was to study the relationship of the eigen values for the different regions. Although, the authors stated in the literature that the best approach to solve transient conductional problems in composite solids with energy generation is the Green's function approach. Feng and Michaelides (1997) state that Greens functions (GFs) is known for obtaining the complete temperature distribution and average properties during transient conduction processes. Although, the authors suggest that such a complete knowledge of the temperature field may be unnecessary. Carslaw and Jaeger (1959) introduced presented an introduction to the use of GF method in heat conduction problems and derived the technique by using Laplace transforms. Green's functions are named after the British mathematician George Green, who first developed the concept in the 1830s.

Numerically solving heat transfer problems makes it an efficient approach. This procedure involves obtaining the solution for the mathematically formulated problems in a finite number of steps to within an arbitrary precision.

Numerical methods produce an approximate solution of a specific problem, and this operation follows a set of guidelines which are known as an algorithm. Esfandiari (2013) further elaborates that the algorithm would be stable if a small change in the initial data will correspond to a small change in the final data. Otherwise, the algorithm is unstable.

For the solutions of systems of algebraic equations, solutions of differential equations used to represent heat transfer, to find the roots of algebraic equations and for many engineering applications, the help of iterative methods is employed by many researchers. Esfandiari (2013) explains the iterative scheme as a method which initiates with an initial guess and computes successive approximations of the solutions of the problem until a relatively accurate approximation is attained. Key thing in the process of iterative approach is how the termination of procedure is reached. There are two ways to end the approximations, firstly, to terminate when the maximum number of iterations is exceeded, and the other is when the approximation calculated in a step is within a prescribed tolerance of the true value. However, commonly true value is not available and therefore, practical form of terminating condition is whether the difference between two consecutive approximate quantities is within the specified tolerance.

A more specific area of heat transfer is evaluated which revolves around the heat related challenges being faced while operating manufacturing machines and what are the main causes and solutions to the problems.

2.7 Thermally Induced Errors in Manufacturing Machines

The metal cutting machine tools have an operating accuracy which is based on the accuracy of the relative movement between the workpiece and tool. If this relative movement becomes inaccurate due to any disturbance, an error is reproduced on the workpiece (Mayr, Ess, Weikert, & Wegener, 2009). In a machine, thermal effect can contribute up to 70% of the overall geometrical inaccuracies of the workpieces. Markus (2012) emphasizes on the necessity of comprehending physics of different shaped components in a machine. Since manufacturing machines are assembled using variety of components which influence the thermal behaviour of the overall structure, therefore, simulating and understanding the thermal behaviour of these components individually is essential as they directly influence the design phase and quality of the structure. Many other scholars (Eneko, Aitor, & Javier, 2013; Bryan, 1991; Dornfeld & Lee, 2008) have also stated that thermal distortion is on the main factors in limiting positional accuracy in the machine tools. Eneko *et al* (2013) also emphasizes on the optimisation of thermal design to prevent distortions in the structure. To reduce the thermal distortions in the structure of the machine, during design stages, engineers aim for obtaining symmetry in the structure and location of heat sources. In addition, it is also pointed out that certain designs of the structure which help in reaching steady state quickly are desirable. Ramesh *et al.* (2000) explain that the

selection of the thermally stable materials plays a vital role in the overall performance of the system. However, these techniques of reducing the thermal deformation in the structure by careful design tends to be very expensive, therefore, just employing thermal compensation methods have been found to be more cost effective. The relative movement between various elements of the machine generates heat which leads to the deformation of the structure and some of the possible heat sources include bearings, gearing and hydraulic oil, drives and clutches, pumps and motors, guideways, cutting action and swarf, and external heat sources. Figure 3 illustrates the main heat source and thermally induced deformation in the structure of a machine.

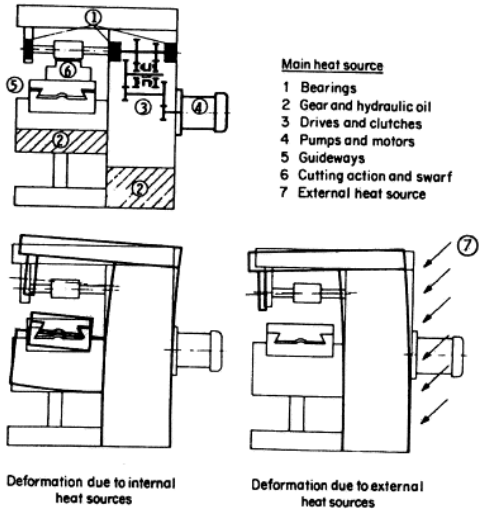

Figure 3: Thermally induced displacements on a milling machine (Week, 1984).

The authors have stated that the complex thermal behaviour is due to the thermally induced error being a time-varying non-linear process caused by a non-uniform temperature variation in the machine structure. Therefore, the interaction between the heat source location, its intensity, thermal expansion coefficient, and machine system's configuration leads to the complexity in the thermal behaviour.

Mian, Fletcher, Longstaff, & Myers (2011) have also considered the thermal errors induced in the machine tool and simulated the structural behaviour using Finite Element Analysis (FEA). The authors investigated the heat distributed in the form of thermal gradients along the structure of the machine which induces linear and nonlinear thermal expansions, and deformations that adversely affect the structural stability to maintain functional accuracy. Bryan (1991) explains that the complex interaction of the components in the structure having various heat sources, thermal time constants and thermal expansions is the reason behind nonlinear structural deformations leading to the thermal errors. Mian *et al* (2011) emphasize on the fact that many of the methods to compensate thermally induced errors in the machine tools require machine downtime where production time in the industries cannot be compromised. The authors utilised FEA to model the structure of

the machine tool and the specified the heat sources in the simulation which included components such as the bearings, belt drive, and motor supporting structure, thus, investigating the thermal behaviour of the structure.

Once the thermal gradients in various structures are accurately simulated and further investigated to reduce the thermally induced errors, it is imminent to study the techniques employed to complete this objective. Therefore, the mathematical model utilized for such object are evaluated for various circumstances in the next section of the literature review.

2.8 Techniques Employed for The Estimation of the Unknown Location and Strength of the Internal Heat Source

Numerous researchers have used various methods to obtain solutions for the conductional heat transfer problems and investigated the accuracy of their approaches along with limitations they pose while some also made a comparison among the mathematical techniques. Neto and Ozisik (1993) utilising conjugate gradient method estimate the location and timewise-varying strength of a plane heat source placed inside a plate with insulated boundaries. The authors utilised computed transient temperature measurements at the insulated boundaries of the structure involved and altered obtained data by adding random errors in order to use it as a simulated experimental data for the inverse analysis. They have also examined the robustness of their methodology by utilising timewise variation in the strength of the heat source taking the form of rectangular, triangular, and sinusoidal functions. Finally, solving the resulting inverse problem using finite difference scheme. Their research aims to estimate the unknown location and strength of heat source while the boundaries are kept insulated. The estimation of unknown strength of the heat source is considered as a function estimation problem and its unknown location as a parameter estimation problem. Neto and Ozisik (1993) employed conjugate gradient method to optimise their solution for the posed inverse problem. They have compared their estimated results of several cases with the exact values and were able to approximate the unknown strength of the heat source with the accuracy error of 2.6% in one of the scenarios while in another situation were able to estimate with only 14% error, these various scenarios represented the measurement errors of standard deviation. However, their research was on a transient one-dimensional heat transfer, and they used inverse estimation of the location and time-wise varying strength of the heat source while the boundaries of the participating region are considered as insulated. Transient temperature data is obtained from both sides of the plate and is utilized as a simulated experimental data to first, determine the temperature field in the region, and followed by the location and strength of the heat source. Similarly, Linhua, Heping, and Qizheng (2000) have also endorsed the conjugate gradient method to estimate the unknown heat source term in a one-dimension problem, their research focuses on a semi-transparent plane-parallel media with opaque and specular reflecting

boundaries. The authors conducting investigation to solve radiative transfer equation and its adjoint equation with the help of discrete ordinates method.

Furthermore, Khachfe and Jarny (2001) extended the works of Neto and Ozisik (1993) to determine both the location and timewise-varying strength of the heat source within a body by utilising temperature measurements across the structure. The researchers conducted thermal experiments as well on the slab under investigation by heating it through internal line heat sources and took the temperature measurements at the boundaries of the structure as demonstrated in Figure 4. The thermocouples utilized for this study were placed at the boundaries as well as in middle of the slab, since it was dissected into pieces for the installation of the heat source, this is illustrated in Figure 4. The researchers have employed numerical methods and computational algorithms for obtaining solution for the inverse heat transfer problem in the two-dimensional enclosure and made a comparison with the experimental results. Their approach comprised of employing the Conjugate Gradient Algorithm (CGA) and the finite element technique and concluded that such combination is well adapted to perform inverse heat flow analysis in various situation including arbitrarily shaped bodies and with temperature dependent properties which belongs to nonlinear problems. Although, they had an extensive access to take the temperature measurements at numerous locations which reduces the number of challenges with estimation of the unknown parameters such as the location and strength of the heat source.

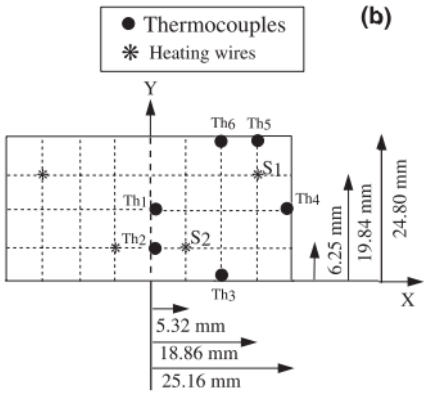

Figure 4: Location of thermocouples and heat wires in the experimental setup of the khachfe & Jarny (2001)

Whereas Lobato, Steffen Jr, & Neto (2010) also determined the unknown heat source term and its location as well. However, their work presented the findings through utilising a different technique known as differential evolution approach in a one-dimensional plate with insulated boundaries. The authors approximated the unknown location and timewise varying strength of a plane heat source inside the plate. They measured

temperature variations dependent on time at both boundaries of the plate and added random errors to it, while this data served as the simulated experimental findings for the inverse analysis.

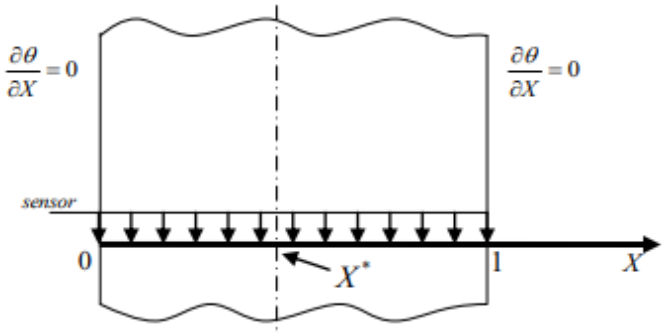

Figure 5: Schematic figure illustrating the plate under investigation for heat transfer problem by Lobato et al (2010)

Figure 5 shows the location of the plane heat source as X^*, however, the total number of sensors used in this research are unclear. The boundary conditions defined for both sides of the structure is insulated. Further investigation by changing the parameter values of the optimisation algorithm and finding out its impact on the performance of the estimation approach would be an interesting finding.

Parwani, Talukdar, and Subbarao (2013) further supported the technique which was employed by Lobato, Steffen Jr, & Neto (2010), and investigated the efficiency of the differential evolution (DE) algorithm in attempts to simultaneously estimate the strength as well as the position of the heat source in the participating medium. Their research revolves around determining the approximation of unknown position and the timewise varying strength of the heat source by employing differential evolution approach. Their investigation is restricted to a two-dimensional region with isothermal and black boundaries containing non-scattering, absorbing, and emitting grey medium. Radiative and conductional heat transfer problem is addressed, and while the solution conclusively projects a success in the given conditions while applying DE algorithm. The authors estimated the unknown location of the heat source with up to 10% relative error in x direction and up to 23.2% in y direction. This error occurred when the number of temperature sensors utilized to record the measurements varied from 9, 15, and 21 within the region. Furthermore, the authors stated that it was also the case that the strength of the heat source was determined with a good correlation with its actual value. The timewise varying strength was in the form of sinusoidal, triangular or step function. While they were able to simultaneously estimate the unknown location and strength of the internal heat source with low relative error, they had placed thermocouples of varying quantity inside the investigating region as illustrated in Figure 6. The availability of numerous thermocouples on a surface of the heat transfer region does increase the accuracy in the estimation of unknown parameters, whereas the three-dimensional aspects of the structure would have posed a further

challenge when estimating the depth of the internal heat source from only one of the external surfaces. Additionally, with only a two-dimensional structure under investigation and ability to take temperature measurements at various locations gave the researchers a better chance at determining the temperature profile and subsequently, came out with estimating the unknown location and the strength of the heat source.

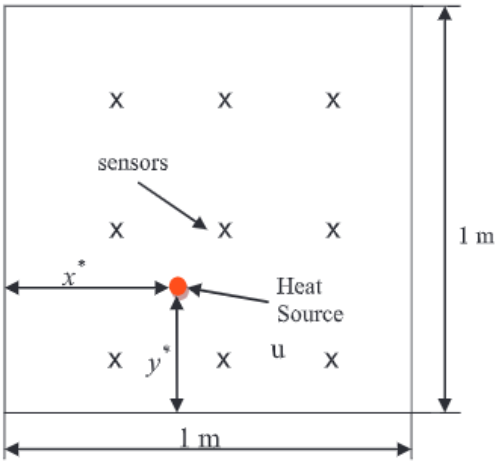

Figure 6: Schematic figure of the investigated problem by Parwani et al (2013) and illustrates the placement of the thermocouples within the structure.

Parwani *et al* (2013) conducted similar study investigating the application of a hybrid differential evolution approach but entirely to estimate the strength of a heat source in a two-dimensional radiatively participating medium. The region under investigation is induced with radiational as well as conductional heat transfer. The authors proposed a hybrid differential evolution method with a local optimisation algorithm to determine the function of the heat source. Intrinsically used the conjugate gradient method with an adjoint equation as a local optimisation algorithm to speed up the convergence speed. For the radiative transfer equation and energy equation, Parwani *et al* made use of finite volume method.

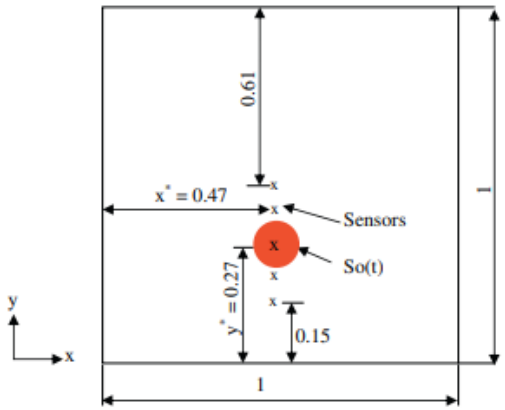

Figure 7: Problem descriptive figure by Parwani et al (2013)

In Figure 7, it can be seen, that the sensors are placed inside the domain and the location of the heat source is a known parameter in their presented work. The temperature field in the domain is determined by using finite volume method and the input it requires is obtained from the thermocouples. The authors were able to determine the functional form of the heat source when the form was of triangular and double sinusoidal. Their comparison deduced better estimation ability of a hybrid differential evolution approach than the normal differential evolution technique. Similar to the previous researchers, the temperature field within the region is determined by mounting the temperature sensors at numerous locations within the structure. When the measurement of the temperature is restricted to limited locations, the difficulty would be different.

Similarly, a three-dimensional investigation was carried out by Beddiaf, Perez, Autrique, & Jolly (2014) to estimate the time varying strength and location of a heat source. The researchers measured temperature on a boundary of the studied three-dimensional geometry and estimated the surface heat flux and heating source's location. The work presented in the outcomes is through utilising conjugate gradient method which is iterative regularisation method. Implementation of such technique consists in the iterative resolution of three well-posed problems: a direct problem (solved by FEM method provided by Comsol-Multiphysics software and interfaced with Matlab), a sensitivity problem (descent depth estimation), and an adjoint problem (descent direction determination). Although, they successfully investigated a challenging objective by heating one surface of the three-dimensional geometry with the fixed heat source while measuring temperature change on the opposite surface, to determine the time-varying strength of the heat flux and fixed location of the heat source by CGM. However, a further research would be interesting by placing the heat source internally in the three-dimensional geometry and investigating its impact on the conjugate gradient method employed by researchers and how the results differ.

Furthermore, to the purpose of determining the unknown heat source function in a heat conduction problem is addressed by Tian, Sun, Xu, & Lai (2011) and they utilized, a completely different approach then what has been discussed so far, a Quantum-behaved Particle Swarm Optimisation (QPSO). PSO is a stochastic method applied in their research without a priori information on the function of the heat source. Furthermore, they employed Tikhonov regularisation method to stabilise the obtained solution.

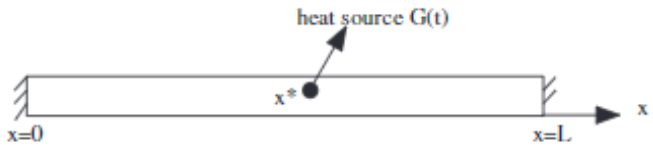

Figure 8: Cross section of the heated rod under investigation by Tian et al (2011)

Figure 8 shows the one-dimensional figure, heat source, and insulated boundary conditions as investigated by Tian *et al* (2011). The work presented considers a plane surface heat source and sensors mounted on both insulated boundaries of the rod. They have first solved the direct problem using the Crank-Nicolson implicit finite difference method. The authors concluded with comparison between PSO, CGM, genetic algorithm (GA), and QPSO in their ability to estimate the time-wise varying strength of the heat source, with remarks for QPSO being prime approach in such heat transfer problems.

2.9 Critical Summary of the Literature Review

The overall findings of the literature review to identify major problems in the relevant field, methodologies applied by previous researchers, and the gap for further research are summarised below.

It is suggested by Esfandiari (2013) that Heat transfer analysis conducted on individual components of the machine structure is essential, since they influence the overall thermal behaviour of the machine structure. Similarly, Han (2012) extended to emphasize on the importance of the initial and boundary conditions and that they must be established before determining the temperature distribution in a structure. Furthermore, it is implied that if the material properties and boundary conditions are independent of time, the problem can be solved analytically. However, if the conditions vary with time, as they do in most real-life applications, then analytically presenting them becomes extremely challenging. In such scenario employing numerical techniques for better approximation is a recommended approach. Esfandiari (2013) supports application of numerical approach to solve heat transfer problems by stating them as an efficient approach which follows certain guidelines known as algorithm.

Another main technique employed in numerous heat transfer scenarios which are thoroughly investigated and solved using analytical approaches and by employing lumped capacitance system to represent thermal behaviours of various structures (Keshavarz & Taheri, 2007); (Su, 2001); (Ostrogorsky, 2008).

Amongst several authors who conducted the study to estimate the unknown location along with the strength of the heat source in both one and two-dimensional mediums, this includes Parwani et al. (2013), Khachfe & Jarny (2001), Beddiaf et al. (2014), Tian et al. (2011), and Lobato et al. (2010). However, all these researchers have a common ground of mounting numerous temperature sensors at various locations of the structures under study and take measurements, this has been a constraint found in the literature in order to reconstruct the temperature distribution within the participating medium. However, restricting the temperature measurement locations would be a challenge to reconstruct the temperature distribution and consequently determine the location of the heat source.

The challenge to determine the unknown location of the heat source depends critically on the knowledge of the temperature distribution of the structure involved. Therefore, the gap identified is to reconstruct the temperature distribution by utilizing reduced number of locations for temperature measurements, and consequently determining the location of the heat source. Such technique would have immense application in three dimensional mediums, where the location of the internal heat source could be determined by only utilizing surface temperatures. The aim and objectives of the research will elaborate how such gap in the literature review will be addressed in this project.

3 Aims and Objectives of the Project

As the literature review identifies a prospect of estimating the location of the heat source utilizing restricted number of temperature measurement locations. Therefore, the aim of the research project is to estimate the unknown spatial location of the internally placed heat source in the given engineering structure.

3.1Objectives

To successfully achieve the aim of the research, following objectives are considered to support the journey of the research,

1. Investigate and estimate the unknown location of the heat source in a one-dimensional medium while the heat transfer is in steady state. The temperature distribution in the medium should also be an unknown parameter and should be determined by measuring temperature change at only at one boundary of the one-dimensional structure.
2. Expand the investigation to one-dimensional transient heat transfer and estimate the unknown temperature field consequently determining the unknown distance to the heat source from the boundary.
3. Generate a comparison between the methodologies used to find the solution to both steady and unsteady one-dimensional heat transfer problems.
4. Further the study of approximation to two-dimensional mediums under transient heat transfer and estimate the unknown spatial location of the heat source. While limiting the temperature measurement to two boundaries in two-dimensional heat transfer analysis.

4 Methodology

The gap identified in the literature review and the formed objectives of the research highlight the main objective of the project which is to determine the location of the heat source in various structures utilizing restricted points of the structure for temperature measurement. It is observed that previous researchers have also determined the unknown location of the heat source in structures; however, to estimate the unknown location, they had to take temperature measurements at multiple positions. The challenge of this research is to estimate the location of the heat source in one and two-dimensional mediums, however, it will be undertaken by utilising only one point for the one-dimensional structures and two points for the two-dimensional structures for extracting the temperature data. This chapter discusses the processes that are used for data collection, experimental setup, computer aided design (CAD) models, mathematical approaches, and explains the reasons behind the each of the techniques being employed.

Since there are a lot of variables involved in the process of heat transfer, it is important to have a correct starting point. Therefore, establishing conditions for the initial study is critical. Similar to the structures investigated by others in the literature review, similarly a metal plate with a heat source was studied for estimating the location of the heat source. The research in this project is conducted on a structure starting with one-dimensional structure and is extended to a two-dimensional structure.

4.1 Finite Element Analysis, Thermal Experiments, and Analytical Approach

Three key processes are involved in the current approach namely thermal experiments, FEA simulation, and the mathematical calculations. Thermal experiments are performed to investigate realistic thermal behaviour of the structure under the influence of a heat source. The experiments will also serve as a validation data for simulated heat transfer on a CAD model. Finally, the mathematical calculations are utilized to determine the location of the heat source using the data from FEA simulation and the thermal experiments. First of all, temperature profiles of the structure are the most prominent requirement when estimating the unknown location of the causing heat source. Once, the temperature profiles are obtained, the data needs to be utilized in mathematical models which may allow to estimate the location of the heat source. In the literature review, several types of optimization techniques are discussed among which are conjugate gradient, differential evolution, and particle swarm optimization. These techniques require complete temperature profile of the surface in order to estimate the location of the heat source. Since, the temperature measurement is restricted to one position in one-dimensional structure and two perpendicular boundaries in two-dimensional structure, these techniques are not suitable. Therefore, the approach to address the main objective of estimating the location of the heat source is

applied through fundamental heat diffusion equation which changes according to the conditions of the heat transfer.

The problem at hand is broken down into four categories namely steady state one-dimensional, transient state one-dimensional, steady state two-dimensional, and lastly transient state two-dimensional heat transfer. Initiating with steady state heat transfer in one dimensional structure allowed to establish a foundation of the approach presented in current research. Generally, heat transfer problems are analysed as one-dimensional, two-dimensional, or three-dimensional. Realistically, heat transfer through a medium is three dimensional which means the temperature varies in all three directions.

Literature states that the Fourier's law of conduction is a strong tool applicable to problems involving conditions such as steady state, transient, multidimensional conduction in complex geometries even when the nature of temperature distribution is not apparent. It is apparent that the full nature of Fourier's law must be fully comprehended to understand heat transfer problems. Incropera et al. (2007) stated that a deeper understanding of Fourier's law is essential and pivotal when dealing with heat transfer problems.

Heat transfer occurs through various modes simultaneously, generally, conduction and convection are found together as the modes of heat transfer in a system (Kothandaraman, 2006). When dealing with two-dimensional heat transfer problems, one can opt for analytical method, graphical methods, or numerical methods. However, for steady state conductional problems, analytical method works best on simplified geometries and when thermal properties are constant, this approach yields exact solution and is sometimes utilised as a benchmark result for numerical approaches. The main objective of the heat diffusion equation is to enable one to determine temperature distribution T (x, y, z, t) in a medium by knowing the temperatures and/or the heat transfer rates on the surface. The heat conduction equation will be modified depending on the conditions of the heat transfer such as steady or transient state or the number of dimensions under study. When the boundary conditions are defined, the temperature distribution can be symmetrical as well as asymmetrical depending upon the conditions. Additionally, the generation and storage terms are irrelevant in the surface energy balance technique. This approach is often utilised and applied at the surface of a medium. Furthermore, the benefit of using surface energy balance is that its applicable in both steady-state and transient state. Incropera et al (2007).

Esfandiari (2013) explains that when an equation involves an unknown function and one or more of its derivatives is known as a differential equation, and it would have two categories: ordinary differential equations (ODEs) and partial differential equations (PDEs). When the unknown function is a function of only one

independent variable or a function of several independent variables then the equation is either ODE or PDE, respectively. The heat equation in the form of differential equation can be solved through various methods such as analytical and numerical approach. For the complex engineering heat transfer problems, Han (2012) incorporates well-known methods of analytical solutions such as Bessel functions, separation of variables, similarity method, integral method, and matrix-inversion to equip professionals with essential knowledge and capability to understand and solve such problems.

Han (2012) emphasizes that to determine the temperature profile of the structure, one must acquire initial and boundary conditions along with material properties which would include thermal conductivity, density, specific heat, and thermal diffusivity. The author highlights that regardless of the nature of the problem such 1-D, 2-D, 3-D, steady or unsteady, could be solved analytically given that the thermal conductivity is a constant parameter, and the thermal boundary conditions are not changing with time. Whereas, in real-life applications, thermal conductivities vary with temperature and heat equation becomes nonlinear which is difficult to solve and represent analytically. The partial differential equation representing the heat flow is utilised and solved using various numerical and analytical approaches, such as separation of variables, energy balance approach, Finite Element Analysis, and lumped capacitance model. The derivation of each approach is presented section 2.2 of the literature review chapter.

Therefore, the main approach would be to analytically utilize the differential equation representing the heat transfer in one and two-dimensional mediums. Furthermore, finite element analysis which is a numerical technique will be applied to obtain data for heat transfer simulations. Similarly, thermal experiments will be performed to investigate and validate the FEA and analytical results.

4.2 Finite Element Analysis

As discussed before the numerical methods are an efficient technique to obtain solutions for multidimensional conduction heat transfer problems. Commonly used technique in numerical approach includes Finite Element Method (FEM), Finite Difference Method (FDM), or Boundary Element Methods (BEM) are utilised due to the flexibility they offer to evaluate complex geometries, nonlinear material properties, and non-simple boundary conditions (Incropera, Dewitt, Lavine, & Bergman, 2007; Hagen, 1999). In FEM, the solution to a discretised partial differential equation is obtained and enables determination of the temperature at only *discrete* points. The geometry of the structure is divided into several building components called the finite elements that conforms the domain. The models are divided into a mesh region and each node is defined by the master finite difference formula,

$$T_{i,j} = \frac{AT_{i-1,j} + BT_{i,j+1} + CT_{i+1,j} + DT_{i,j-1} + BiT_{\infty} + (E\dot{q}\,\Delta^2 + q\Delta + \frac{\dot{Q_s}}{\delta})/k}{F + Bi} \quad \text{Eq. 22}$$

$$Bi = \frac{h\Delta}{k} Biot\ number$$

$$T_{\infty} = Fluid\ temperature$$

$$\Delta = Node\ spacing$$

$$\dot{q} = Internal\ heat\ generation\ (\frac{W}{m^3})$$

$$q = Heat\ flux\ (\frac{w}{m^2})$$

$$Q_s = Point\ Heat\ Source\ (W)$$

$$h = Heat\ Transfer\ Coefficient\ (\frac{W}{m^2} \times C)$$

In this research, the data to heat transfer for the structure under investigation will be mainly obtained by utilising the FEA software namely Abaqus/CAE 2020. Whereas the validation of the obtained temperature profile will be conducted by comparing the results obtained through physical thermal experiments.

4.3 Thermal Experiments and Equipment

Thermal experiments are performed on a steel plate. The apparatus for the thermal experiments mainly includes a metal plate with a heat source attached to it. The power source for the heater, thermocouples for monitoring the temperature of the heat source along with the laboratory temperature to observe external factors. The surface temperatures of the metal plate are extracted using a thermal imaging camera. The temperature data is captured and recorded by utilising a thermal imaging camera (A615) and its accompanying software called ResearchIR. The power supply's accuracy is tested by connecting a multimeter to it and checking against current and voltage, and the thermal imaging camera has the accuracy of $\pm$ 2℃ and thermal sensitivity of $<$ 0.05℃. The experiments performed are restricted to number of positions of the heat source attached to the backside of the metal plate.

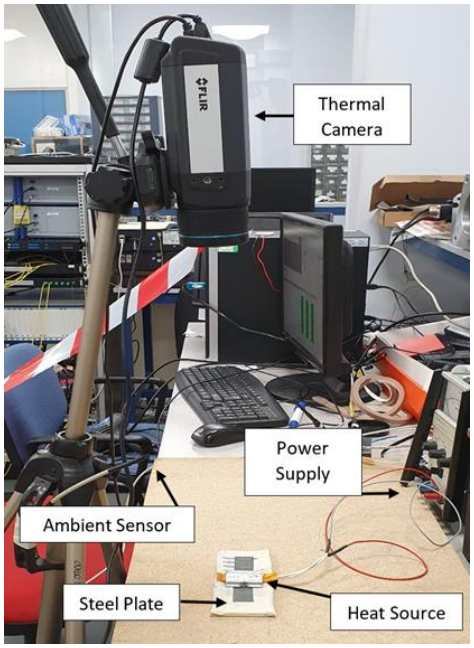

Figure 9: Thermal Experiment setup illustrating the equipment.

In Figure 9, the equipment illustrated shows the heat source attached to the back side of the steel plate. For the actual experiment, the steel plate is flipped over, and the top surface is capture for thermal response by the thermal imaging camera. This set up is to create as close as possible to a one-dimensional heat transfer. The thickness of the steel plate is only 4mm. The height of the heat source and the plate is both 40mm. Insulation foam is wrapped around the edges of the plate to restrict the loss of heat through convection to minimum. Three sensors are also placed to measure the ambient temperature around the set up in the laboratory. The data captured by the thermal camera is processed in the FLIR ResearchIR software and the temperature profiles across the surface and boundary points is extracted as an excel file. Furthermore, similar experiments are performed on another plate with bigger dimensions which would reflect a two-dimensional heat transfer.

4.4 Mesh Convergence – Benchmark Study

The benchmark study is conducted to establish and validate the correct application of the thermal properties applied in the heat transfer simulation. For this purpose, Abaqus CAE software is utilized to create the CAD models of the steel plate and attach a heat source to it. Further conditions are defined such as material properties, heat transfer conditions including initial temperature, ambient temperature, duration of heat transfer, mesh type, and body heat flux. The CAD model is simulated to produce its thermal behaviour under the conditions predefined for it.

The mesh properties are evaluated to study its influence on the outcome. Abaqus offers different types of element shapes when creating the mesh for the CAD model.

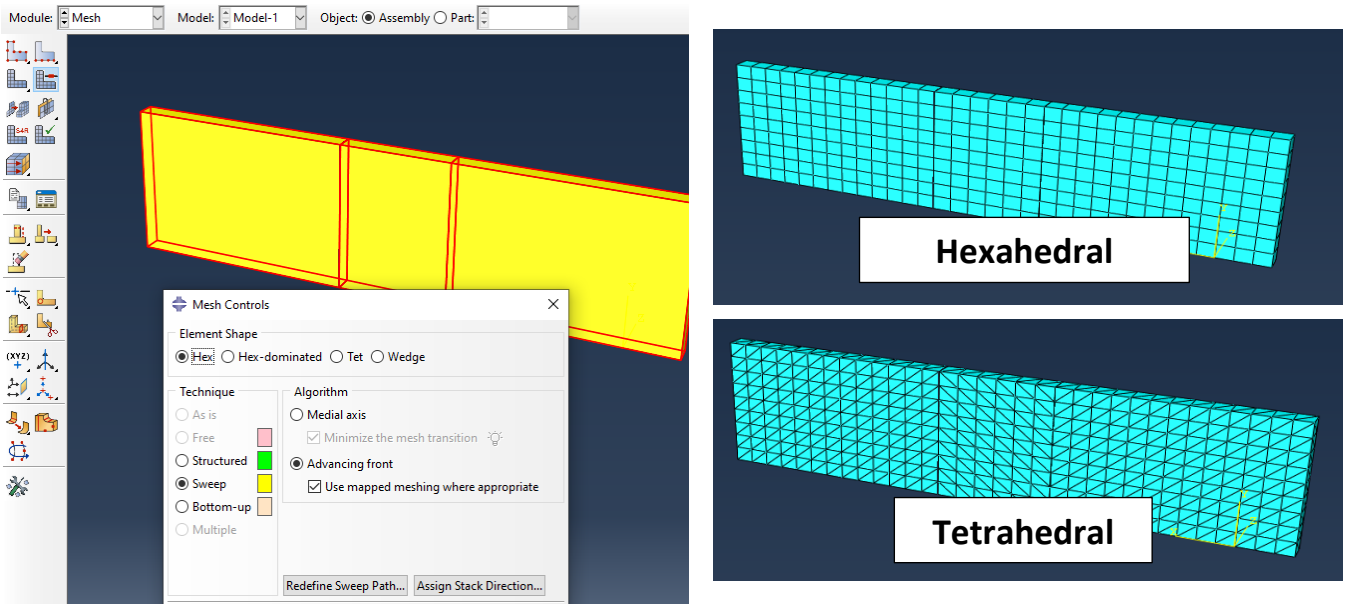

Figure 10: Mesh controls illustrating the element shapes offered in Abaqus.

Figure 10 illustrates the element shapes which will be studied for the purpose of its influence on the outcome. In addition, it also shows the two types of element shapes applied to the assembled steel plate with an attached heat source in the middle. The simulation for these two element shapes will be conducted and the mesh convergence study will be concluded.

4.4.1 Hexahedral Meshing

The steel plate is simulated using hexahedral meshing technique and the element size is defined approximately to 4.5mm (seeding). This meshing discretised the structure under study into 288 linear hexahedral elements. The total CPU time required for the hexahedral meshing for the heat transfer simulation is only 13 seconds. In Figure 11, the maximum temperature in the plate for the transient simulation of 600 seconds produced 56.071℃.

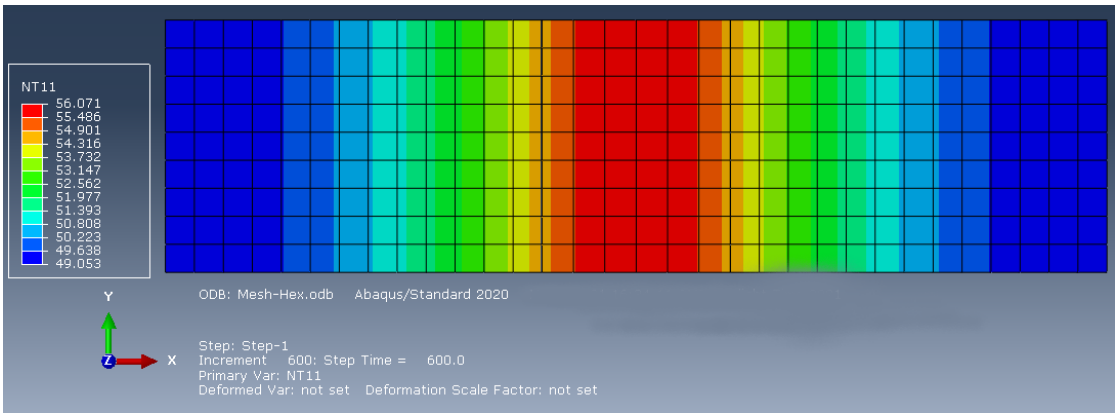

Figure 11: Temperature profile across the steel plate – Hexahedral Meshing.

4.4.2 Tetrahedral Meshing

The steel plate is simulated using tetrahedral meshing technique and the element size is defined approximately to 4.5mm (seeding). This meshing discretised the structure under study into 3406 linear tetrahedral elements. Total CPU time to solve for tetrahedral meshing is 49.5 seconds. Whereas the maximum temperature for the transient simulation of 600 seconds produced $56.068℃$, this is illustrated in Figure 12. The difference in the maximum temperature in both types of meshing is negligible.

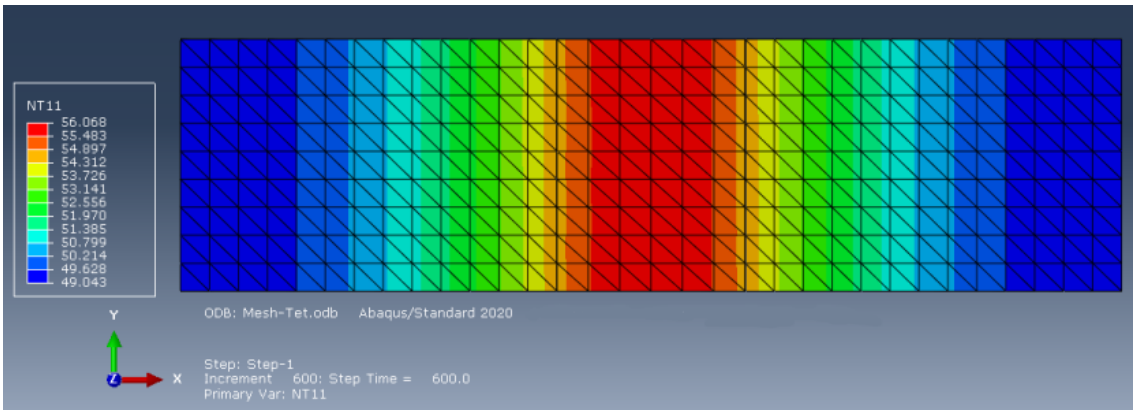

Figure 12: Temperature profile across the steel plate – Tetrahedral Meshing.

4.4.3 Mesh Sensitivity – Hexahedral

Since, both tetrahedral and hexahedral have negligible impact on the maximum temperature in the transient heat transfer. A further investigation into the element size is conducted to study the mesh convergence.

Element Size (mm)	Number of Elements	CPU Time (Seconds)	Maximum Temperature
6	175	11.6	56.015
5	240	12.1	56.070
4	380	16.7	56.070
3	1300	35.8	56.070
2	4500	103.1	56.064
1	30000	622.1	56.070

Table 1: Mesh convergence study - Hexahedral

The results in Table 1 show the varying element size and corresponding number of elements in the meshing of the steel plate. Subsequently, the CPU time and the maximum temperature for increasing number of elements is illustrated. It is noted that with smaller element size the CPU time increases as a greater number of elements need to be solved in order to obtain the solution for the heat transfer simulation. Whereas the maximum temperature in the plate is still at $56.07℃$. As the geometry of the structure is simple plate with an attached heat source, it does not change the maximum temperature as much. Using element size of 3 – 4 mm for the plate produces the same result within shorter time as compared to utilizing 1 – 2 mm element size. This research is concerned with the temperature values and with a finer mesh the accuracy is not improving. Therefore, for the rest of the investigation, the element size will be used as 4 mm.

4.5 Limitations in methodology

The most important limitation in the current methodology is the fact that it is only applied to one and two-dimensional structures. Which are also in a simplified shape of a plate with an attached heat source. However, within the investigation of one and two-dimensional structures, experimentally, the flow of heat transfer is not completely restricted in neither one now two dimensions. As the heat transfer realistically takes place in all three dimensions. However, the insulation around the plate did minimize the loss of heat through boundaries. And for the purpose of negligible temperature difference across the thickness of the steel plate, a 5mm thick plate was chosen. This allowed maximum transfer of heat from the backside of the plate where the heat source was attached to the top surface from which the temperature profile was being measured by the thermal imaging camera. There was also loss of heat from the other surface on the heat source which was in contact with the medium-density fibreboard (MDF). Moreover, the thermal contact conductance between the heat source and the steel plate was assumed to be negligible, whereas an epoxy was used to attach the heat source to the back side of the steel plate.

5 Results and Discussion

This chapter discusses the methodology applied in the current research and initiates by one-dimensional steady state heat transfer. The approach develops further when several positions of the heat source is determined under steady state condition. Consequently, it is extended to the transient heat transfer which creates an opportunity for a parametric analysis on the properties involved in the thermal behaviour of the structure under study. In Addition, it discusses the outcomes from the finite element analysis along with the experimental findings. This allows to make a comparison and further validate the approach of the current research. Finally, the application of the approach employed for one-dimensional structures is applied to two-dimensional and the outcome is presented.

The heat transfer under realistic conditions in a machine structure occurs in three-dimensions and due to the complexity of the assembly, it is challenging to mathematically model the heat transfer in the whole structure. However, looking at heat transfer within individual components which consequently contribute to the overall performance could be a starting point. Therefore, in this research heat transfer is evaluated through physical thermal experiments and FEA simulation. The heat transfer under realistic conditions is difficult to restrict to only one-dimension so for this purpose reliability is considered in the FEA analysis. The results are presented for both one and two-dimensional heat transfer under steady and unsteady conditions.

The first section of the results chapter presents the steady state heat transfer in a one-dimensional structure. The results include the estimated outcome for the strength of the internal heat source as well as its location which is determined utilising temperature data extracted from only end of the one-dimensional structure. This is then followed by performing thermal experiments on a similar metal plate to evaluate conductional heat transfer under realistic conditions. Once the data is extracted from thermal experiments, likewise conditions are applied in the FEA simulation to recreate the heat transfer in a transient and more realistic format. Thereafter, the dependency on the FEA simulations was established due to its repeatability, efficiency, and adaptability to modifications in the applied parameter to create situations which would have been time consuming as well as prone to errors if performed in the thermal experiments. The results within the FEA simulation for the heat transfer only take few minutes to compute for the similar data, thermal experiments could take few hours. Therefore, the simulated data from the FEA software is employed as an input to the mathematical approaches applied to determine the spatial location of the heat source within the structure in both one and two-dimensional steady as well as the unsteady heat transfer. The overall analysis investigates how the location, strength, and geometrical size of the internal heat source influences the temperature profile at the boundary while estimating the unknown location of the internal heat source in each case.

5.1 Known Parameters and Assumptions to Estimate the Location of the Heat Source

The applied approaches to solve for the unknown location of the heat source from the boundary or the surface of the structure is to establish fundamental results. The unknown parameters are only two in this research namely the location or the distance to the heat source and its strength. These two parameters are estimated using the temperature measurements carried out on the boundary or the surface of the structure, whereas the known parameters considered in study include the dimensional size of the structure, dimensional size of the heat source, boundary conditions, and the material properties.

5.2 One-Dimensional Steady State Heat Transfer Analysis

As shown in the methodology section 2.3, the heat diffusion equation reduces to the following expression when the system is in a steady state with uniform internal heat generation,

$$\frac{d^2T}{dx^2} + \frac{\dot{q}}{k} = 0$$

In this steady state, the position of the heat source will be determined using boundary temperatures. Along with an investigation into the role that convectional coefficient plays in the heat transfer.

5.2.1 Centrally Positioned Heat Source

In problem 1, a steady state conductional and convectional heat transfer through a thin steel plate with constant thermal conductivity and internal heat source is investigated. The boundary conditions are illustrated in the schematic Figure 13: Schematic diagram of 1D heat transfer with an internal heat source in the plate. with convection on two sides and insulated on the other two ends to restrict the heat flow in one dimension. In this section the strength of the heat source body is determined. The dimensional parameters of the plate under the analysis are 150 x 40 x 5 (mm). Additionally, the known parameters are listed in the Table 2 along with the unknown parameters to be addressed in this problem. An FEA simulation (Abaqus/CAE) is used to model the heat transfer process in the plate and the temperature profile from the simulation will be compared with the calculated values.

Known Parameters	Value	Units	Unknown Parameters
Thermal Conductivity	52	W/m.C	Heat Source Strength
Plate mass	0.0936	Kg	Location of Heat Source
Specific Heat Capacity	473	J/Kg.C	Steady State Boundary Temperature
Heat Source Volume	0.000006	m^3	Boundary Heat Flux

Table 2 The known parameters before the solution and the unknowns to be determined – Problem 1.

The simulation on the FEA software is a transient heat transfer until the system approaches the steady state. Transient temperature change on the boundary until it reaches a steady state is extracted and utilised along with the value of steady-state's temperature at only one end of the plate. The Schematic Figure 13 illustrates the dimensions of the structure and thermophysical properties involved in the heat transfer. Part A and C are the non-generating, and part B is the generating one since it is the internal heat source.

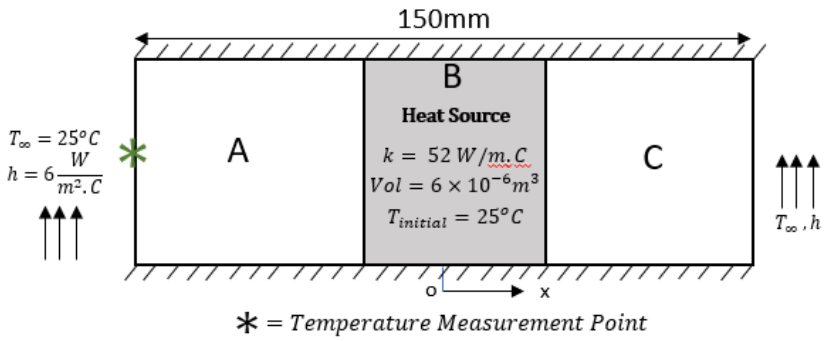

Figure 13: Schematic diagram of 1D heat transfer with an internal heat source in the plate.

$T_{initial}$ is the initial temperature of the whole structure. The temperature change on the boundary is observed over time and the obtained data will be used to determine the strength of the heat source. Temperature Sensor location is the boundary under observation for the temperature change in the plate for both sides. A constant strength of the heat source is applied in the FEA simulation under the body heat flux conditions. The rest of the plate are given material properties and convectional heat loss condition is also applied to both ends of the plate.

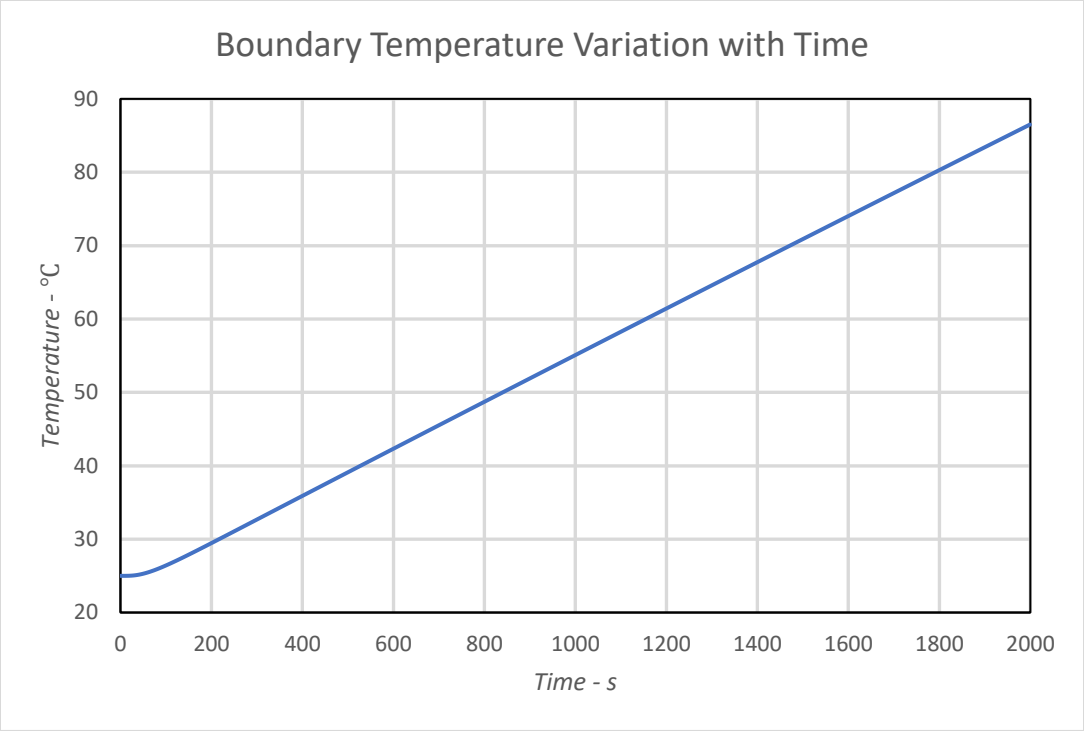

Figure 14: Transient state temperature change at boundary point '*' – data extracted from the FEA simulation.

The temperature measured on the boundary is extracted from the FEA simulation and plotted in Figure 14. Since the heat source is centrally positioned. To examine the behaviour at the boundaries, rate of change of temperature is calculated for 10 second interval. The outcome is illustrated is plotted in Figure 15. It can be observed that the temperature change is slowly decreasing after 300 seconds have passed, the rate of change in temperature decreases slowly from this point onwards as the system will eventually approach the steady state, the rate of change will reach zero as well.

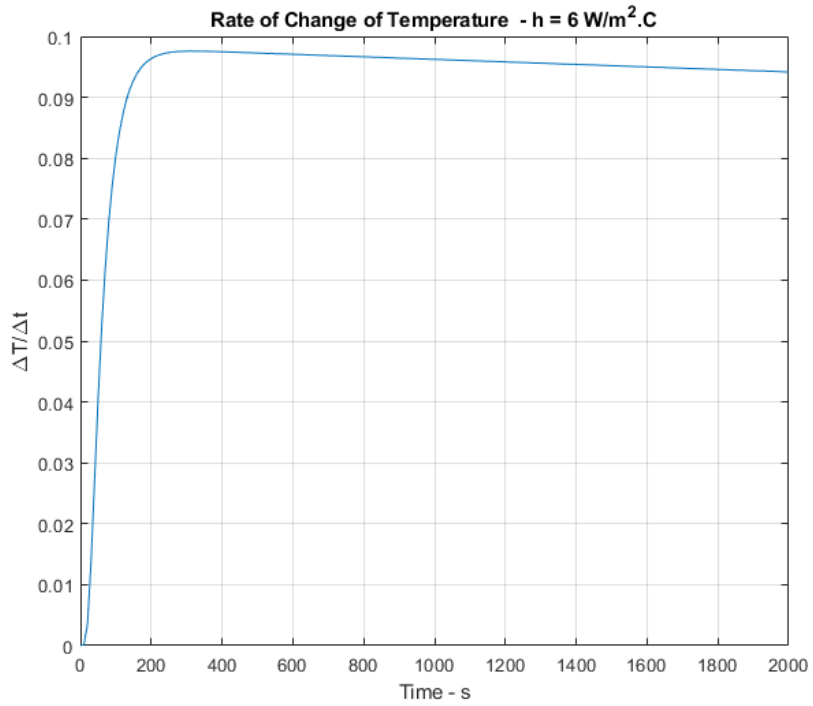

Figure 15: Rate of change of temperature on the boundary of the one-dimensional plate.

Therefore, two values of rate of change are taken from the slow decreasing phase in Figure 15. The two values are used to calculate the average rate of temperature change per second for the phase close to a steady state of rate of change of temperature. This consequently assisted in determining the energy being used to cause the rate of temperature change.

$$\frac{\Delta T}{t} = \frac{T_2 - T_1}{t_2 - t_1}$$

$$\frac{\Delta T}{t} = \frac{70.86 - 42.29}{900} = 0.0317℃/s$$

Using specific heat capacity equation provides the energy for the calculated temperature change, however, before using this equation, the gradient will be multiplied with time as 1 second to change the units to ℃, hence,

$$Q = mC\Delta T = 0.0317 \times 473 \times 0.234 = 3.514\,J$$

The energy will be converted to power,

$$Power = \frac{Energy}{Time} = \frac{3.514\,J}{1\,s} = 3.514\,W$$

This is the power being used to cause the temperature change in the structure, however, the heat generation is not by the entire plate. Therefore, dividing power value by the volume of the heat source body will retrieve the strength of heat source. The following step is carried out to determine the strength of the heat source present in the plate,

$$Body\ Heat\ Flux = \frac{Power}{Volume} = \frac{3.514W}{6 \times 10^{-6}m^3} = 5.86\ \times 10^5\ W/m^3$$

Whereas the actual body heat flux applied in the FEA simulation was $6\ \times 10^5\ W/m^3$.

Since all the energy produced by the heat source dissipates in the negative and positive directions of the x-axis, utilising the energy balance on the heat source body while keeping in mind that there is no inflow of the energy and with steady states there is no energy is being stored either. The heat flux being dissipated by the heat source can be determined by applying energy conservation on the heat source body,

$$\dot{E}_{in} + \dot{E}_g - \dot{E}_{out} = \dot{E}_{st}$$

$$-q" + \dot{q}L - q" = 0$$

$$-2q" = -\dot{q}L$$

$$q" = \dot{q}L/2$$

$$q"\ (Heat\ Flux) = \frac{\dot{q}L}{2} = \frac{5.86 \times 10^5\ \times 0.03}{2} = 8790\ W/m^2$$

Whereas with the actual body heat flux value, the surface heat flux would be and illustrated in Figure 16,

$$q"\ (Heat\ Flux) = \frac{\dot{q}L}{2} = \frac{6 \times 10^5\ \times 0.03}{2} = 9000\ W/m^2$$

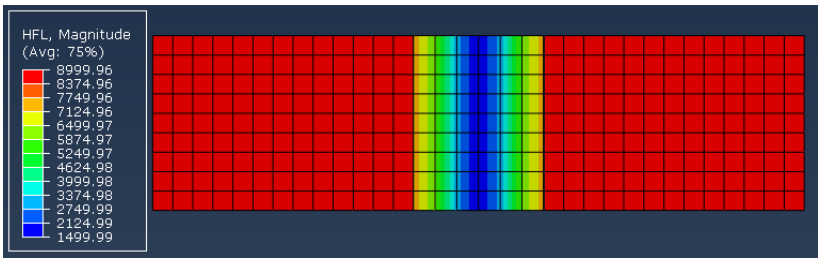

Figure 16: FEA simulated heat flux magnitude in the one-dimensional plate at the steady state of heat transfer.

5.2.2 Convectional Coefficient Analysis and Estimation of Location

In this section the convection applied at the boundaries as illustrated in Figure 17 will be varied and the steady state profile will be evaluated while keeping the rest of the parameters unchanged.

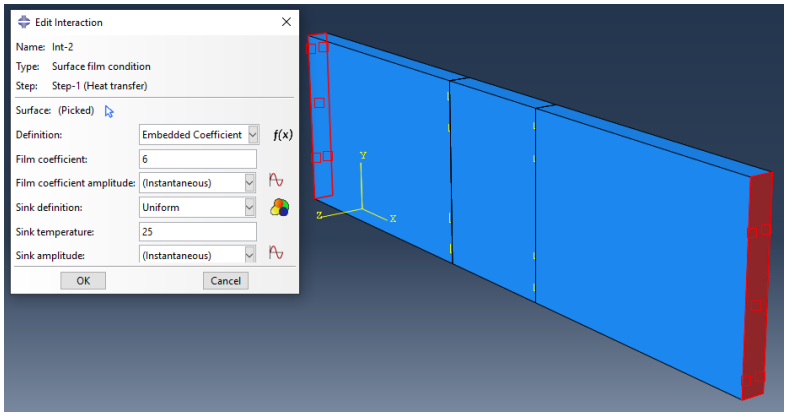

Figure 17: Convectional boundary conditions applied to the ends of the plate to obtain a one-dimensional heat transfer.

The boundary temperature (T_s) at steady state can be determined by the following equation,

$$T_s = T_\infty + \frac{\dot{q}L}{h}$$

Where T_∞ is the ambient temperature, $\dot{q}$ is the BHF value for the heat source, L is the size of the heat source, and h is the convectional coefficient. Since there is no inflow of energy into the plate, the energy generated by the heat source will be equal to the outflow energy.

$$T_s = 25 + \frac{\frac{6 \times 10^5}{2} \times 0.03}{50} = 205°C$$

Convectional Coefficient $W/m^2°C$	FEA – Steady State		Calculated – Steady State
	Temperature – °C	Approx. Time to Steady State	Temperature – °C
6	1525	350x10^3 seconds	1525
50	205	70 x10^3 seconds	205
300	55	12 x10^3 seconds	55
600	40	7 x10^3 seconds	40
1000	34	4 x10^3 seconds	34

Table 3: Parameters involved in the convection analysis and calculated steady state temperatures.

The steady state temperature in the FEA simulation was obtained as $34℃$ whereas the calculated temperature is also $34℃$. Using the calculated heat flux and boundary temperature, the temperature profile is determined using the Fourier's law. The Figure 20 shows linear temperature distribution inside the whole plate and is illustrating the intersection point, which obviously would be the centre point of the whole plate.

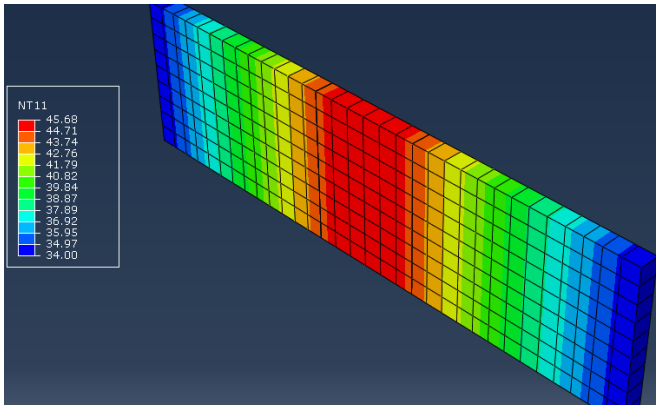

Figure 18: FEA simulated temperature distribution with internal heat generation.

In Figure 18, the plate illustrated is at steady state of the heat transfer process and the boundary temperature is $34℃$ whereas the convectional coefficient is maintained at $1000\ W/m^2℃$.

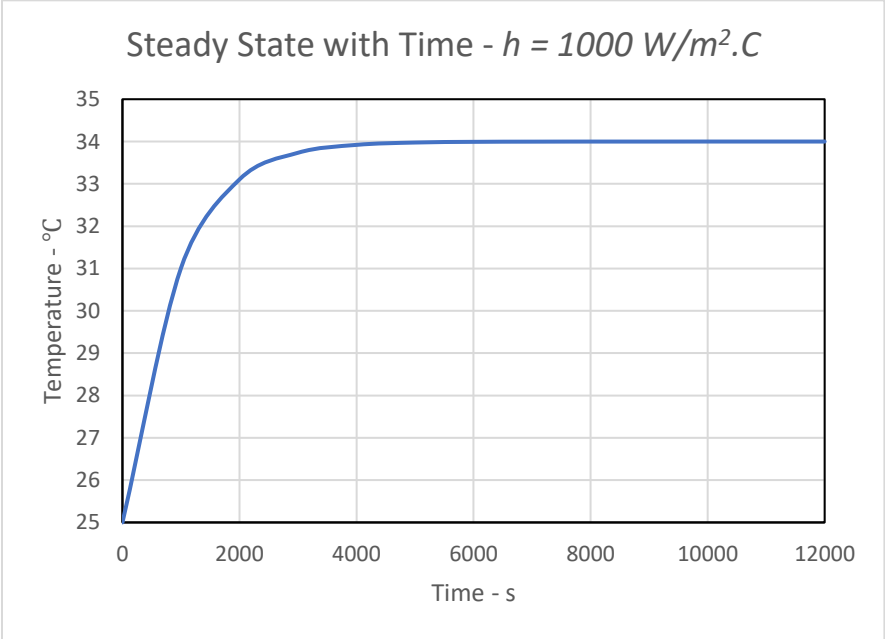

Figure 19: Steady state being reached at the boundary extracted from FEA simulation.

To show the steady state being reached in the FEA simulation is supported by the Figure 19, the maximum temperature is $34℃$ while the calculated maximum temperature in the plate was estimated to be $45.68℃$. This

shows the results are accurate when the temperature data when the temperature measurements are only taken from one end of the plate. The temperature approaching the steady state on the boundary was estimated with the value 34℃. Since, part A and C are non-generating, the temperature profile would be linear in both, and a rearranged form of the Fourier's law can be used to determine the temperature profile. Both parts are then considered 30mm wide, the temperature at 30mm from both boundaries and in between distances is given by,

$$q" = -k\frac{\Delta T}{\Delta x}$$

$$T = \frac{q"}{k} \times L + T_B$$

$$T_A = \frac{9000}{52} \times 0.06 + 34 = 44.385℃$$

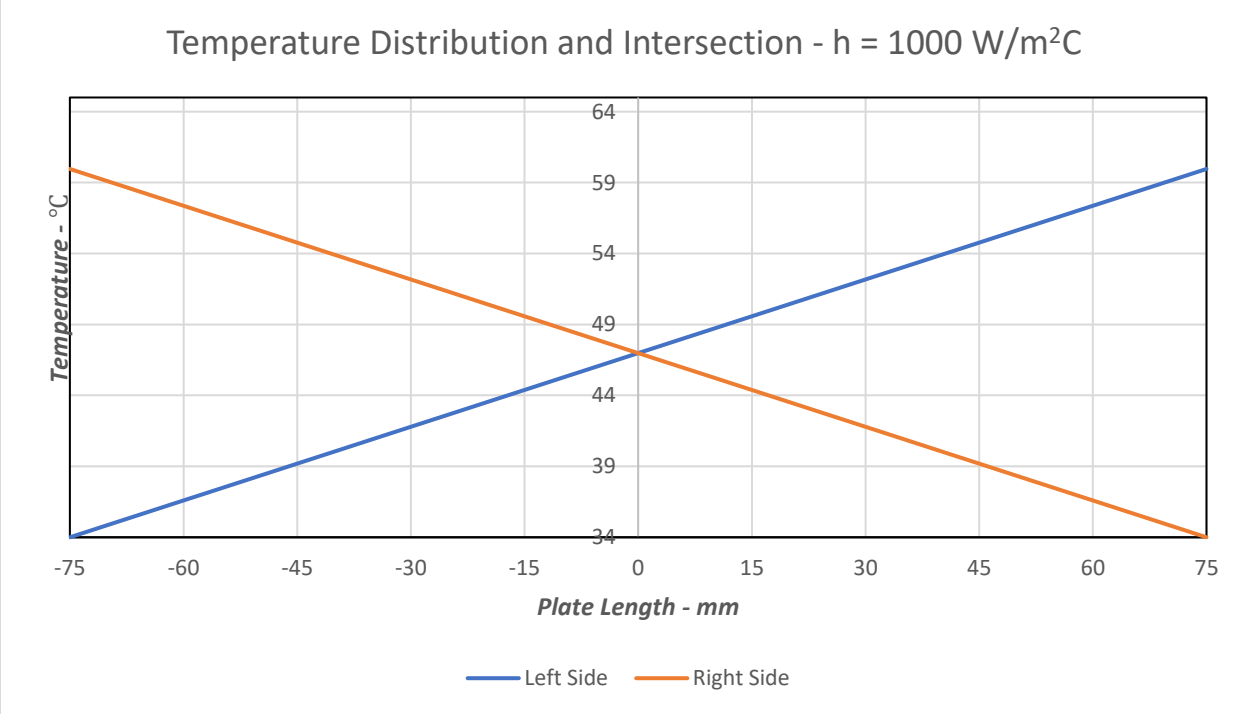

Figure 20: Linear temperature distribution calculated from both boundaries and intersection point is shown.

These steps allow to determine the linear temperature profile within the non-generating parts of the plate. However, the heat source body will not possess a linear distribution, therefore, the governing Eq. 15 for the heat source's temperature distribution is,

$$T(x) = -\frac{\dot{q}}{2k}x^2 + C_1x + C_2$$

C1 and C2 are the boundary condition of the heat source, in this case, the temperature calculated at 30mm away from both boundaries will be used to fully determine the temperature profile in the generating part B.

$$T(x) = \frac{\dot{q}\mathrm{L}^2}{2k}\left(1 - \frac{x^2}{L^2}\right) + \frac{T_{s,2} - T_{s,1}}{2}\frac{x}{L} + \frac{T_{s,1} + T_{s,2}}{2}$$

Additionally, the centre point is considered as origin point on the axis. This means 30mm of the heat source's length is extending on both side of the origin. The temperature values determined at 30mm from each boundary is,

$$T(-0.015) = 44.38 \; and \; at \; T(0.015) = 44.38$$

When values are substituted in the equation, the outcome is,

$$44.38 = -\frac{6 \times 10^5}{2 \times 52}(-0.015)^2 + C_1(-0.015) + C_2$$

Rearranging this equation to make C2 the subject gives,

$$C_2 = 45.648 + 0.015C1$$

Substituting C2 back in Eq. 15 and taking $x = 0.03$ gives,

$$44.38 = -\frac{6 \times 10^5}{2 \times 52}(0.015)^2 + C_1(0.015) + 45.648 + 0.015C1$$

$$C_1 = 0$$

When C1 and C2 are substituted by the surface temperatures of the heat source, the equation takes the following form and represents the temperature distribution within the heat source body,

$$T(x) = -5769.23x^2 + 45.68$$

$$T(max) = 5769.23(0)^2 + 45.68 = 45.68℃$$

Combining the heat diffusion equation for the heat source and basic Fourier's law for non-generating parts, temperature distribution inside the plate can be fully put together. The calculated temperature distribution inside the plate and FEA simulated temperature distributions are plotted together on Figure 21 to compare the obtained results.

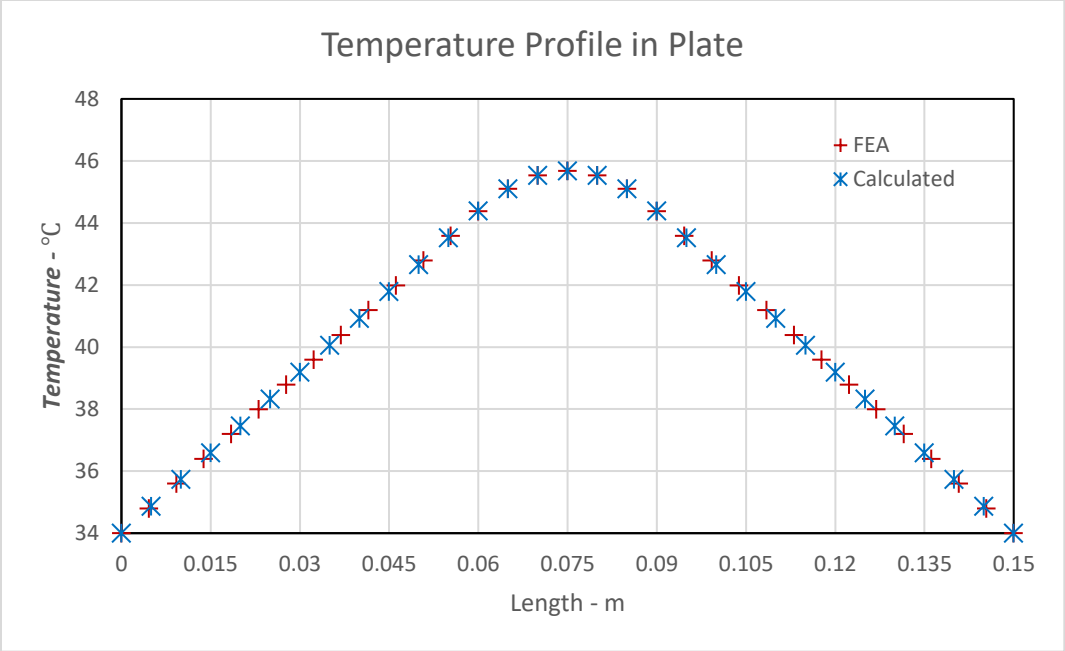

Figure 21: Steady state one-dimensional temperature profile – Numerical and Analytical Approach

The estimated location and strength of the heat source, and the temperature field in the plate is in good correlation with the values extracted from the FEA simulated heat transfer in the plate. The temperature field is plotted in Figure 21 together for both the calculated and FEA.

5.2.3 Non-Centrally Positioned Heat Source in a Steady State Problem

In this section, the distance to the heat source determined by measuring temperature change at one end of the plate. Initiating by conducting an FEA simulation, the heat source and the plate is simulated until it reaches the steady state.

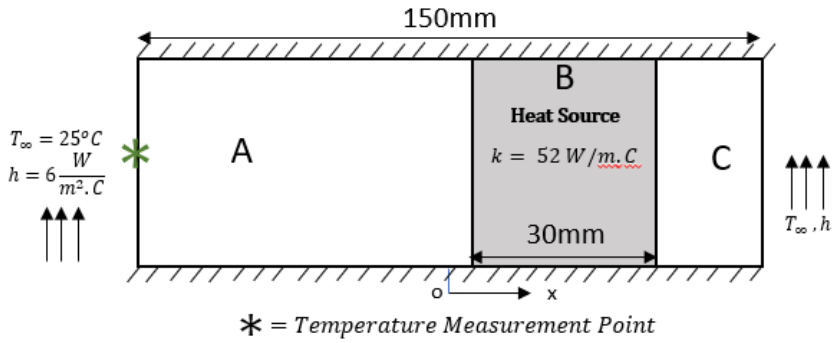

Figure 22: Schematic diagram of a non-centrally positioned heat source within a one-dimensional plate.

Although, the temperature data extracted from the FEA simulation will be only from one boundary and the position is illustrated in the schematic Figure 22 as '*'. Distance from both boundaries to the heat source will be determined. At '*' position, the steady state temperature will be obtained from the FEA simulated data. The transient temperature data can also be used to estimate the strength of the heat source as previously shown in the section 5.2.1. Otherwise, if the strength is considered as a known value, then only steady state temperature is sufficient to predict the location. The known parameters include the total length of the plate, dimensional size of the heat source body, material properties, ambient temperature, and convectional coefficient. Using the known parameters, the steady state temperature at the '*' position is calculated using the following expression,

$$T_s = T_\infty + \frac{\dot{q}L}{h}$$

Where T_∞ is the ambient temperature, $\dot{q}$ is the BHF value for the heat source, L is the size of the heat source, and h is the convectional coefficient.

Known Parameters	***Values***
Total Length	150mm
Heat Source	30mm
Ambient Temperature	25 °C
Convectional Coefficient	6 W/m^2 C
Body Heat Flux	600000 W/m^3

Table 4: Known parameters for estimating the location of a non-centrally positioned heat source.

However, the steady state temperature is extracted from FEA simulation to use as a reference value to correlate with the calculated one. Figure 23 shows the temperature distribution in the plate at steady state and the temperature at the near end of the plate is $1530.1℃$.

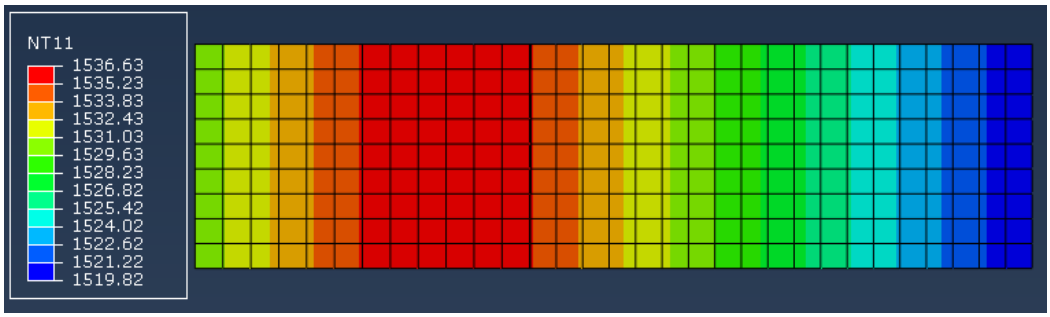

Figure 23: FEA simulated temperature distribution within the plate at steady state of the heat transfer.

The transient temperature profile at the position is also plotted to demonstrate system reaching the steady state in Figure 24.

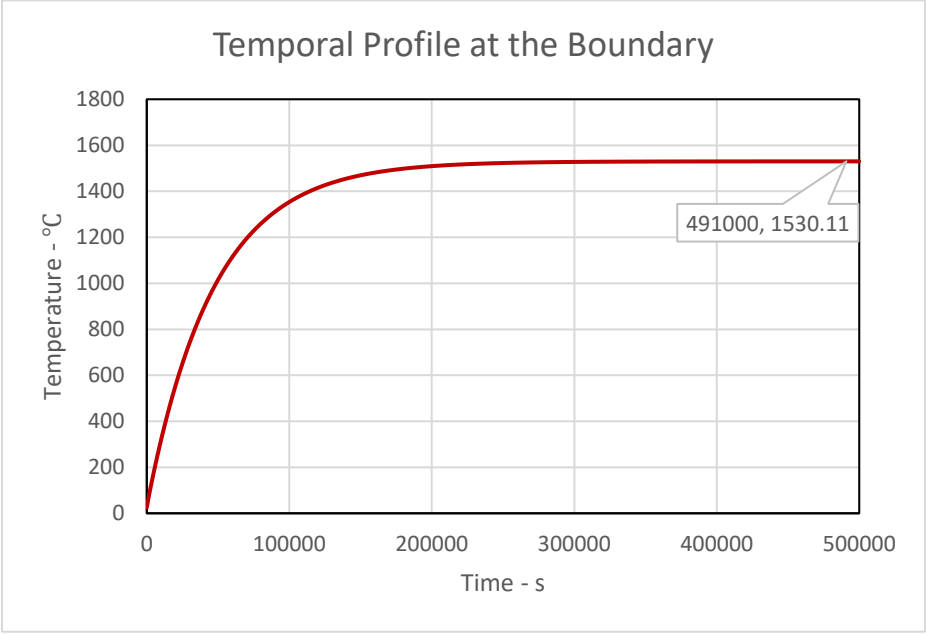

Figure 24: Transient temperature at the position '*' reaching the steady state obtained from FEA simulation.

Using the following equation to calculate the steady state temperature at the boundary while reducing the body heat flux value with various ratios and the one that matches closest to the FEA steady state temperature is at 0.502 of the total body heat flux which gives the temperature value,

$$T_s = 25 + \frac{301200 \times 0.03}{6} = 1531℃$$

Ratio	*BHF – W/m³*	*Steady State Temperature* - ℃
1	600000	3025
0.502	301200	1531
0.498	298800	1519

Table 5: Steady state temperature at the boundary and the corresponding ratio of the body heat flux.

Now calculating the surface heat flux of the body heat source,

$$q^{"} = \dot{q}L = 600000 \times 0.03 = 18000\ W/m^2$$

Multiplying the surface heat flux with the corresponding ratios gives heat flux in each direction,

$$q^{"} = \dot{q}L = 18000 \times 0.502 = 9036\ W/m^2$$

$$q^{"} = \dot{q}L = 18000 \times 0.498 = 8964 W/m^2$$

Using the Fourier's Law and the heat flux at each boundary, the linear temperature profile from both sides, A and C, can be plotted to find the intersecting point.

$$q" = -k\frac{\Delta T}{\Delta x}$$

$$T = \frac{q"}{k} \times L + T_B$$

$$T_c = \frac{9036}{52} \times 0.15 + 1530.11 = 1556.18℃$$

$$T_A = \frac{8964}{52} \times 0.15 + 1519.8 = 1545.66℃$$

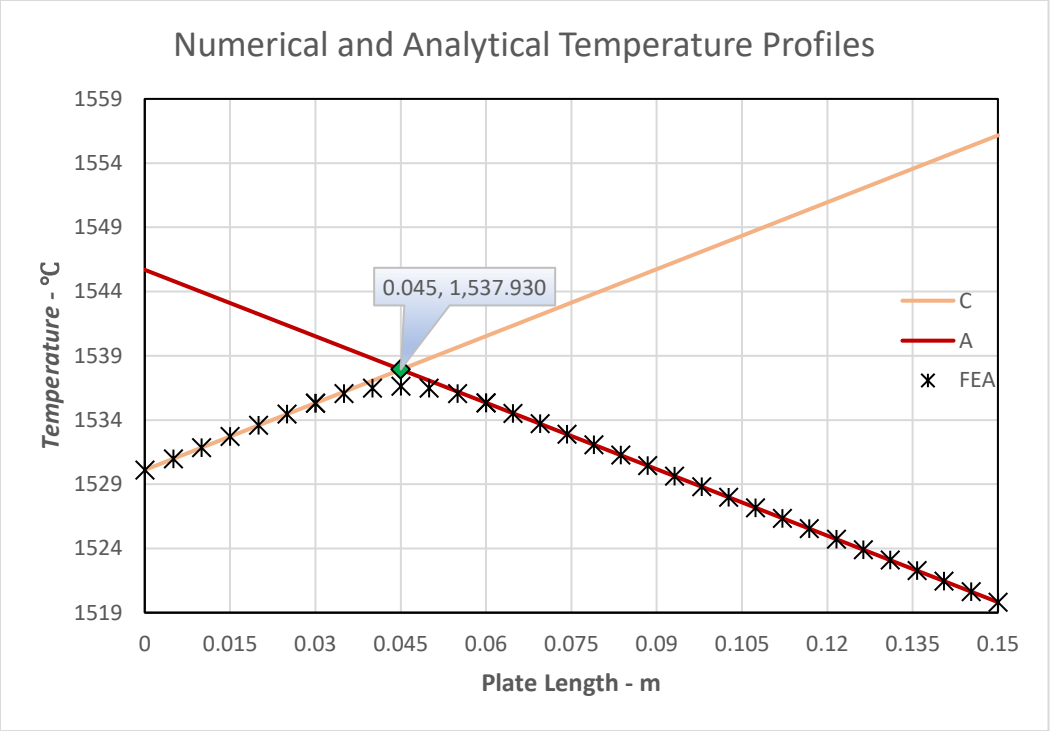

Figure 25: Temperature profiles plotted for FEA simulated results and calculated using Fourier's law in one-dimensional plate.

The intersecting point in Figure 25 is 45mm and 105mm from both ends and represents the central point of the heat source body. From the intersecting point, the body of the heat source extends 15mm in each direction. And the temperature profile within the heat source body can be determined using the following expression,

$$T(x) = \frac{\dot{q}\mathrm{L}^2}{2k}\left(1 - \frac{x^2}{L^2}\right) + \frac{T_{s,2} - T_{s,1}}{2}\frac{x}{L} + \frac{T_{s,1} + T_{s,2}}{2}$$

Where $T_{s,1}$ and $T_{s,2}$ are the temperatures at the surface of the heat source body and can be extracted from the linear temperature profile.

5.2.4 Heat Source Location in One-Dimension

Final investigation is carried in this section which will conclude the one-dimensional steady state conductional heat transfer. The solutions are obtained following the same steps applied in section 5.2.3 to further investigate factors that could influence the accuracy of the results obtained so far, this section will include changing the location of the internal heat source within the plate and altering the dimensional size of the heat source body as well. Likewise, in this study the estimation for the unknown location is determined by utilising only one side of the plate and measuring the temperature at the boundary position - (*A*). The transient temperature data is

extracted from the FEA simulation to estimate the strength of the heat source body. Additionally, the dimensional size of the heat source is a known parameter in each case under study.

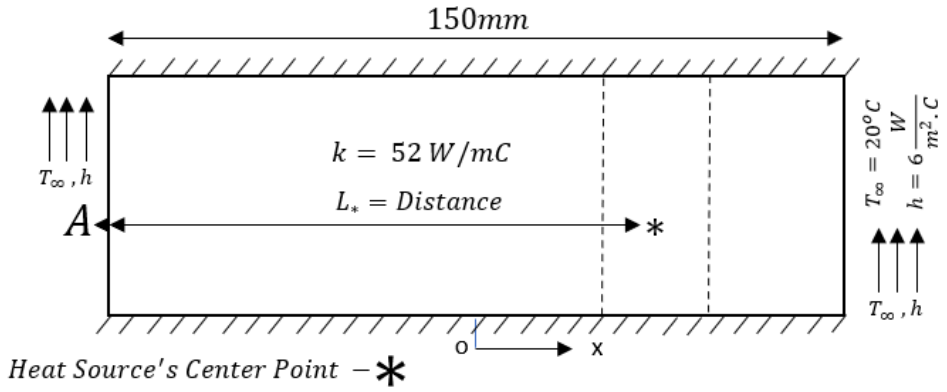

Figure 26: Schematic diagram for the inverse heat conduction problem.

The total length of the plate is an unchanged parameter in the analysis whereas, the position of the internal heat source is varied in each simulation. From the observing boundary (*A*), L_* is the unknown distance to the centre point of the heat source body. The approach for the solution of this problem is to measure the temperature as the plate approaches the steady state. The internal heat source is positioned at different distances from the observing boundary and the unknown length to its centre from the boundary is estimated. The investigation is conducted for nine different positions of the internal heat source as illustrated in

Known Parameters	***Values***
Total length	150mm
Thermal conductivity	52
Convection coefficient	100
Body heat flux	600000
Heat source length	30mm
Ambient Temperature	25

Table 6: Known parameter for estimating the various positions of the heat source using boundary temperatures – One Dimensional.

$$T_s = T_\infty + \frac{\dot{q}L}{h}$$

Where T_∞ is the ambient temperature, $\dot{q}$ is the BHF value for the heat source, L is the size of the heat source, and h is the convectional coefficient.

Steady state temperature calculated for the first situation where central point of the heat source is at 30mm from the boundary,

$$T_s = 25 + \frac{322800 \times 0.03}{100} = 121.84℃$$

Ratio	***BHF – W/m³***	***Steady State Temperature -*** ℃
1	600000	205
0.538	301200	121.84
0.462	277200	108.16

Table 7: Steady state temperature at the boundary and the corresponding ratio of the body heat flux.

Actual Distance L_*- mm	***FEA Steady State – Boundary Temperature***	***Calculated Steady State – Boundary Temperature***
30	121.81	121.84
40	119.97	119.95
50	118.45	118.42
60	116.94	116.98
70	115.42	115.45
80	114.58	114.55
90	113.06	113.02
100	111.55	111.58
110	110.03	110.05

Table 8: Steady State temperatures at the boundary for various positions of the heat source – Calculated and FEA simulated values.

The results obtained and displayed in table 8 are plotted in Figure 27 which illustrates the steady state temperature for FEA and the corresponding temperature obtained through hand calculations.

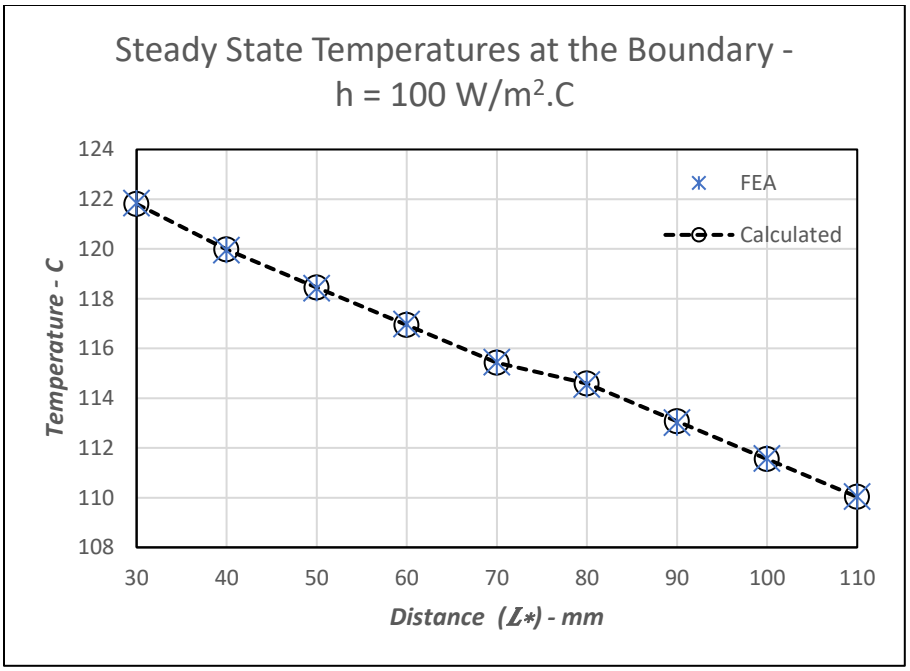

Figure 27: Steady state temperature at the boundary from FEA and calculated.

Calculations to plot the linear temperature distribution within the plate using the Fourier's law in the case where heat source is 30 mm away from the temperature measurement boundary.

$$T = \frac{q"}{k} \times L + T_B$$

$$T_A = \frac{9680.67}{52} \times 0.03 + 121.84 = 127.42℃$$

$$T_C = \frac{8319.33}{52} \times 0.12 + 108.16 = 127.35℃$$

The estimation to the distance of internal heat source in a one-dimensional heat transfer under steady state is concluded with these last calculations. Various distances were tested in the FEA simulation, and each one of them are calculated from only end of the plate. The result for one case of 30mm away heat source is illustrated in the Figure 28. The rest of the distances are also determined using the same steps are the accuracy for each distance is concluded in Figure 29. The results and the approach in a steady state one-dimensional heat transfer with utilising temperature measurements at only one end of the plate are very accurate and robust.

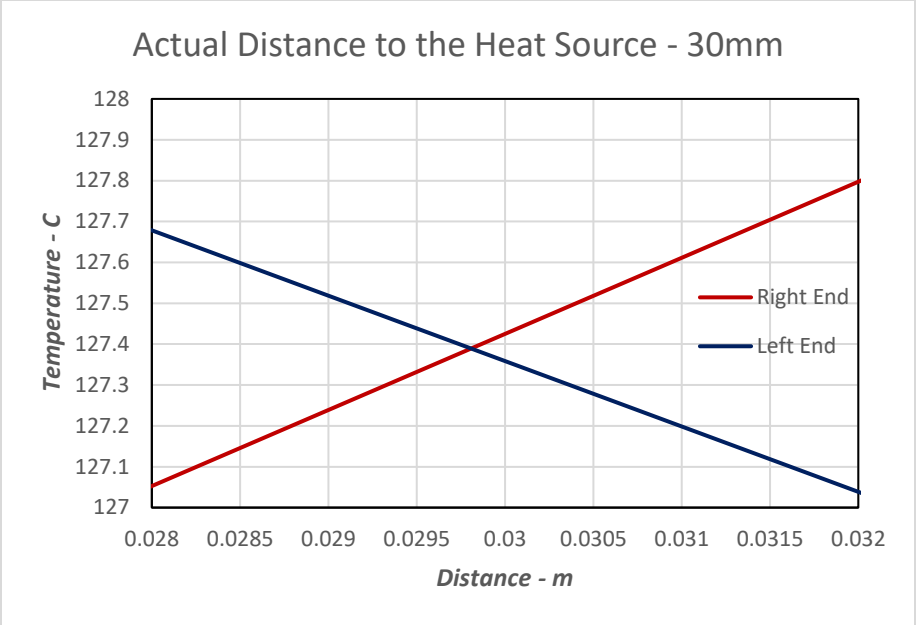

Figure 28: Intersecting point represents the central position of the internal heat source from each end of the one-dimensional plate.

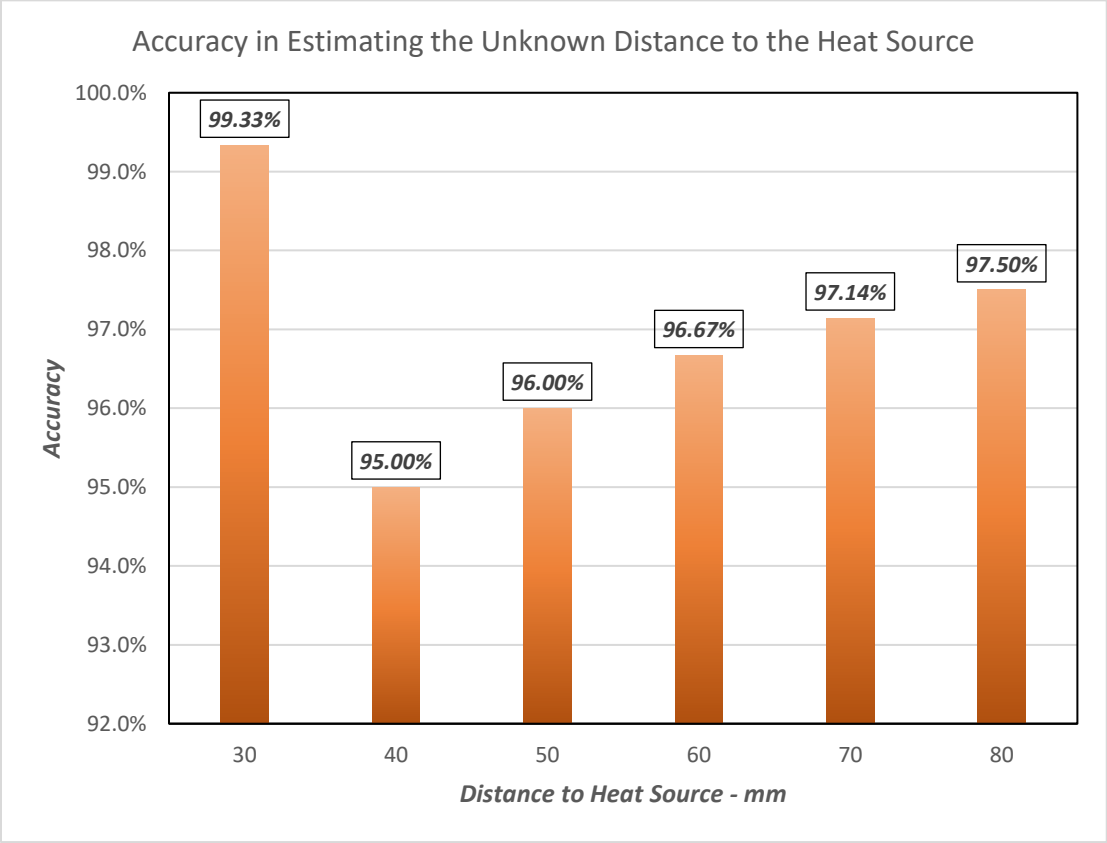

Figure 29: Estimation of distance to the heat source from the boundary of the one-dimensional plate.

5.3 One-Dimensional Thermal Experiment

The heat transfer in a solid induced by a heat source is investigated by setting up an experimental analysis. The setup included the use of a steel plate, heat source, power supply, thermal imaging camera, insulation and masking tape, and ambient temperature sensors. In Figure 30, thermal imaging camera is setup perpendicular to the steel plate. An aluminium heat source is attached to the backside of the steel plate with the use of an epoxy. The power to the heat source is controlled via a power supply monitoring the constant current and voltage supplied to the heat source. The temperature data is captured and recorded by utilising a thermal imaging camera (A615) and its accompanying software called ResearchIR. The power supply's accuracy is tested by connecting a multimeter to it and checking against current and voltage, and the thermal imaging camera has the accuracy of $\pm\ 2℃$ and thermal sensitivity of $< 0.05℃$. For further comparison, a thermocouple is attached to the heat source to monitor its temperature through a temperature controller.

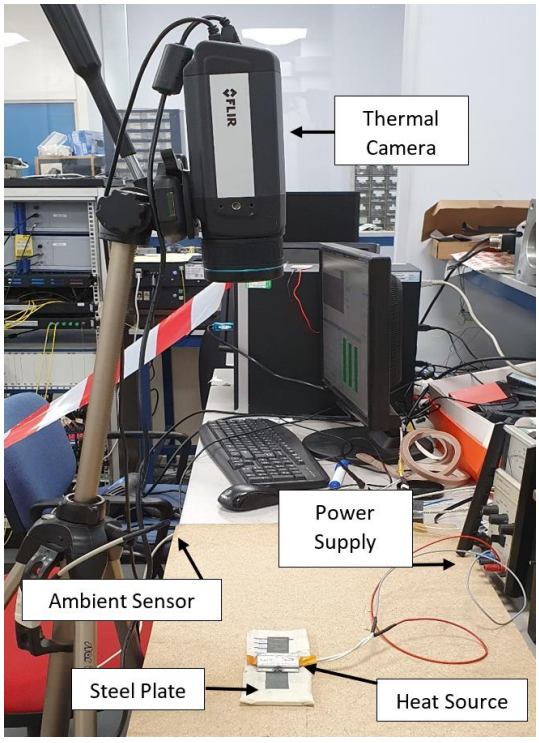

Figure 30: Thermal Experimental Setup.

The experiment is conducted for various positions of the heat source which is attached to the backside of the steel plate. While the top and bottom side of the plate is insulated to obtain a one-dimensional heat transfer. The thickness of the plate is 4mm so temperature variance in that direction is negligible. The heat source is kept on for 720 seconds with a constant power and the recorded temperature data is extracted from the thermal imaging software to plot the temporal profile for further analysis and calculations.

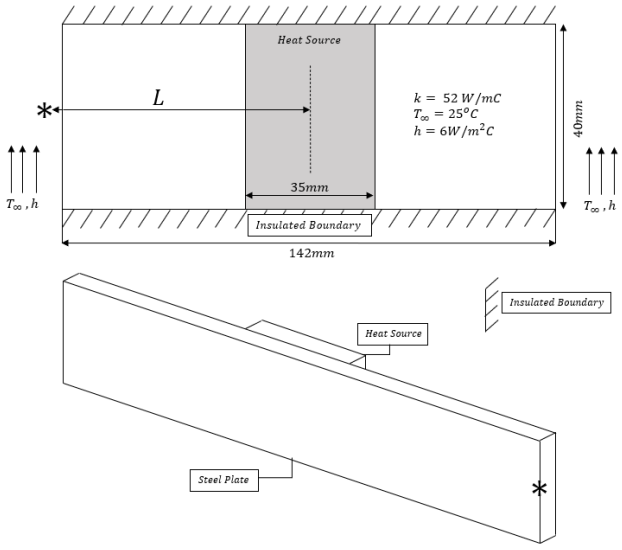

Figure 31: Schematic Diagram illustrating the position of the heat source and steel plate for thermal experiment.

After obtaining the thermal imaging data for the experiment, temperature snapshots are also plotted for four stages as they are illustrated in Figure 32, these are captured by the thermal imaging camera. The temperature profiles across the face of the steel plate for initial stage at the start of the experiment and through different intervals of time untill it reaches 1200 seconds of the experiment is also plotted in Figure 33 for better presentation of temperature change with time.

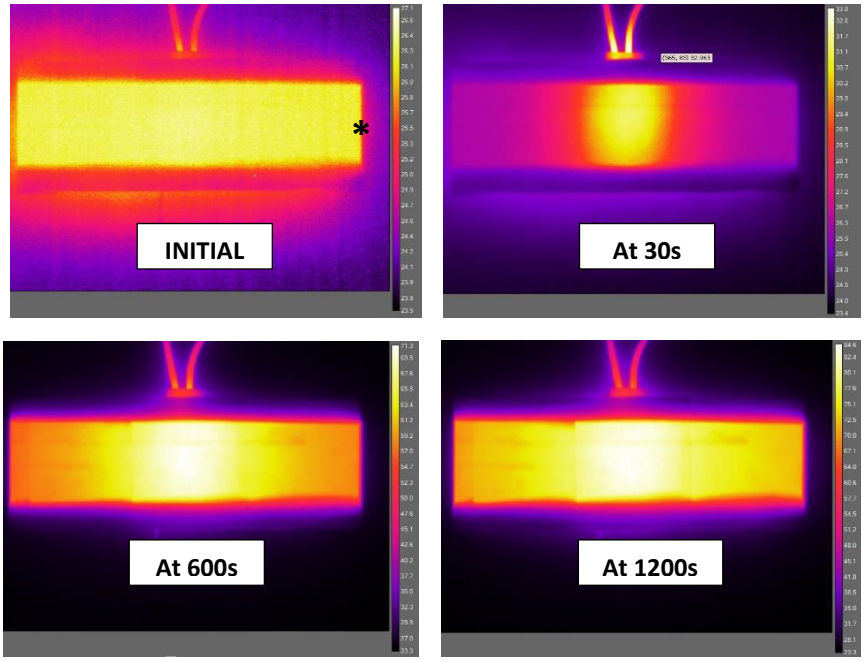

Figure 32: Instances from heat transfer experiment on a steel plate, illustrating from initial stage up until 1200 seconds.

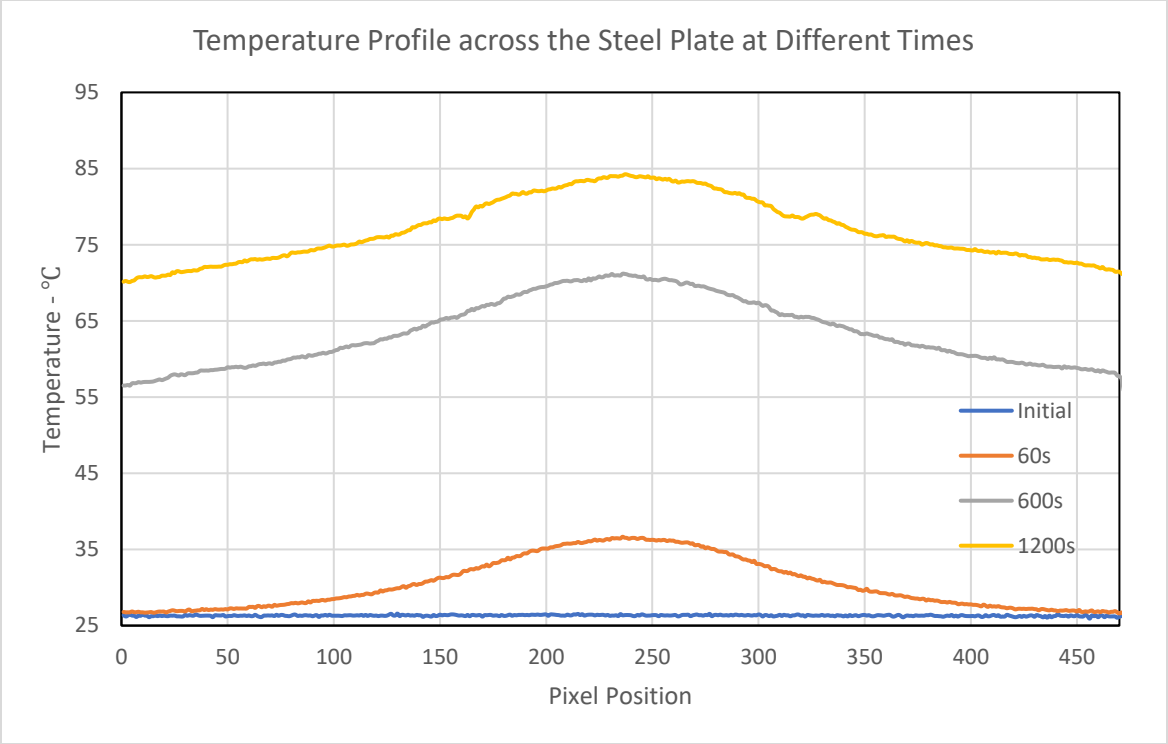

Figure 33: Temperature profile across the surface facing thermal camera for four stages such as initial up until 1200 seconds of heat transfer in the steel plate.

In Figure 33, at the initial stage the temperature across the whole steel plate is at $\approx 26℃$. The next is after 60 seconds have passed on, this curve clearly shows higher distribution in the central region of the plate whereas the edges are not yet highly induced. Although, after much of the time has passed, the temperature across the whole steel plate is risen to a maximum of $\approx 71℃$ whereas at both edges is $\approx 56℃$. The same profile with approximately similar temperature difference at 1200 seconds exists, at this point the maximum temperature at the central region is $\approx 84℃$ and at the edges $\approx 70℃$. However, the interest of this research is at the boundary of the plate and its temporal profile. As shown in Figure 27, the steric $(*)$ point on the edge of the steel plate will be of investigation this point forward. For various position of the heat source attached to the plate, the temporal profile for the boundary point will be plotted and investigated how it varies with respect to the

position of the heat source. The distance ‘L’ is to the centre point of the heat source from the observing position (∗) and will be changed each time the heat source is relocated.

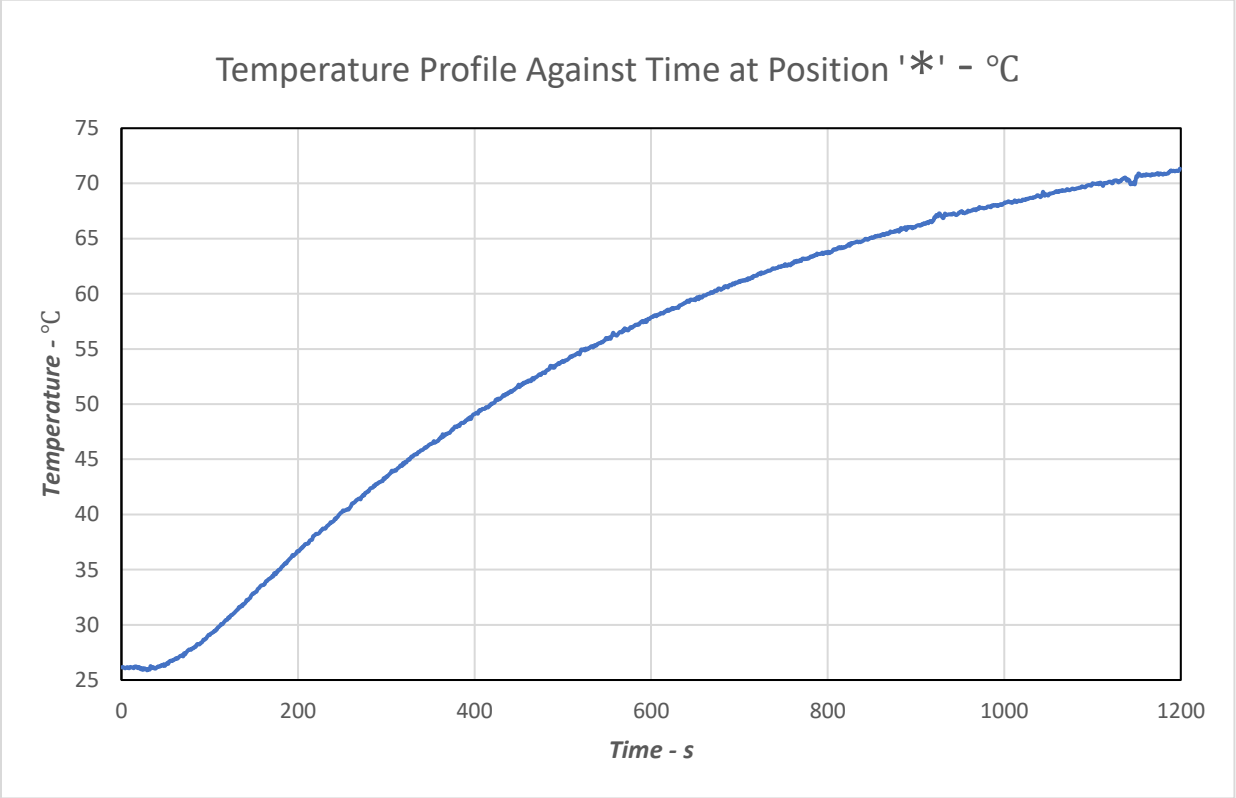

Figure 34: Temperature change at the boundary of the steel plate when the heat source is centrally positioned.

Figure 34 shows the induced temperature change with time due to the presence of the heat source attached to the back side of the steel plate. In this case, the heat source is centrally placed on the steel plate. Therefore, the temperature change at the edge of the plate takes longer which is reflected in the trendline during the first 60 seconds of the curve.

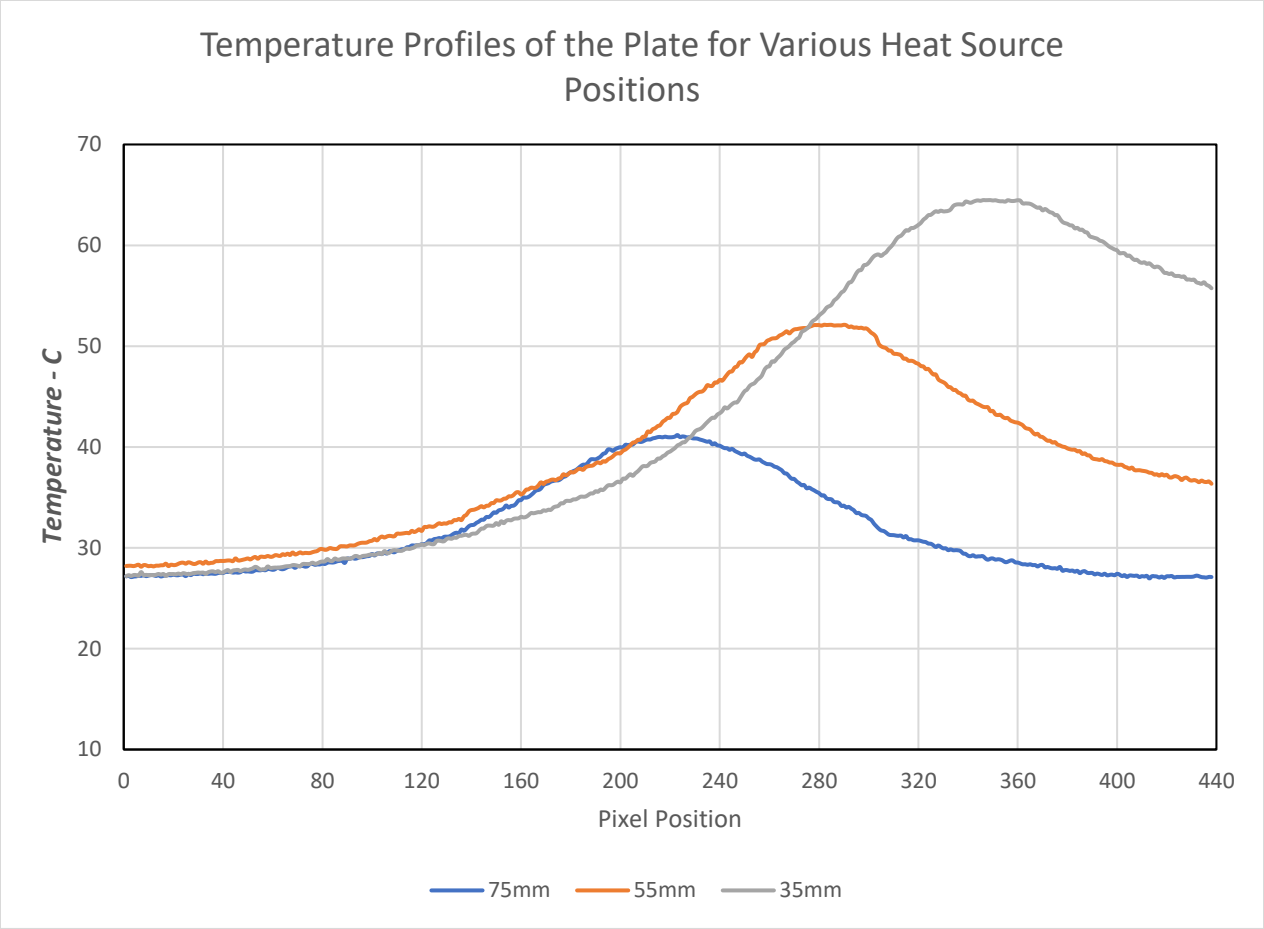

Figure 35: Three different locations of the heat source attached to the backside of the plate and the temperature profiles, respectively.

The distance of the heat source is moved closer to the edge of the plate to investigate its behaviour in the temperature profile within the plate as it being illustrated for three different positions in Figure 35. Further analysis and temperature data is obtained through FEA simulation and presented in the following section.

5.4 One-Dimensional Finite Element Analysis for the Heat Transfer

For the purposes of recreating the thermal experiment performed in the section 5.3 and for further analysis, the FEA software used is Abaqus CAE 2020. FEA allows to make more precise alterations in the placement of the heat source attached to the backside of the steel plate and efficiently simulates the heat transfer. The parameters applied to the computer aided model (CAD) of the steel plate in the simulation restricts the flow of heat transfer in one-dimension, and a comparison of the results can be made between numerical and analytical approaches. Additionally, the thermal contact conductance between the heat source and the steel plate is considered as a negligible parameter for complete transfer into the plate without any resistance or loss of heat. In Figure 36, steps to create the heat transfer simulation involved defining the surface conditions for convection,

initial temperature, ambient temperature of the surroundings, material properties, and the load of the heat source. Followed by meshing of the model. With all parameters correctly applied, the simulation computed and the results in the form of temperature profiles at various instances such as at 15 and 1200 seconds is presented where the NT11 is the temperature at that step of the heat transfer simulation.

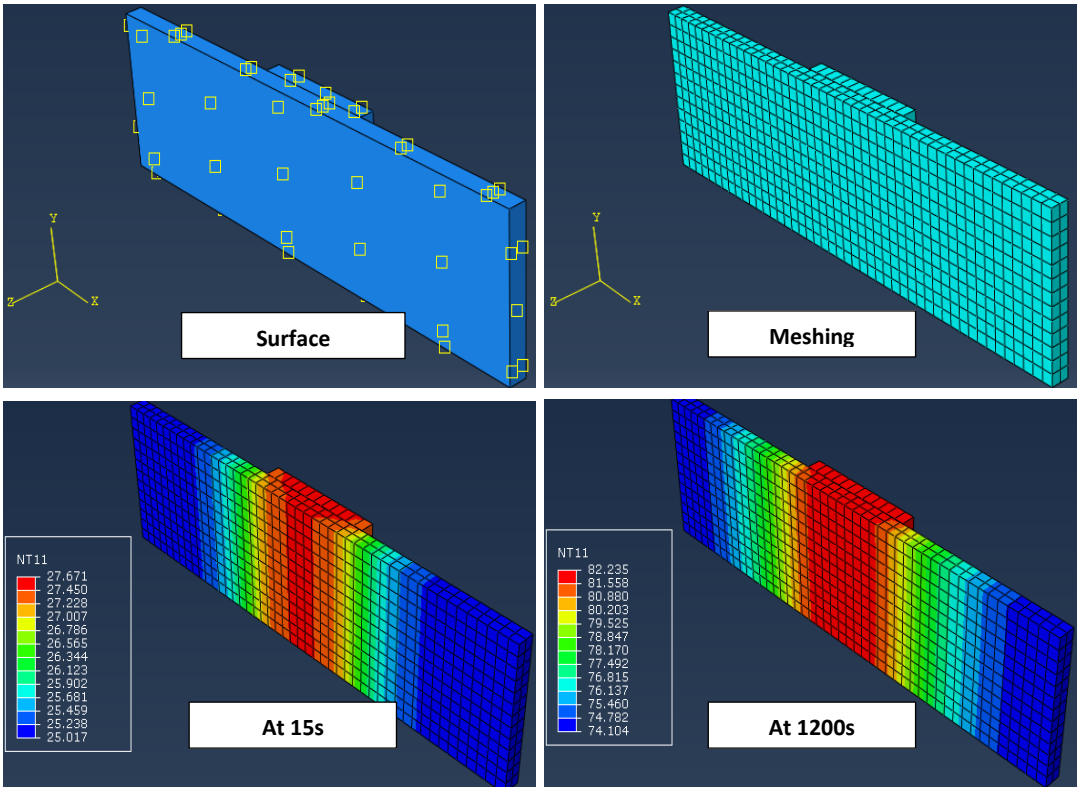

Figure 36: Finite Element Modelling of the steel plate with a heat source attached and simulated for heat transfer.

Whereas Figure 37 shows how various positions of the heat source attached to the backside of the steel plate influence the temperature at the boundary. It is obvious that if the heat source is closer to the boundary, the temperature will rise at that end. Consequently, the temperature data at the boundary is extracted to determine the distance to the heat source. Figure 38 represents the temperature profiles in the graphical format respectively as the data to plot is also obtained from the Abaqus FEA heat transfer simulation.

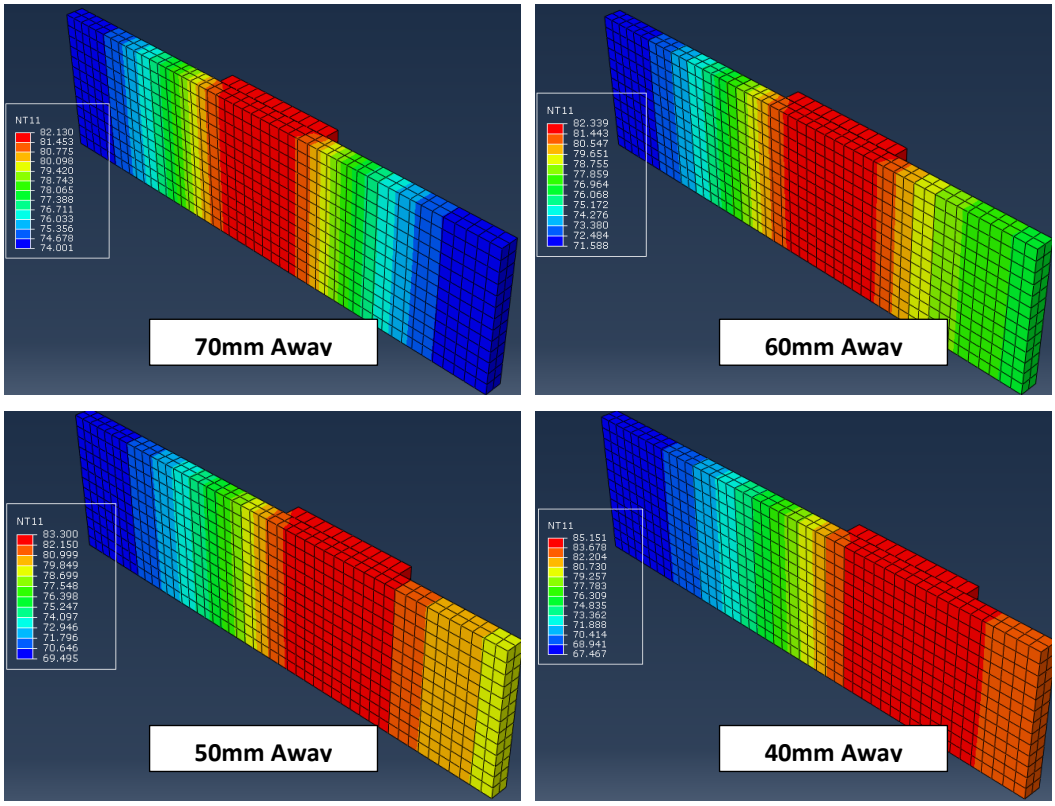

Figure 37: One dimensional heat transfer with various positions of the heat source from the near boundary of the plate.

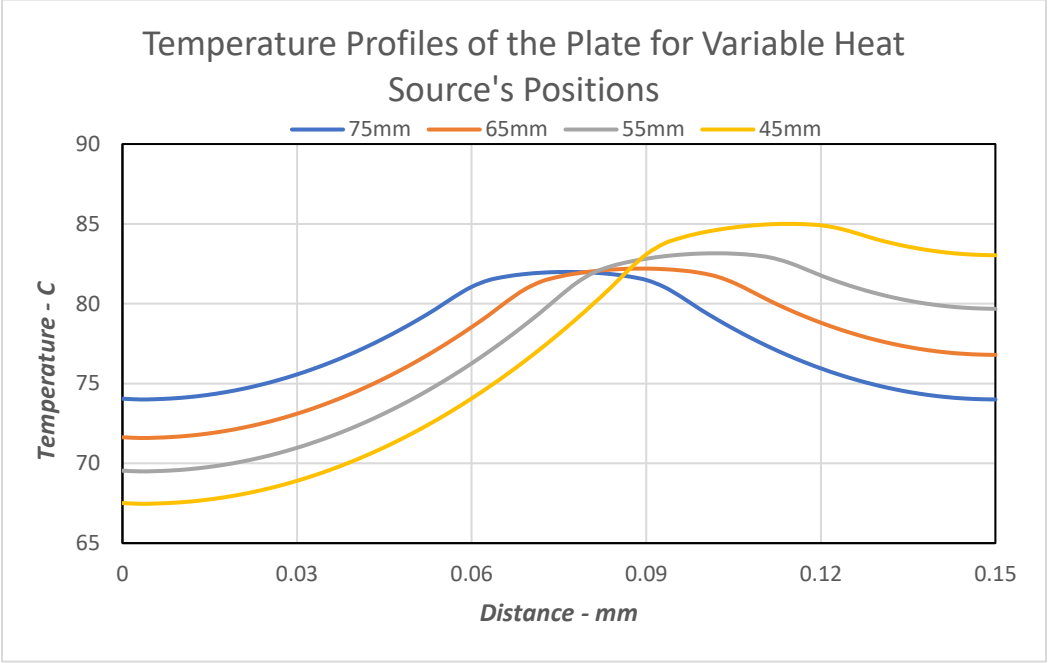

Figure 38: Temperature profile of the steel plate at 720s and with variable positions of the heat source.

Figure 38, illustrates the temperature profile in the steel plate and how it varies when the position of the heat source is altered. At 75mm the heat source is exactly positioned at the centre of the plate, the temperature profile is also symmetrical. However, as the heat source is moved away the profile becomes asymmetrical because the material of the plate is less on one side and longer on the other. This makes the shorter side become hotter as the temperature rise at the far end takes longer. Similar temperature profiles can be in the experimental data in Figure 35.

5.5 One-Dimensional Transient Heat Transfer – Parametric Analysis

In this section, the dimensional size of the heat source, convectional coefficient, the strength of the heat source is analysed in a transient heat transfer. While the unknown location and the strength is also determined utilising temperature measurements from only one boundary of the structure which is same as Figure 31. For this purpose, a Matlab code is written to compute the transient temperature profiles and plot the rate of change of temperature as well. After that, the maximum value for each curve is extracted and plotted for the respected position of the heat source. The Matlab code for all these results in added in the Appendix B – Matlab Algorithm

Since a lot of variation is required to establish different relationships among parameters and formulate a methodology applicable for the estimation of the unknown location of the heat source, the FEA software is heavily used for heat transfer simulation instead of performing thermal experiments physically. The FEA simulated data is obtained for various placements of the heat source within the structure.

Parameters Investigated in the Parametric Analysis	
Distance to the heat source from the boundary	20, 25, 35, 45, 55, 75, 85, 95, 105, 105, 115, and 130mm
Convectional Coefficient	6, 100, 1000 W/m^2.C
Strength of the Heat source	6, 9, and 18 W
Dimensional Size of the heat source	10 and 30 mm wide

Table 9: Parametric investigation of various parameters involved in a heat transfer.

The total length of the structure utilised is 150mm and the distance of the heat source from one of the boundaries is varied between 20 – 130 mm and is presented as scenario 1 – 13 in the plots, 1 being the closed to the boundary. The temperature data is obtained from only one side of the structure for all observations and illustrations. The transient temperature profiles at the boundary for each scenario is plotted in Figure 39 using three different convectional coefficients, presented on the left side. Whereas on the right side within the Figure 39, curves plotted represent the rate of change of temperature in each case.

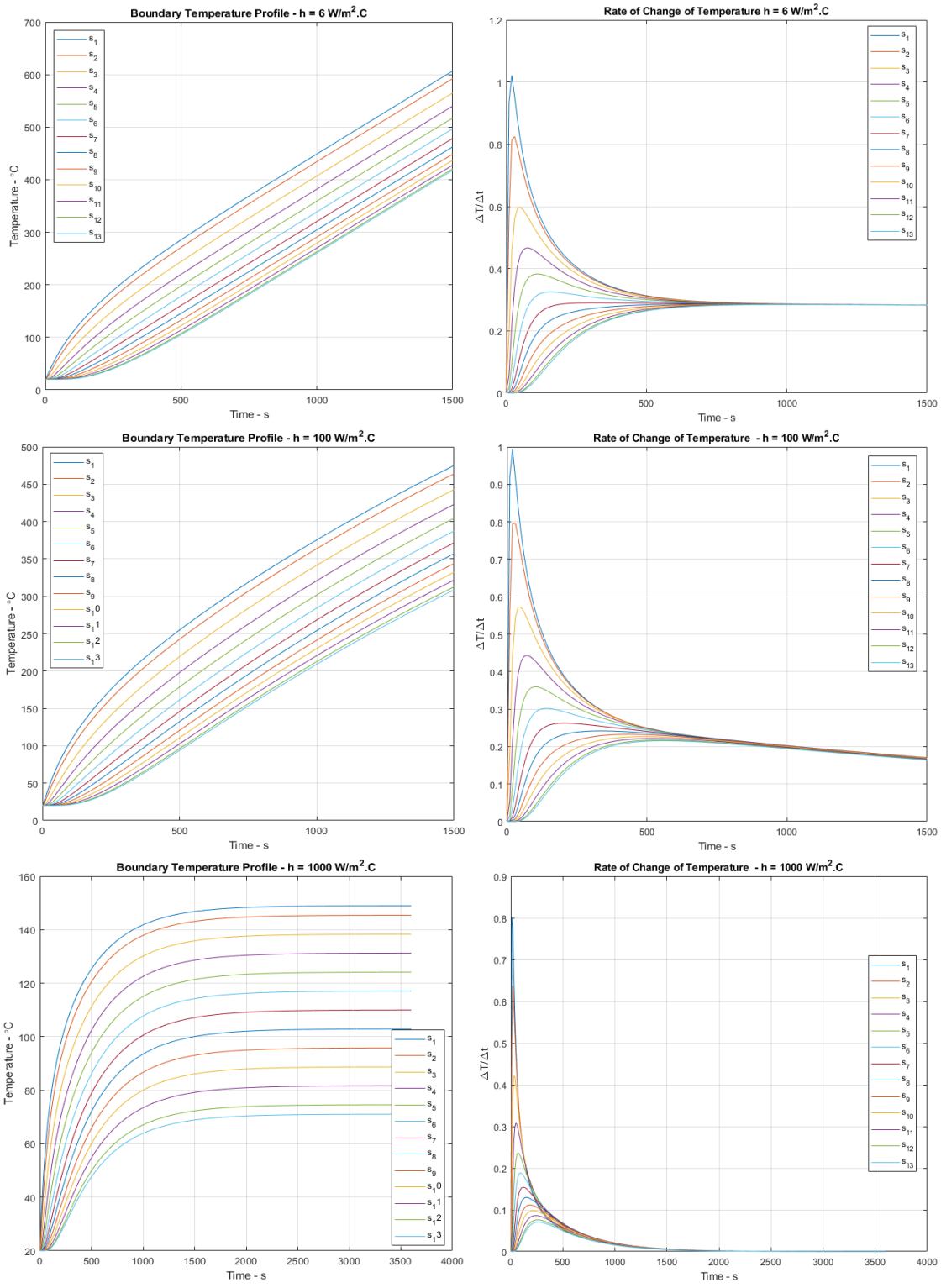

Figure 39: FEA simulated transient temperature profiles at the boundary for 13 different positions of the heat source and the rate of change of temperature curves.

As the Figure 39 illustrates the rate of change of temperature on the right side, and it was observed that these curves follow a similar pattern, a relationship is deduced here between rate of change and the relevant location of the heat source. The maximum rate of change of each curve for each convectional coefficient is extracted and plotted against the distance. When the convection is high such as $1000\ W/m^2.C$, the temperature in the structure rapidly approaches the steady state of heat transfer. Which is also reflected in the rate of change plots where the curves sharply depreciate to zero. However, since the strength of the heat source is kept unchanged in all three cases, the influence of convectional coefficient on the maximum rate of change of temperature at the boundary is negligible. Therefore, a further study is conducted on the dimensional size and power of the heat source.

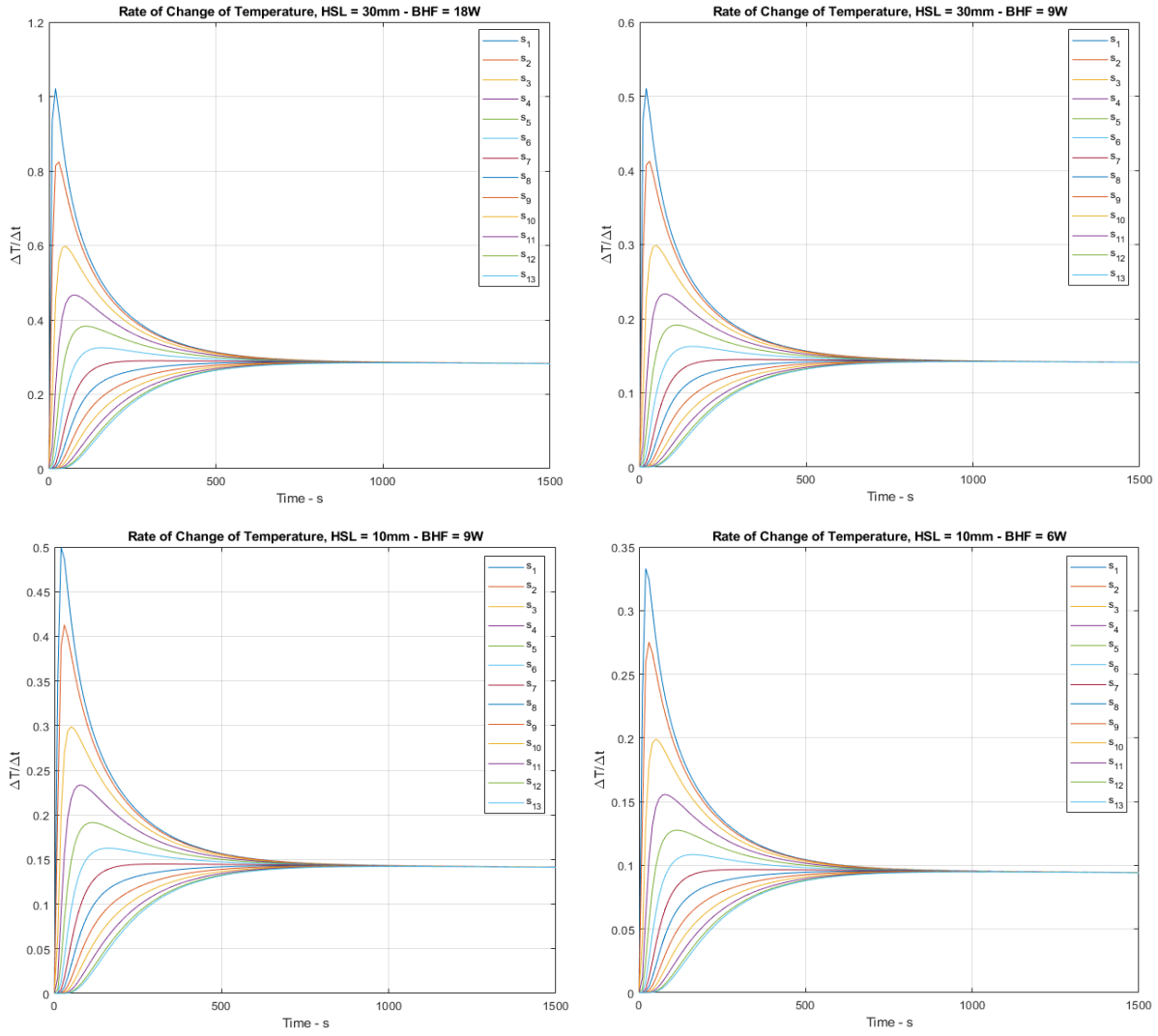

Figure 40: Rate of change of temperature for 30 and 10mm wide heat source with power of 18, 9, and 6W.

Figure 40 represents the rate of change of temperature with natural convection applied to the surface of the structure. The strength is half in one of the cases which can be seen in the outcome as the rate of change of temperature. It is noted that for the first six positions of the heat source (20 – 65 mm) the trendline for the rate of change of temperature has a peak between the range 0 – 200 seconds. This also indicates that the heat source is nearer to the boundary.

The first graph on top left within Figure 40 represent when heat source length (HSL) is 30mm and the power of 18, this produces the maximum change of $\frac{\Delta T}{\Delta t} \approx 1℃/s$ for when the heat source is 20 mm away from the boundary. Whereas, with half the strength of heat source at the same distance generates maximum rate of change of $\frac{\Delta T}{\Delta t} \approx 0.5℃/s$ since the power of the heat source is also reduced by half to 9 Watts. However, the dimensional size of the heat source plays negligible role, since the bottom left graph represents the rate of change of temperature when the length of the heat source is 10 mm, and the power is 9 Watts. The comparison between the 30mm and 10mm wide heat sources when the power is same for both shows that they can generate same rate of change of temperature regardless of their volumetric size. This is further established when one third power of the first case (18W and 30mm) is applied to a 10 mm wide heat source. The bottom right graph in Figure 40, represents the change in temperature with the internal heat source of 6 Watts and 10 mm wide. The maximum $\frac{\Delta T}{\Delta t} \approx 0.33℃/s$ which is one third of the maximum change generated by an 18 Watts heat source. These key observations are summarised in Table 10, analysis on the strength and size of the heat source was conducted for 13 different placements of the heat source whereas the temperature measurements are again only extracted from one boundary of the structure.

Heat Source Size	***Heat Source Strength***	***Maximum $\frac{\Delta T}{\Delta t}$ from 20 mm***	***Reduction Percentage***
30 mm	18 W	1.0217	100%
	9 W	0.5109	50%
10 mm	9 W	0.4994	100%
	6 W	0.3329	66%

Table 10: Parameters investigated in a transient heat transfer parametric study.

In this analysis, the overall length of the structure is not changed along with material properties, convection coefficient etc. The only variables were the dimensional size and power of the heat source, and location of the heat source.

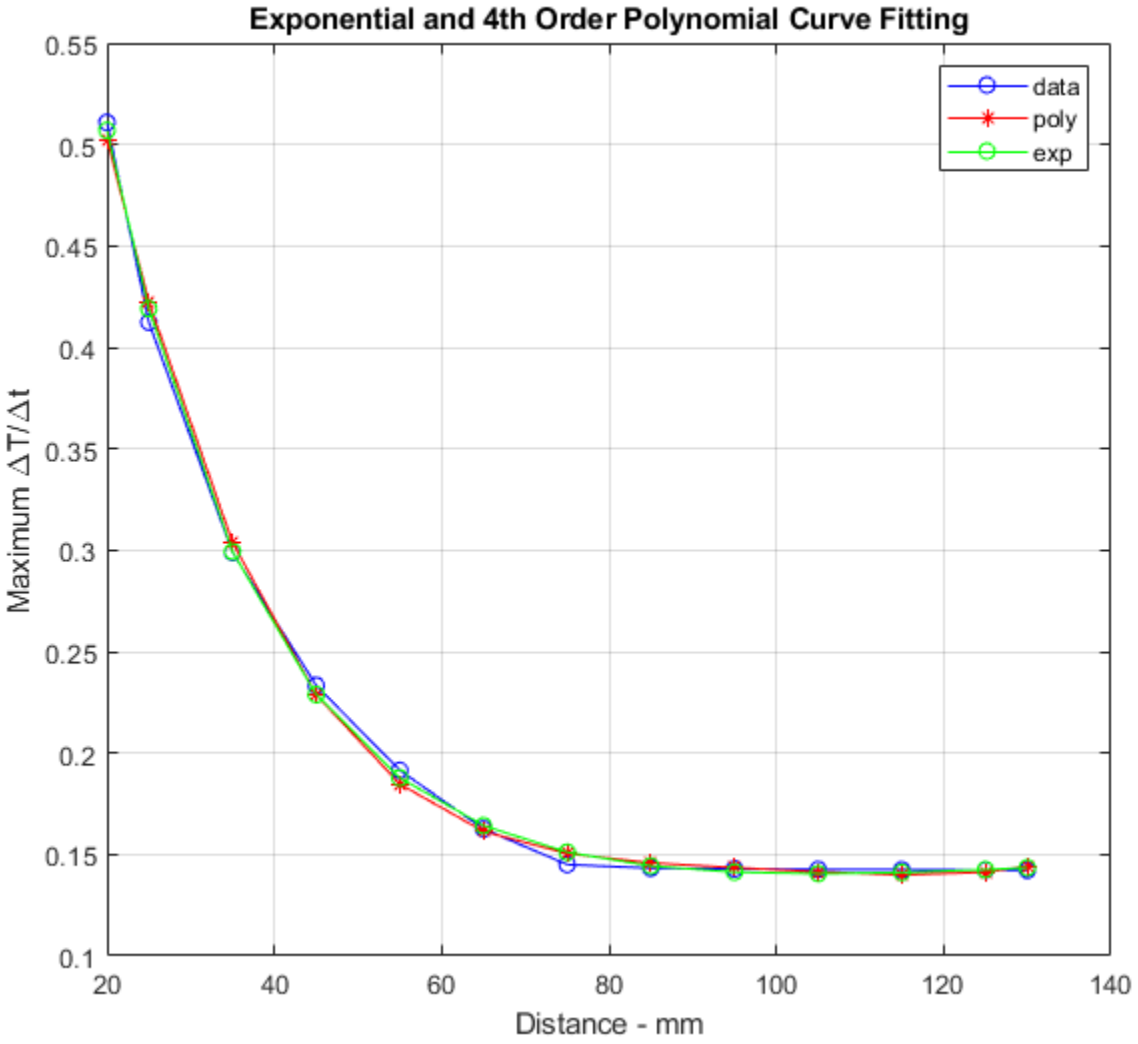

Figure 41: Maximum rate of change of temperature at each location of the heat source extracted from the transient heat transfer simulation and curve fitting using 4th order polynomial and exponential function.

It is observed that the location of the heat source and the maximum rate of change have a relationship that can be utilized to estimate the location of the heat source. Moreover, Figure 42 displays the application of 3rd order polynomial fitting on the data for heat source with the power of 18W, 9W, and 6W. Furthermore, a test on another position of the heat source is carried of for estimating the location of the heat source through the means of interpolating, such temperature profile at the boundary of the structure is illustrated in Figure 43.

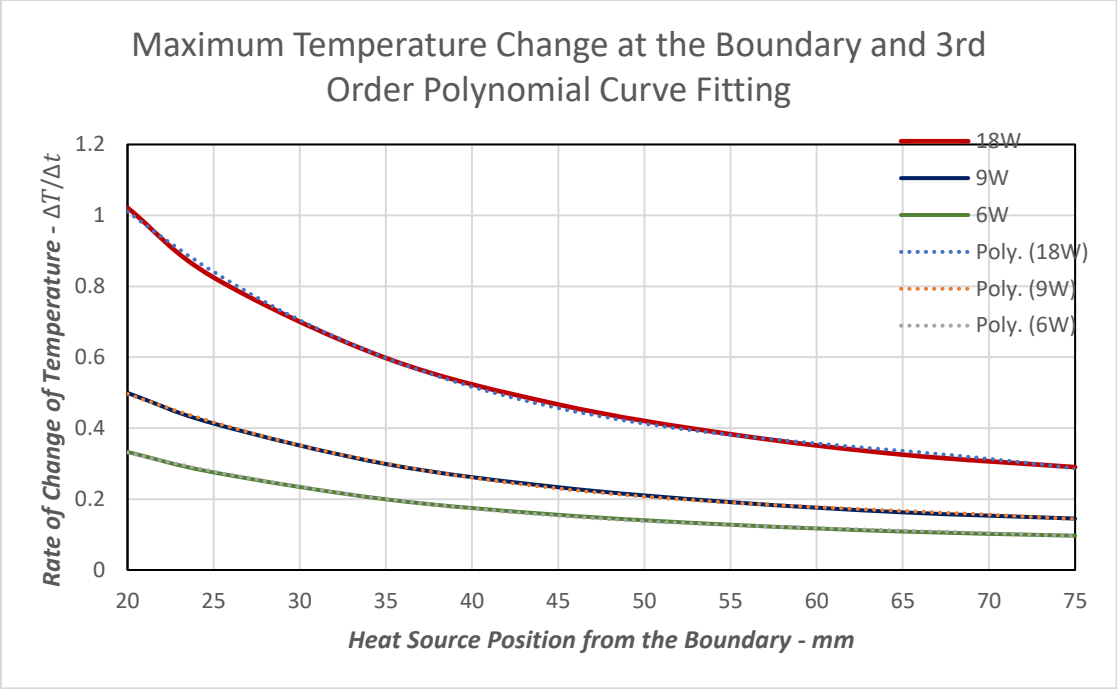

Figure 42: Maximum rate of change of temperature at the boundary with heat source at various placement – Polynomial curve fitting.

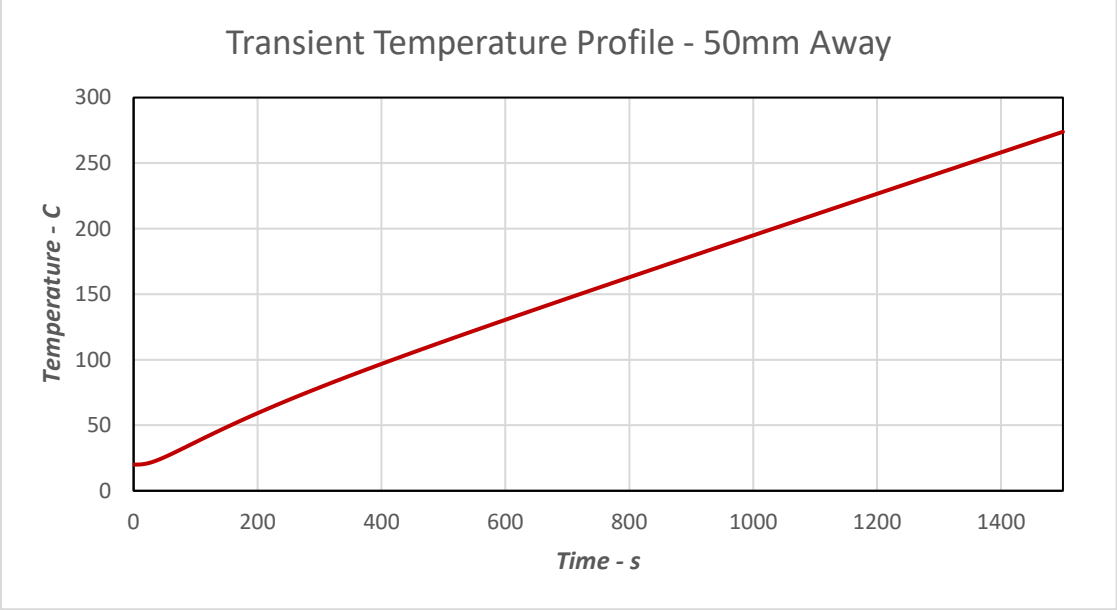

Figure 43: Transient temperature profile at the boundary – Distance to heat source is unknown.

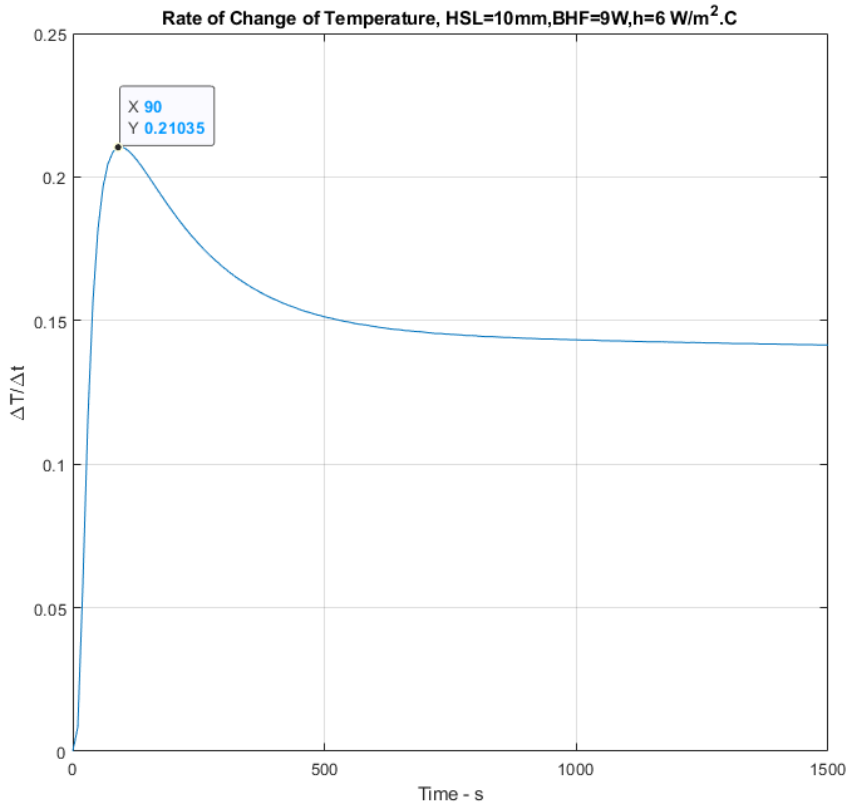

Figure 44: Rate of change of temperature with time at the boundary.

Using the curve fitting equation to interpolate for unknown location gave promising results for the tested positions of the heat source with an accuracy up to 96%. The power of the heat source can be determined with accuracy of 97% using only the transient temperature change at the boundary such as illustrated in Figure 44. Additionally, the rate of change at the boundary determined for the boundary point, the maximum temperature change as highlighted in Figure 44, is estimated using the curve fitting equation from Figure 42. The trendline for the rate of change of temperature in Figure 44 also indicates the heat source location to be closer to the boundary with the peak existing within the first 200 seconds of the total data. Based on this observation, a better prediction can be made to estimate the location of the heat source using the exponential trend it follows against the location of the heat source.

5.6 Two-Dimensional Thermal Experiment

A steel plate with the dimensions of $\approx 150 \times 100 \times 10mm$ is utilised to perform the thermal experiment while employing the same heat source that was used for the one-dimensional heat transfer. Vernier calliper is used to measure the dimensions of the plate which had the accuracy of $\pm 0.01mm$. In Figure 45, the thermal camera is right above the steel plate to record the temperature change across the surface of the plate. While it also shows the backside of the plate where the heat source is attached using epoxy and the power supply providing the current to the heat source. Additionally, a foam tape is used on the backside of the plate as well to have minimum contact with plywood surface.

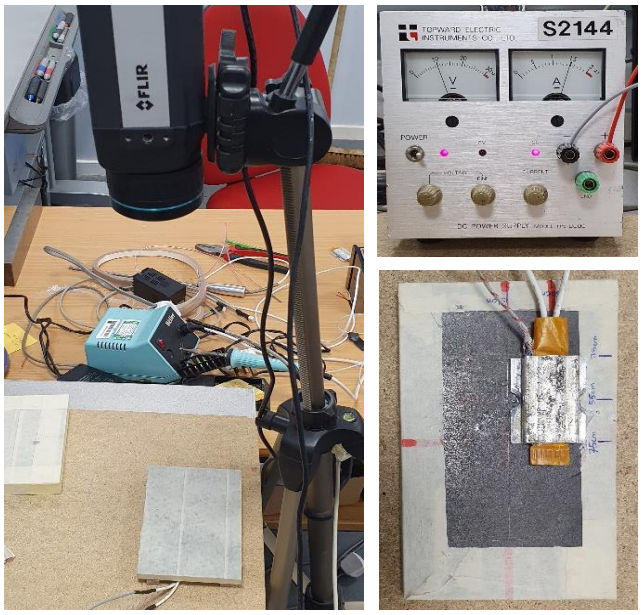

Figure 45: Experimental setup for the steel plate, heat source, thermal camera, and power supply.

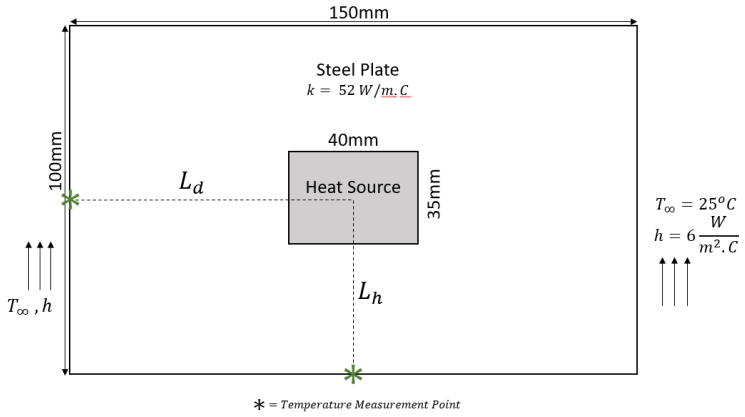

Figure 46: Schematic diagram of the steel plate and the position of the heat source attached to the backside of the plate.

Figure 46 illustrates the dimension of the steel plate and the heat source in a two-dimensional system. L_d and L_h is the length from two edges to the centre of the heat source. All sides experience normal convection although the bottom surface will lose heat due to the convection much slower as it has foam tape to lift it so that the plate has either no or minimum contact with the plywood surface. The point of interest will be the temperature profile at the edge of the steel plate and using the recorded data, the depth and height to the heat source will be estimated. Figure 47 demonstrates the temperature sensors mounted for measuring the ambient temperature of the laboratory. It also shows the temperature controller which is utilized to monitor the temperature of the heat source during the experiment.

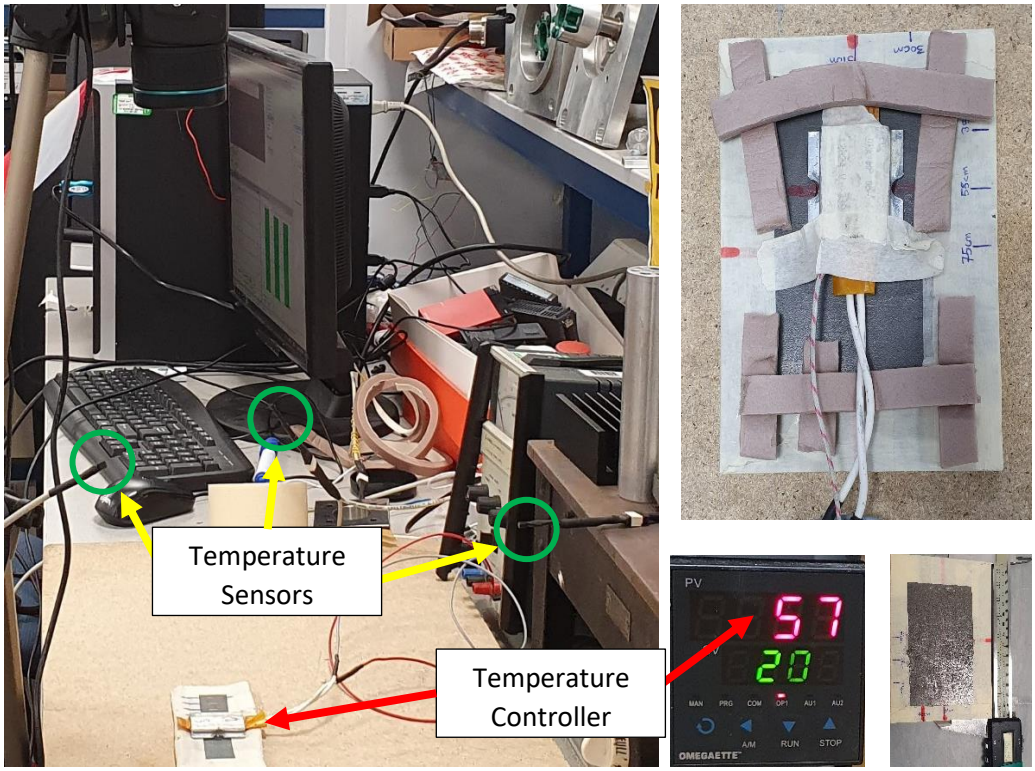

Figure 47: Temperature sensors to monitor ambient temperature, vernier calliper to measure the dimensional parameters, and the temperature controller to monitor the temperature of the heat source.

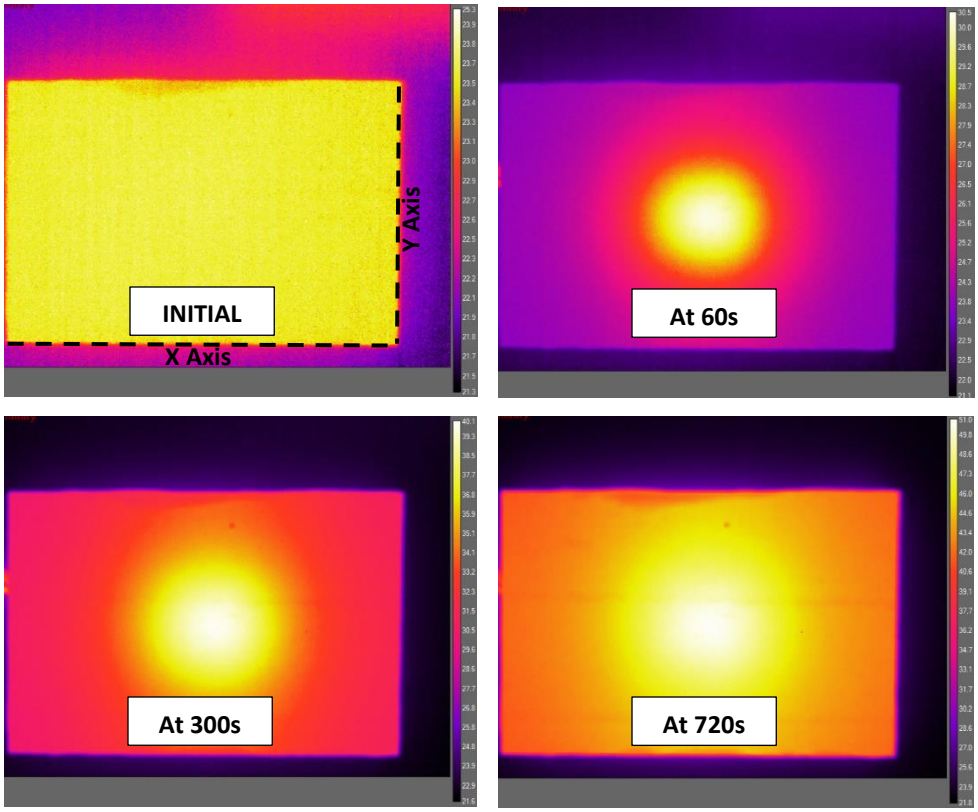

Figure 48: Snapshots from the thermal imaging camera, capturing the surface of the steel plate while illustrating the temperature change at different stages of time.

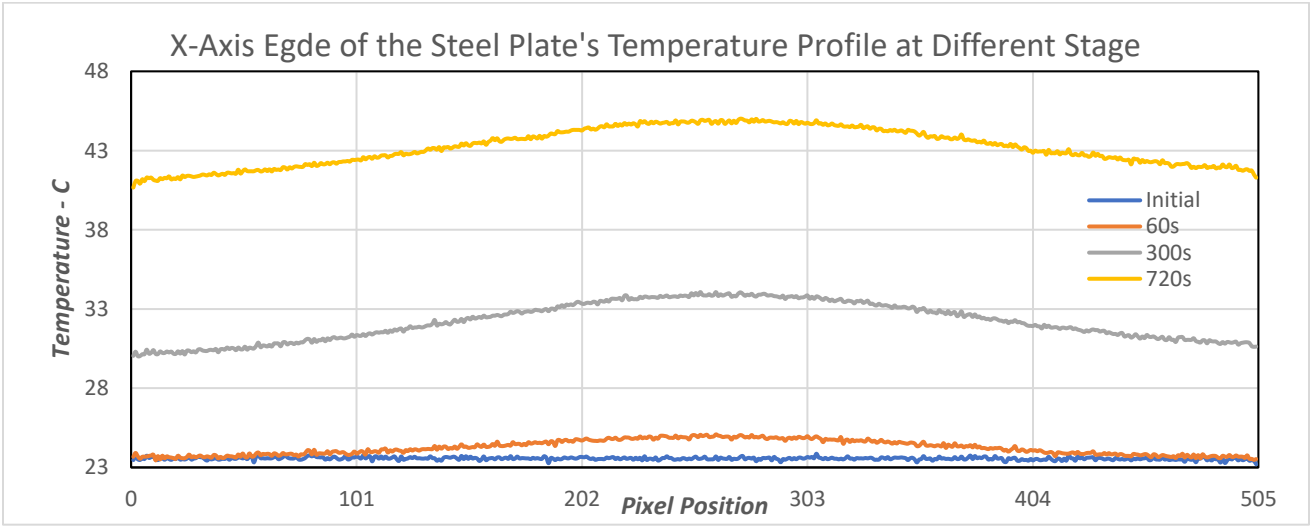

Figure 49: Temperature profiles plotted for the x-axis boundary of the steel plate at four different stages of transient heat transfer.

The experiment conducted on the steel plate is captured by the thermal imaging camera and is illustrated at different stages in Figure 48. Whereas the Figure 49 shows the temperature profile at the x-axis edge of the steel plate at different instances of time. Initially the plate is at $\approx 23°C$, after 60 seconds of the heat source dissipating heat into the steel plate, temperature is higher around the central region and its influence on the corners is slower. Although, as time passes the temperature profile maintains the similar curve where central region has higher temperature range which indicates that the heat source in approximately centrally aligned with x-axis. A further approximation from the boundary profile can be made once observing the temperature profile on the y-axis boundary as well.

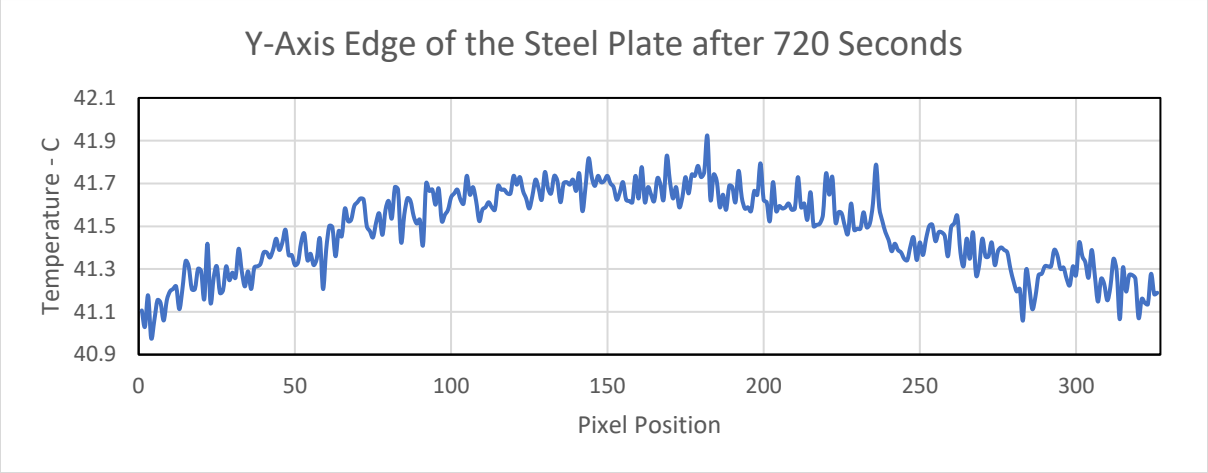

Figure 50: Experimental temperature profile plotted for the y-axis boundary after 720 seconds of the heat transfer.

However, in Figure 50 in contrast to Figure 49, it illustrates the temperature profile for the y-axis edge for only final instance as the temperature difference is very small. Although, the maximum temperature also exists in the central region therefore, with just observing both boundaries it can be approximated that the heat source is in the central position on the backside of the steel plate.

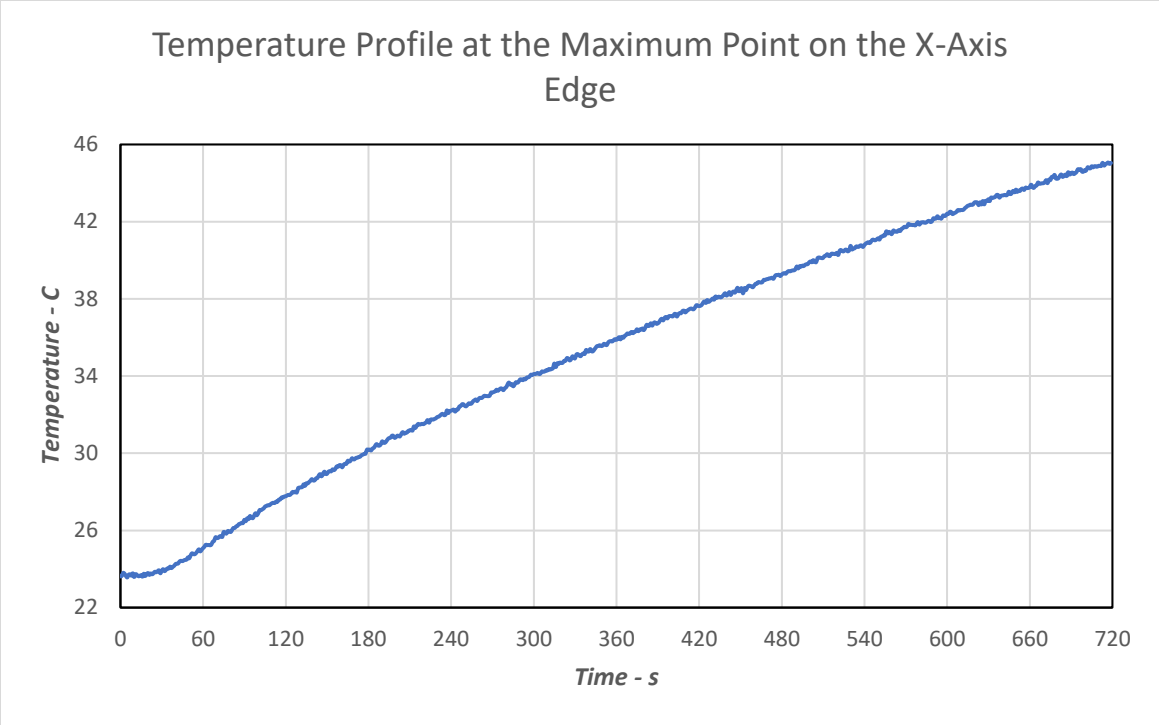

Figure 51: Experimental transient temperature curve for the highest temperature point at the boundary.

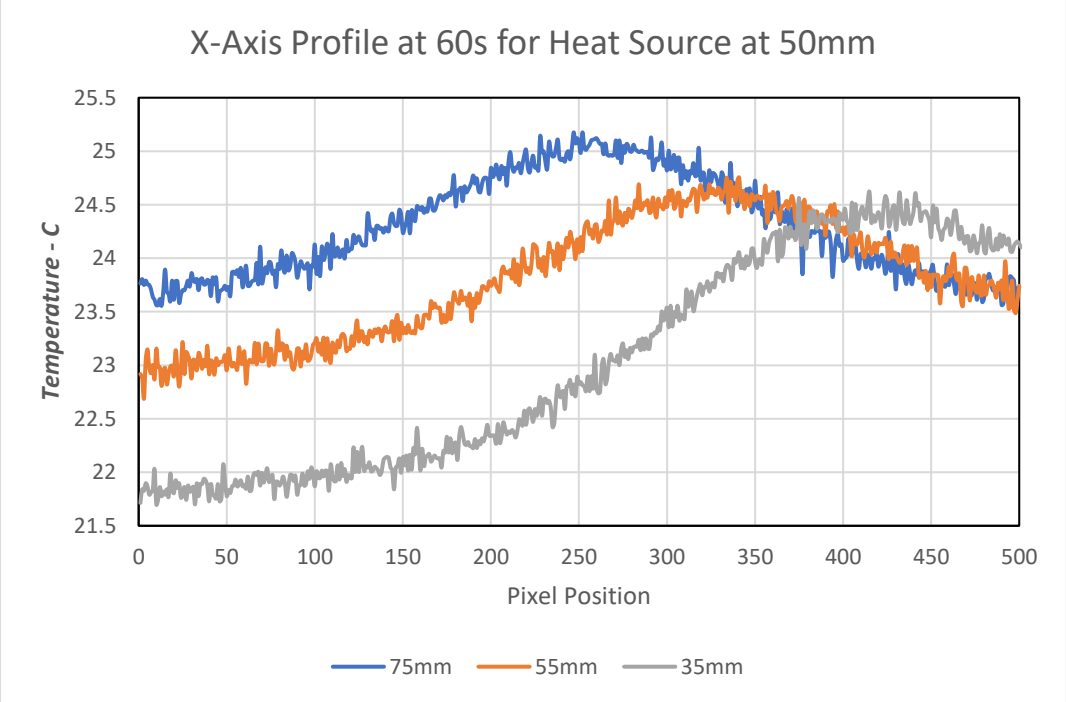

Figure 52: Experimental temperature profiles after 60 seconds for three different positions of the heat source from y-axis while at fixed position of 50mm from x-axis boundary.

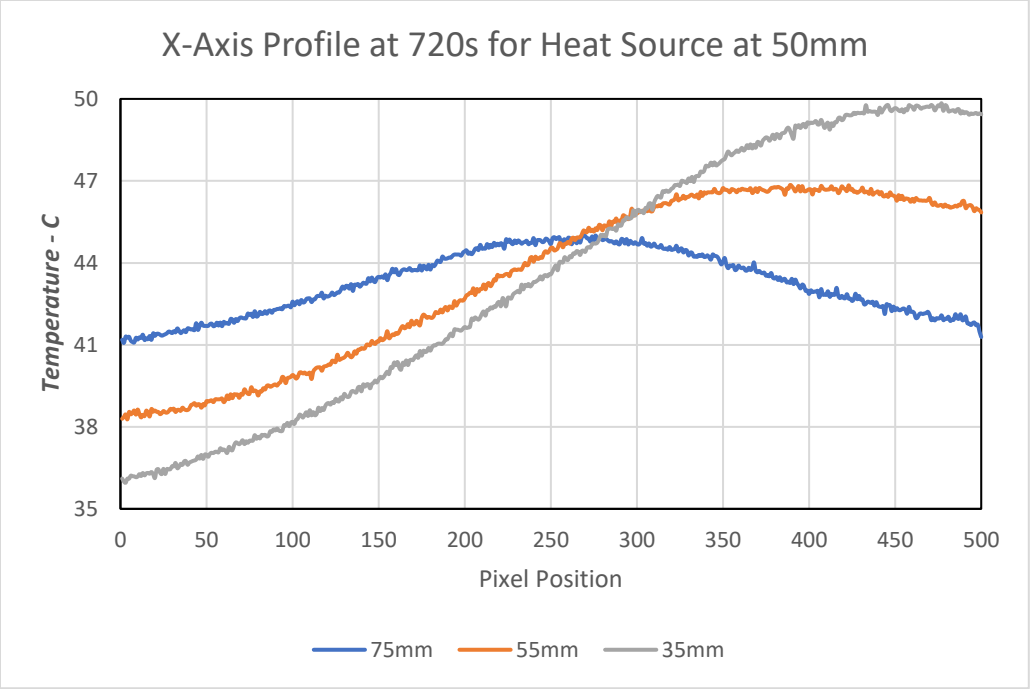

Figure 53: Experimental temperature profiles after 720 seconds for three different positions of the heat source from y-axis while at fixed position of 50mm from x-axis boundary.

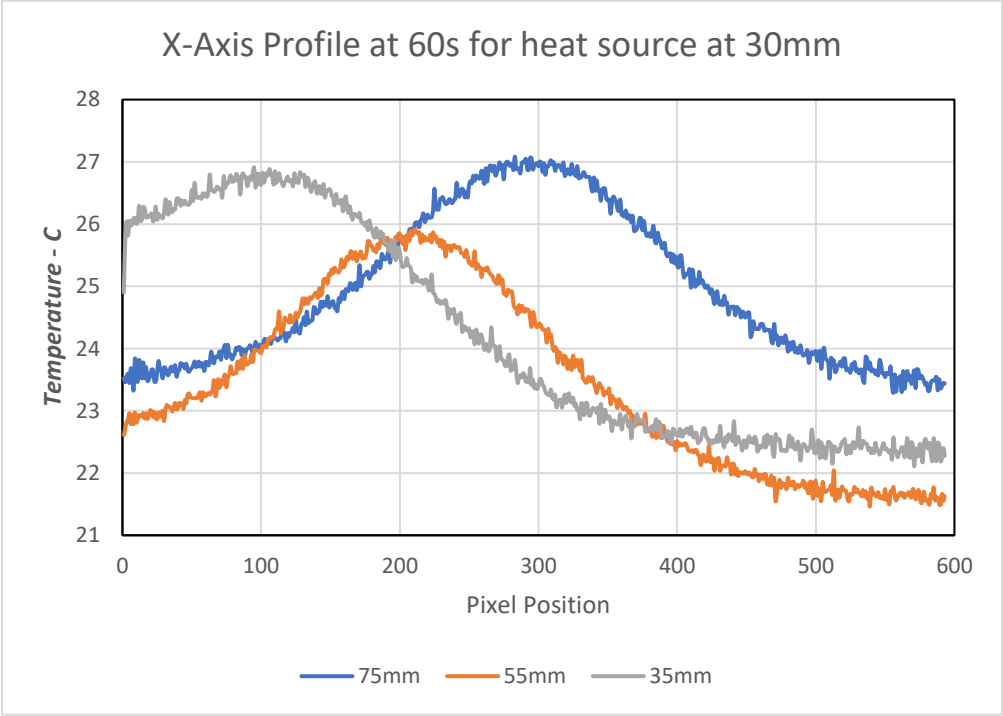

Figure 54: Experimental temperature profiles after 60 seconds for three different positions of the heat source from y-axis while at fixed position of 30mm from x-axis boundary.

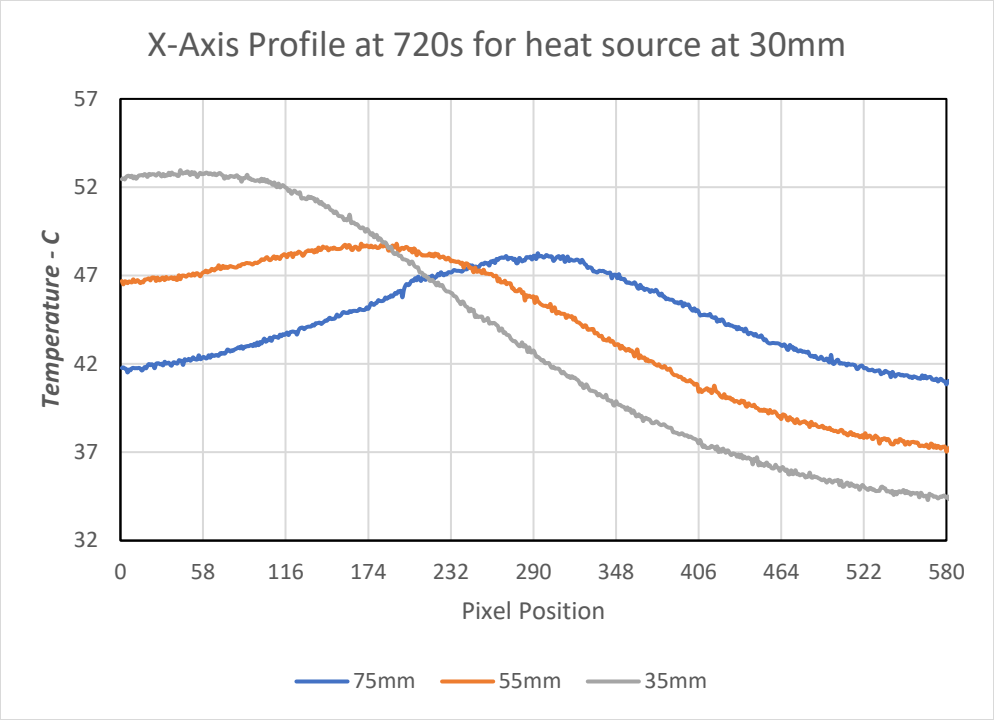

Figure 55: Experimental temperature profiles after 720 seconds for three different positions of the heat source from y-axis while at fixed position of 30mm from x-axis boundary.

The analysis conducted in section 5.5 is extended to the thermal experiment where five different locations of the heat source from the boundary are evaluated using the transient temperature data. From Figure 46, the length L_d is changed between 35, 55, 75, 95, and 115 mm. The maximum temperature on the surface of the steel plate is plotted in Figure 51 which illustrates the temperature profile for 720 seconds of the heat source inducing temperature change. In addition, between Figure 52 - Figure 55, the temperature profile for x-axis boundary is plotted which also indicates the position of the heat source with the maximum temperature point in line with the actual position of the heat source. For these figures between 52 – 55, the L_h is maintained at 50 mm from y-axis boundary. The temperature data is obtained from the thermal camera from one boundary position only and the profiles for each distance are plotted in Figure 56.

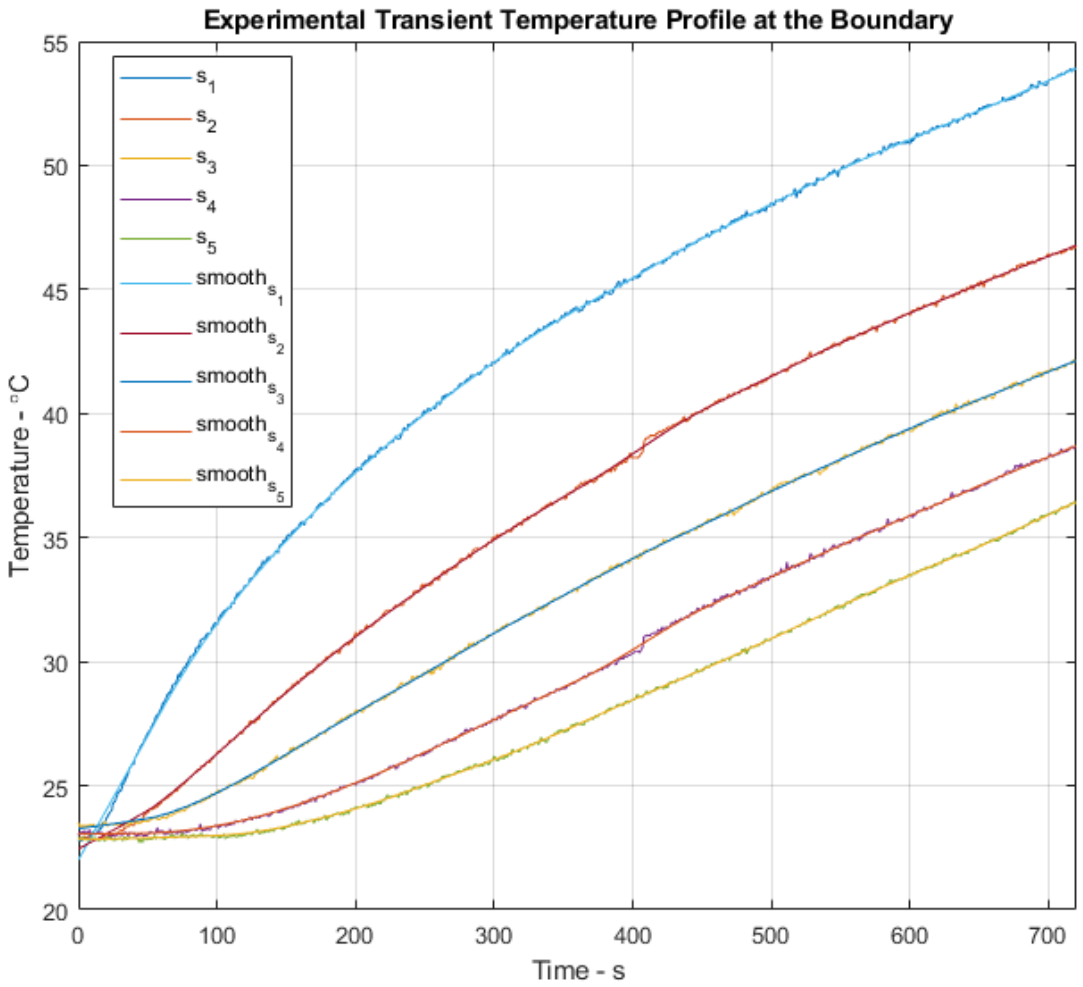

Figure 56: Thermal experimental transient temperature profiles at the boundary and the curves for smoothed data are also plotted with raw data.

Figure 56 shows five temperature profiles, heat source at 35 – 115mm (s1 – s5) each with 20 mm difference, the raw data obtained is smoothed using a technique which uses the locally weighted linear regression to smooth the data. For this purpose, in Matlab, the code is defined for Lowess curve fitting which does the polynomial (Quadratic) model in the regression. The smoothing factor of 0.1 is used. After the data is smoothed, the rate of change at the boundary is calculated within the code and is plotted against the time in Figure 57.

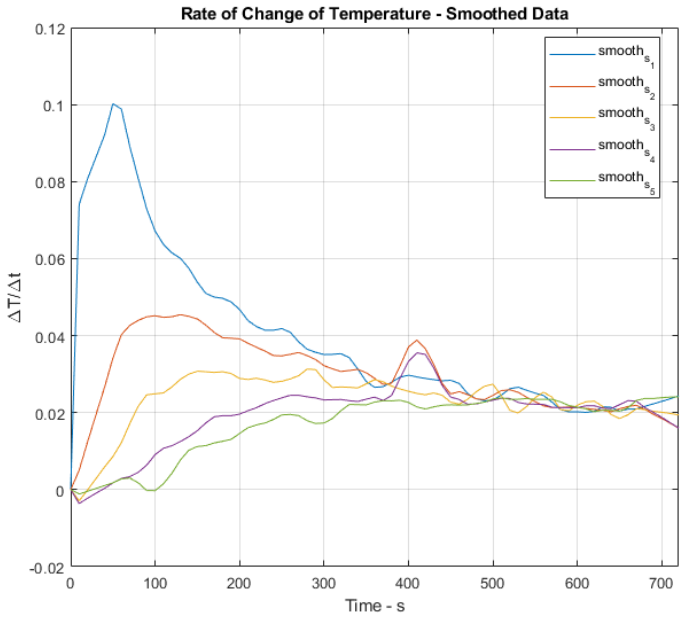

Figure 57: The rate of change of temperature at the boundary for the experimental data.

Figure 57, the scenarios where the heat source is closer to the boundary has the peak early in the transient heat transfer. The maximum rate of change of each curve is extracted from the data and plotted against the position of the heat source Figure 58. The exponential curve fitting shows better trendline than the polynomial fitting. When the heat source is 95 mm away from the boundary, exponential curve shows lower value of maximum rate of change compared to 75 mm position. Whereas, the raw data had this abnormality, which is corrected by the exponential fitting instead of polynomial.

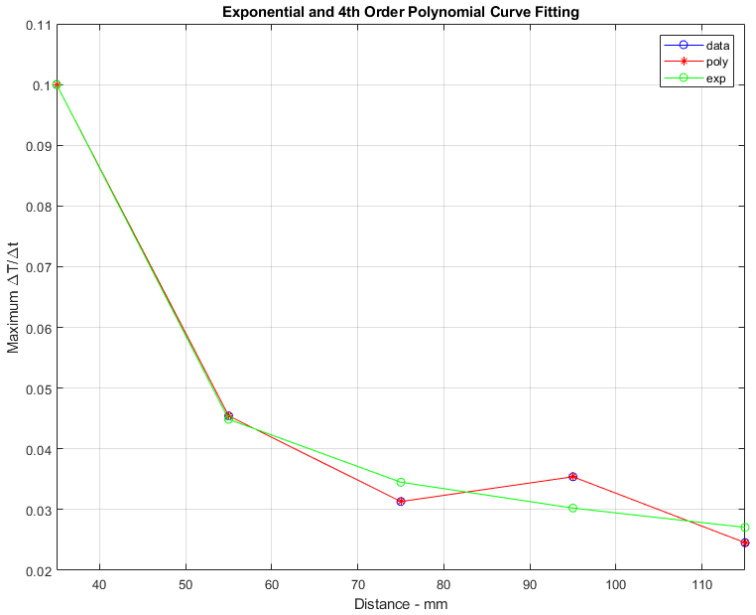

Figure 58: Exponential and Polynomial curve fitting to the experimental data.

5.7 Two- Dimensional Transient Finite Element Analysis for the Heat Transfer

As the experiment is conducted on a steel plate is section 5.6, similar CAD model is created Abaqus software, and the FEA heat transfer simulation is conducted. All the boundary and initial conditions, material properties, heat source parameters are defined as accurately as possible to the experimental values. The Figure 59 shows the parameters and mesh applied to the CAD model and the heat transfer simulation intervals.

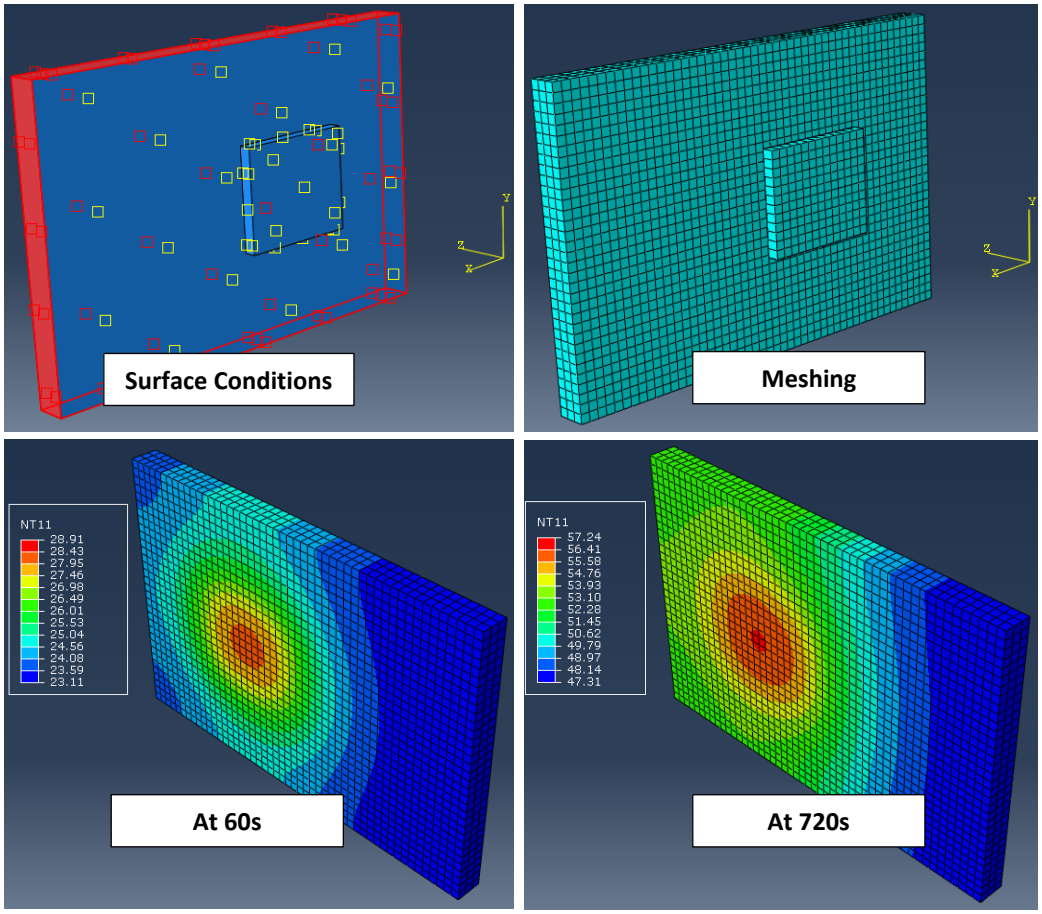

Figure 59: FEA modelling of the plate and attached heat source to simulate two-dimensional heat transfer.

Temperature data is extracted from the boundary point and the profiles are plotted in Figure 60 - Figure 61.

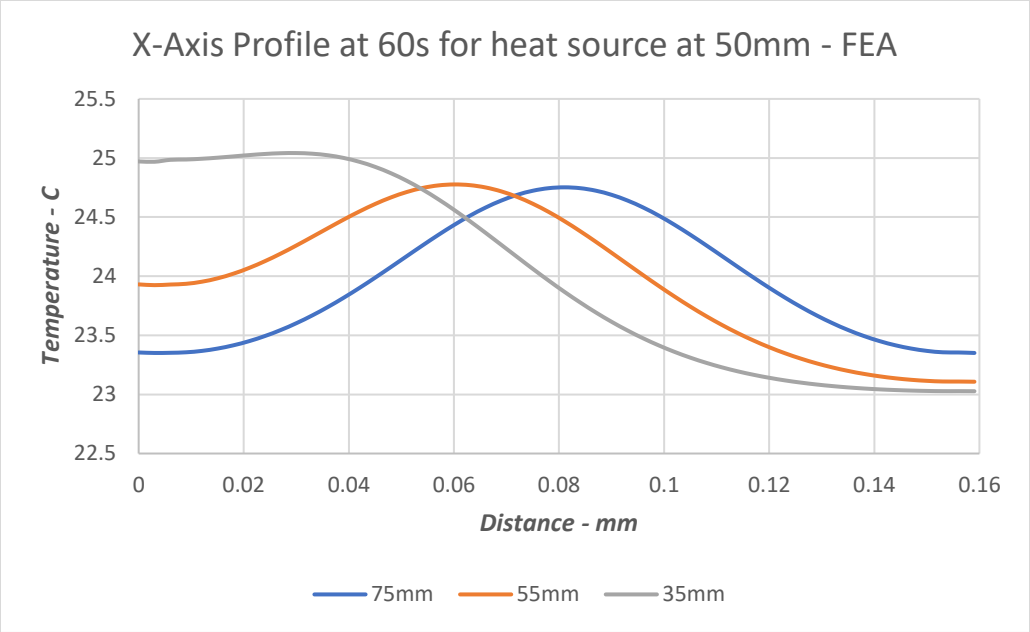

Figure 60: Temperature profiles obtained from FEA simulation after 60 seconds for three positions of the internal heat source attached to the plate.

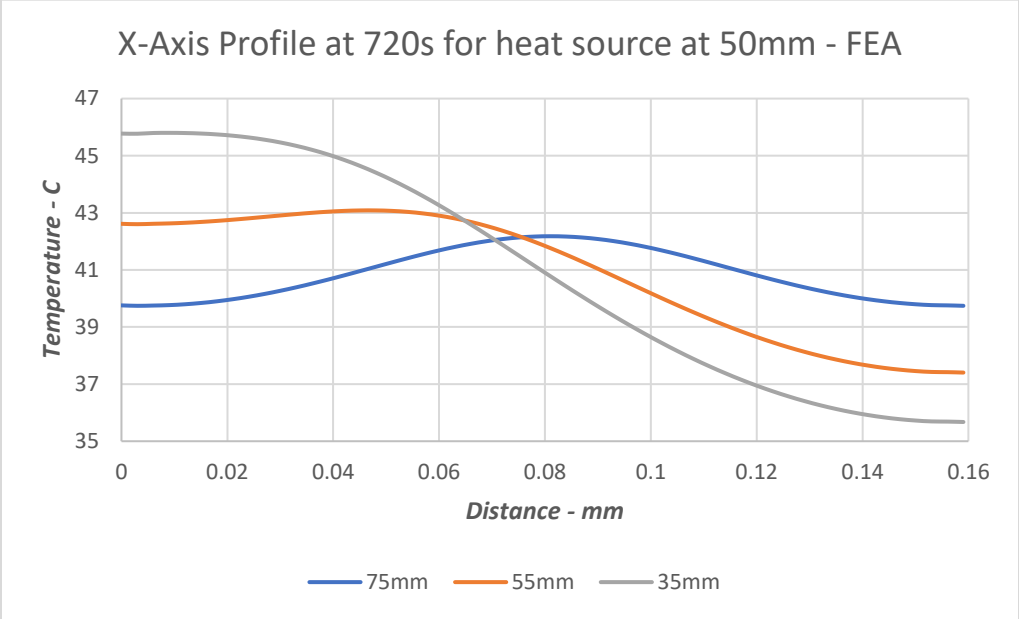

Figure 61: Temperature profiles obtained from FEA simulation after 720 seconds for three positions of the internal heat source attached to the plate.

In Figure 60 and Figure 61, the similar positions of the heat source are defined in the FEA simulation as they were in experiment and plotted in Figure 52 and Figure 53, whereas, the temperature profiles obtained from the FEA simulation also follow the same trendline and are plotted for 60 seconds and 720 seconds of the simulation.

5.8 Transient Heat Transfer Analysis

Using the energy balance technique and lumped capacitance model to estimate the temperature profile at the boundary while optimising for the depth of the heat source from the boundary surface of the plate. This approach assumes the temperature gradients within the structure are negligible and is only applicable to heat transfer models when the Biot number is less than 0.1. Therefore, this approach can be applied to one and two-dimensional heat transfer.

$$\dot{E}_{in} - \dot{E}_{out} = \dot{E}_{st} \text{ or } q_o^{"} - h(T - T_\infty) = \rho L C_p \frac{dT}{dt}$$

To estimate time to reach a steady state for a system, first thermal constant needs to be calculated which is obtained by,

$$\tau_t = R_t^{"} C_t^{"}$$

First, the Biot number will be determined to establish that the system behaves as a lumped capacitance model. This can be calculated by,

$$Bi = \frac{hL}{k} < 0.1$$

$$Bi = \frac{6\frac{W}{m^2}.C \times 0.1mm}{\frac{52W}{m}.C} = 0.01 \; which \; meets \; the \; condition \; of \; < 0.1$$

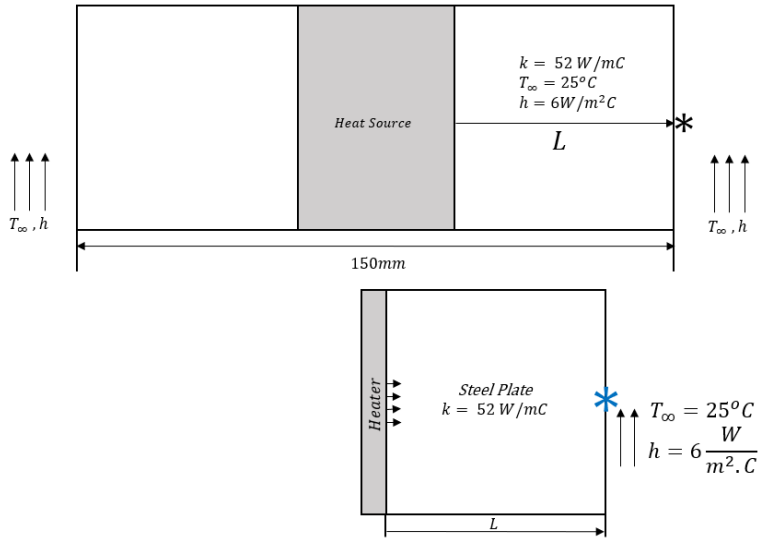

Figure 62: Schematic diagram for transient heat transfer analysis to estimate the depth of the heat source from the boundary.

Using interactive heat transfer 4.0 to solve the equations mentioned above in this section. The L in the equations represents the depth of the heat source from the boundary, this will be calculated by comparing the temporal profile at the boundary obtained through FEA simulation and the calculate one. Through optimisation the depth of the heat source will be determined. Using this method, a preliminary result is obtained to showcase the difference between thermal experiment temperature measurement, FEA simulation, and the lumped capacitance method.

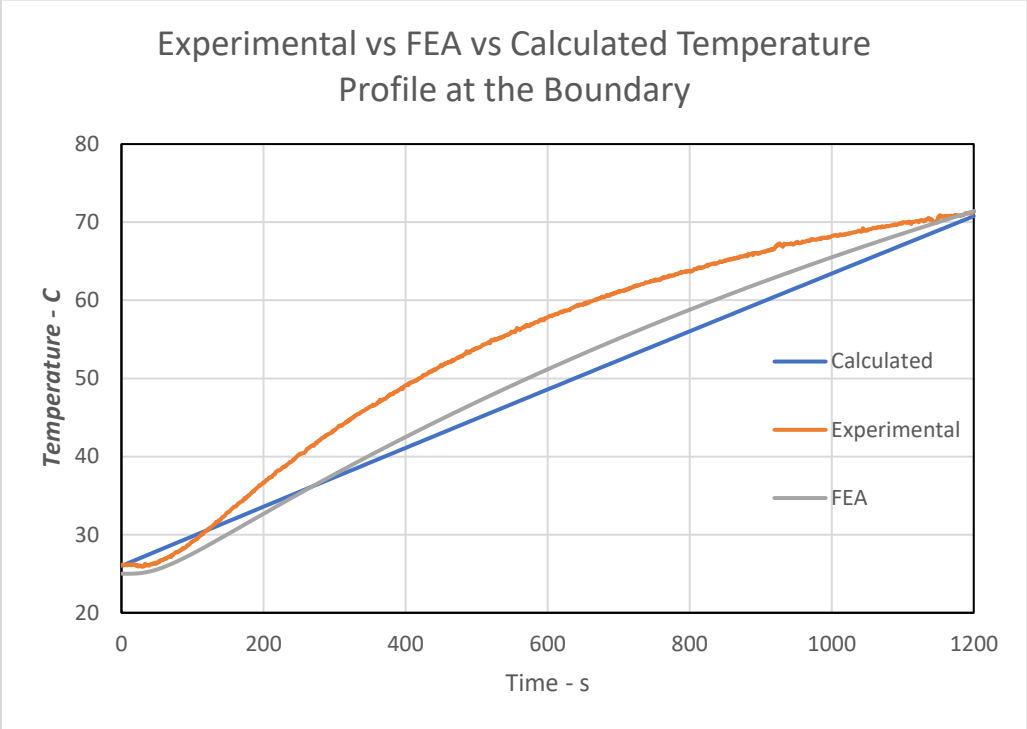

Figure 63: Temperature profiles for obtained through the thermal experiment, FEA simulation, and mathematical approach.

In Figure 63, the results for all three approaches are presented together for the experiments, FEA, and analytical approach. The profiles plotted together show the results of the lumped capacitance system used for the transient temperature calculation at the boundary of the plate. The thermal experimental profile is same as illustrated in Figure 34.

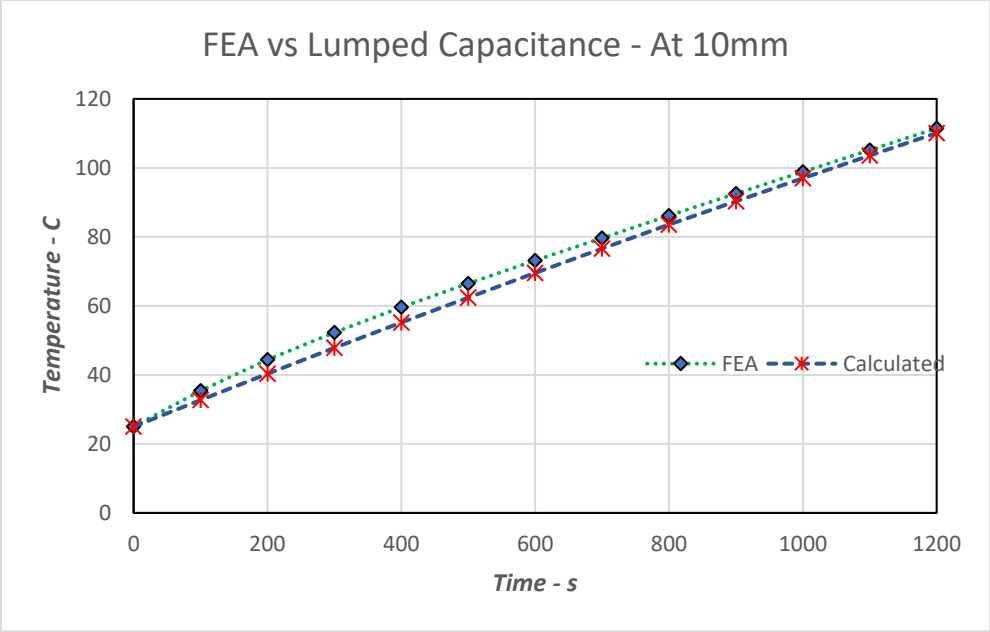

Figure 64: Transient temperature profile at the boundary determined for when heat source was 10mm away and a comparison with FEA temperature profile.

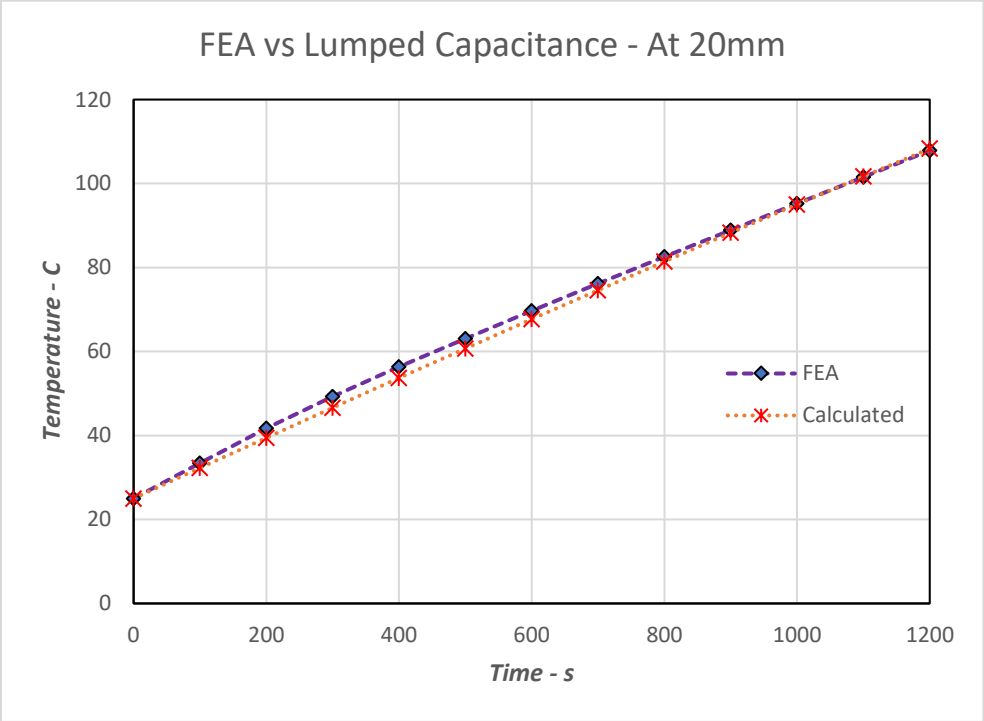

Figure 65: Transient temperature profile at the boundary determined for when heat source was 20mm away and a comparison with FEA temperature profile.

In Figure 64 and Figure 65, the results are illustrated for the boundary point for both FEA and Lumped capacitance model. The correlation between FEA and calculated temperature profile are well correlated.

6 Conclusion and Suggestion for Further Work

Main objective of the current research was to determine the unknown location of the heat source utilizing only one of the boundaries of the structure for the temperature measurements. The methodology employed in this project led to estimate the location of the unknown heat source in a one-dimensional plate. Where the heat source was placed at several different locations. For each of the locations, the estimation of the distance to the heat source has been determined with the maximum error of only 5%. These results for the steady state heat transfer are presented in section 5.2.4. The estimation to the location of the heat source relied mostly on the knowledge of the steady state temperature at the boundary of the structure. Utilizing the temperature of the boundary when it was at a steady state as per FEA simulation, the data applied in the analytical approach provided the unknown distance of the heat source from the boundary.

However, under realistic conditions, structures with an attached heat source would take much longer to reach a steady state along with the loss of heat through normal convection as well. Therefore, thermal experiments conducted for this research are used as benchmark and validation of FEA simulations. The validation of FEA simulated heat transfer aided in investigating numerous situations which otherwise would be time consuming for thermal experiments.

Utilizing simulated heat transfer model allowed further parametric analysis on important parameters such as the convectional coefficient and its influence on the boundary temperature. The main finding on the convectional coefficient was that with higher convection, the temperature at the boundary was lower when compared with lower convection condition and the structure itself reaches the steady state rapidly with higher convection. However, the convectional coefficient had negligible influence on the rate of change of temperature at the boundaries, hence the rate of change of temperature was unchanged regardless of the magnitude of the convectional coefficient. The rate of change of temperature at the boundary was impacted only by the parameters specified for the heat source. These results are presented in section 5.5.

Moreover, an investigation into the parameters specified for the heat source such as the strength and dimensional size of it, illustrated their relationship with the thermal behaviour of the structure. As a result, the analysis on the size and strength of the heat source revealed that the strength of the heat source has a prominent role in affecting the rate of change of temperature at the boundary of the structure. Whereas the dimensional size of the heat source had no impact on the rate of temperature change at the boundary. It is also observed that if the dimensional size of the heat source is considered as an unknown parameter, then it would be a difficult task to determine the size, strength, and the location of the heat source.

The objectives were further achieved when the study was continued into two-dimensional heat transfer investigation, where transient analysis was conducted, and thermal experiment were also performed on a steel plate with a heat source attached to the backside of it. Subsequently, the analysis was conducted on estimating the unknown location of the heat source using only two perpendicular boundary temperatures in this study as well. For two-dimensional estimation, the data obtained through thermal experiment was applied into a Matlab code for further analysis. The transient temperature profile at the boundary of a two-dimensional model from the experiment was plotted, and the data was smoothened by utilizing a regression technique. The technique extended further by calculating the rate of change of temperature and finding the maximum change at each location of the heat source. This enabled to plot the maximum temperature change against the relevant positions of the heat source. The obtained trendline for the plot followed an exponential behaviour which was used to interpolate for new locations of the heat source under same conditions specified for the heat transfer. Furthermore, the lumped capacitance model was applied to predict the location of the heat source utilizing the heat flux at the boundary of the plate. Preliminary results of lumped capacitance were correlating with the FEA as well as the experimental outcomes. The methodology employed to estimate the unknown location of the heat source using only the surface or the boundary temperatures was conducted on a one and two-dimensional structure. A comparison between analytical, numerical, and experimental approach was made which enabled to establish a validation for the technique being used to obtain the results. This research comprises the novelty of estimating the location of the heat source by utilizing only one point of temperature measurement in one dimensional structure and two perpendicular boundaries for a two-dimensional structure. The methodology utilized kept the estimation of the heat source as a central point in each section. This allowed to expand the estimation in steady and transient heat transfer within a one and two-dimensional structures. However, there are some assumptions and limitations to the methodology, and these are discussed in the following section.

6.1 Limitations

Few assumptions were also considered to obtain the presented solution, among other assumptions, knowing the volumetric size of the heat source was one of the main one. Whereas if this parameter is considered an unknown parameter when estimating the unknown location of the heat source, it could further open another perspective of research and could robust the technique which would estimate the parameters such as the size, location, and the strength of the heat source utilizing only one surface of a three-dimensional structure for the temperature measurements. Moreover, the simplification of the structure under investigation needs to be

extended into more complex assembled shapes. This would also involve other parameters such as thermal contact conductance between surfaces and different material properties could certainly challenge the approach.

6.2 Scope for future work

The results achieved through this research can be considered as a benchmark for estimating the location of the heat source utilizing limited temperature measurement locations in both one and two-dimensional structures. However, further prospect of the work is in three dimensional simplified structures. The structural shape and dimensions could be another aspect to further investigate. The approach needs to be applied to assembled structures as well, along with defining further realistic properties such as thermal contact conductance.

List of References

AbdulShahed, A., Longstaff, A., & Fletcher, S. (2015). The application of ANFIS prediction models for thermal error compensation on CNC machine tools. *Applied Soft Computing*, 158-168.

Antoniou, A., & Lu, W.-S. (2007). *Practical Optimization.* New York: Springer.

Beck, J. V., Blackwell, B., & St. Clair, C. R. (1985). *Inverse Heat Conduction: Ill-Posed Problems.* New York: John Wiley.

Beddiaf, S., Perez, L., Autrique, L., & Jolly, J.-C. (2014). Simultaneous determination of time-varying strength and location of a heating source in a three-dimensional domain. *Inverse Problems in Science and Engineering*, 166-183.

Bryan, J. (1991). International Status of Thermal Error Research (1990). *CIRP*, 645-656.

Carslaw, H. S., & Jaeger, J. C. (1959). *Conduction of Heat in Solids.* London: Oxford University Press.

Correa, E., & Cotta, R. (1998). Enhanced lumped-differential formulations of diffusion problems. *Applied Mathematical Modelling*, 137-152.

Dornfeld, D., & Lee, D. (2008). *Machine Design for Precision Manufacturing.* Boston: Springer verlag.

Eneko, G., Aitor, O., & Javier, O. (2013). Methodology for the design of a thermal distortion compensation for large machine tools based in state-space representation with Kalman filter. *International Journal of Machine Tools and Manufacture*, 100-108.

Esfandiari, R. S. (2013). *Numerical Methods for Engineers and Scientist Using MATLAB.* Boca Raton: Taylor & Francis Group.

Ess, M. (2012). Simulation and compensation of thermal errors of machine tools. *Semantic Scholar*.

Feng, Z.-G., & Michaelides, E. (1997). The use of modified Green's functions in unsteady heat transfer . *Int. J. Heat Mass Transfer*, 2997-3002.

Hagen, K. (1999). *Heat Transfer with Application.* New Jersey, USA: Prentice-Hall.

Han, J.-C. (2012). *Analytical Heat Transfer.* New York: Taylor & Francis Group.

Incropera, F., Dewitt, D., Lavine, A., & Bergman, T. (2007). *Introduction to Heat Transfer.* John Wiley & Sons.

Joel, R. (1974). *Basic Engineering Thermodynamics in SI Units.* London: Longman.

Keshavarz, P., & Taheri, M. (2007). An improved lumped analysis for transient heat conduction by using the polynomial approximation method. *Heat Mass Transfer*, 1151-1156.

Khachfe, R. A., & Jarny, Y. (2001). Determination of heat sources and heat transfer coefficient for two-dimensional heat flow – numerical and experimental study. *International Journal of Heat and Mass Transfer*, 1309-1322.

Kothandaraman, C. (2006). *Fundamentals of Heat and Mass Transfer.* New Age International.

Ling, S. J., Moebs, W., & Sanny, J. (2016). *University Physics* (Vol. 2). Houston, Texas, USA: OpenStax.

Linhua, l., Heping, T., & Qizheng, Y. (2000). Inverse radiation problem in one-dimensional semitransparent plane-parallel media with opaque and specularly reflecting boundaries. *Journal of Quantitative Spectroscopy and Radiative Transfer*, 395-407.

Lobato, F. S., Steffen Jr, V., & Neto, A. J. (2010). Simultaneous Estimation of Location and Timewise-Varying Strength of a Plane Heat Source using Differential Evolution. *2nd International Conference on Engineering Optimization*, (pp. 1-7). Lisbon.

Mayr, J., Ess, M., Weikert, S., & Wegener, K. (2009). Compensation of Thermal Effects on Machine Tools using a FDEM Simulation Approach. *semantic*.

Mian, N. S., Fletcher, S., Longstaff, A. P., & Myers, A. (2011). Efficient thermal error prediction in a machine tool using finite element analysis. *MEASUREMENT SCIENCE AND TECHNOLOGY*.

Monte, F. d. (2000). Transient heat conduction in one-dimensional composite slab. A `natural' analytic approach. *International Journal of Heat and Mass Transfer*, 3607-3619.

Monteiro, E. R., Macêdo, E. N., Quaresma, J. N., & Cotta, R. (2009). Integral transform solution for hyperbolic heat conduction in a finite slab. *International Communications in Heat and Mass Transfer*, 297-303.

Neto, A. J., & Ozisik, M. N. (1993). Simultaneous Estimation of Location and TimewiseVarying Strength of a Plane Heat Source. *Numerical Heat Transfer*.

Ostrogorsky, A. (2008). Transient heat conduction in spheres for Fo<0.3 and finite Bi. *Heat Mass Transfer*, 1557-1562.

Parwani, A. K., Talukdar, P., & Subbarao, P. (2013). Performance evaluation of hybrid differential evolution approach for estimation of the strength of a heat source in a radiatively participating medium. *International Journal of Heat and Mass Transfer*, 552-560.

Parwani, A. K., Talukdar, P., & Subbarao, P. (2013). Simultaneous estimation of strength and position of a heatsource in a participating medium using DE algorithm. *Journal of Quantitative Spectroscopy & Radiative Transfer*, 130-139.

Postlethwaite, S., Allen, J. P., Ford, & G, D. (1998). The use of thermal imaging, temperature and distortion models for machine tool thermal error reduction. *Journal of Engineering Manufacture*, 671-679.

Raju, K. (2011). *Fluid Mechanics, Heat Transfer, and Mass Transfer.* John Wiley & Sons.

Ramesh, R., Mannan, M., & Poo, A. (2000). Error compensation in machine tools — a review: Part II: thermal errors. *International Journal of Machine Tools and Manufacture*, 1257-1284.

Rao, S. S. (1996). *Engineering Optimization.* (Third, Ed.) Toronto: John Wiley & Sons.

Su, J. (2001). Improved lumped models for asymmetric cooling of a long slab by heat convection. *Int. Comm. Heat Mass Transfer*, 973-983.

Su, J., & Cotta, R. M. (2001). Improved lumped parameter formulation for simplified LWR thermohydraulic analysis. *Annals of Nuclear Energy*, 1091-1031.

Tian, N., Sun, J., Xu, W., & Lai, C.-H. (2011). Estimation of unknown heat source function in inverse heat conduction problems using quantum-behaved particle swarm optimization. *International Journal of Heat and Mass Transfer*, 4110-4116.

Tikhonov, A. N., & Arsenin, V. Y. (1977). *Solutions of Ill-Posed Problems.* New Jersey: Winston and Sons.

Week, M. (1984). *Handbook of Machine Tools: Metrological Analysis and Performance Tests.* John Wiley and Sons .

Appendix A – CAD Modelling of Plate and Heat Source

The CAD models of the heat source and the plate were created using Abaqus CAE 2020.

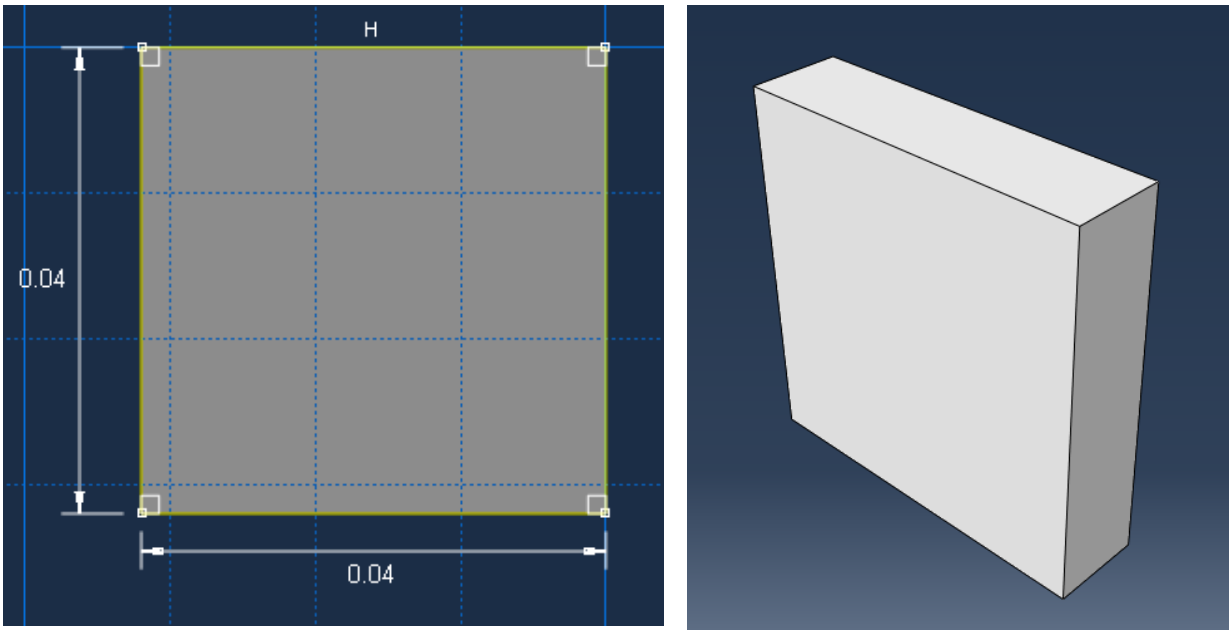

Figure 66: Heat Source Dimensions

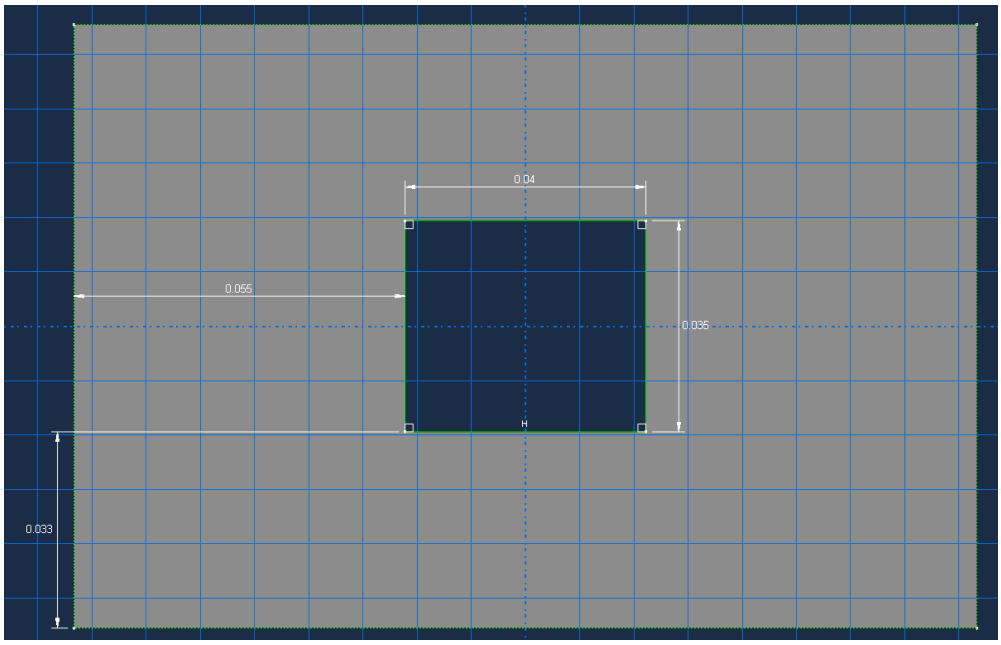

Figure 67: Dimensions of the plate with cut out for the heat source.

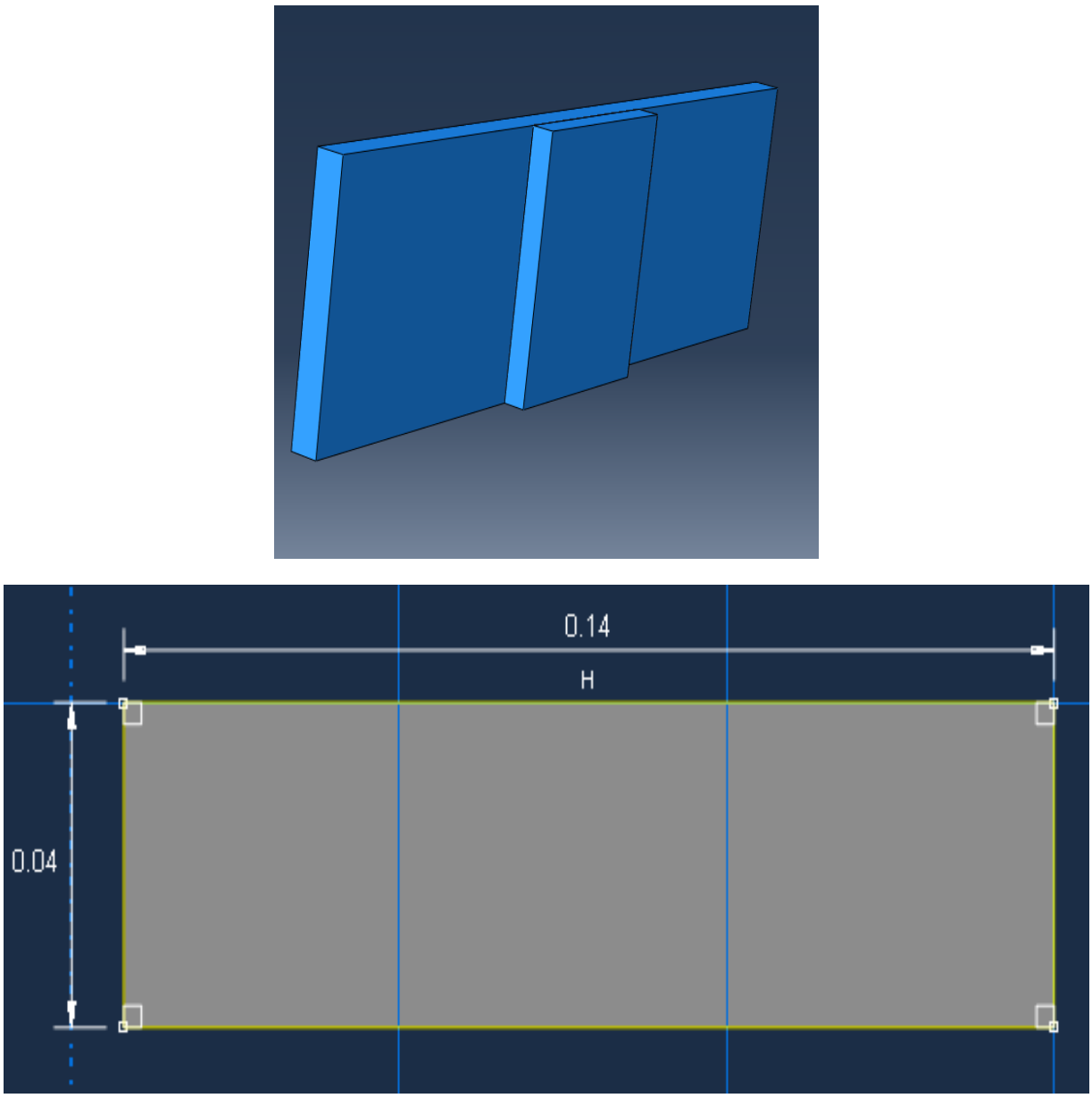

Figure 68: One-dimensional heat source and the plate dimensions.

Appendix B – Matlab Algorithm

This program generated the transient temperature profiles, rate of change of temperature, maximum rate of change of temperature against respected position of the heat source, and curve fitting using exponential and polynomial functions.

FEA - BHF, Heat Source length, and Plate Length Analysis

BHF = 9W

Plate Length = 150mm

Heat source size = 30mm h = 6 W/m^2.C

```
load ('Temp_h_6_BHF_9')
load ('time_data')
tRange = (0:10:1500)';
[dataNum, scenarioNum] = size(Temp_h_6_BHF_9);
Tdata4 = zeros(scenarioNum, 151);
lgnd = {};
for scenario = 1: scenarioNum
    STemperature = reshape(Temp_h_6_BHF_9(2:end,scenario), [10 150]);
    T_change1 = arrayfun(@(x) (STemperature(end,x)-STemperature(1,x))/10,
1:size(STemperature,2));
    T_change1 = [0 T_change1];
    Tdata4(scenario, :) = T_change1;
    lgnd{end+1} = sprintf('s_{%d}', scenario);
end
plot(tRange,Tdata4)
grid on
title('Rate of Change of Temperature, HSL = 30mm - BHF = 9W')
%title('Rate of Change of Temperature  - h = 6 W/m^2.C')
xlabel('Time - s')
ylabel('\DeltaT/\Deltat')
legend(lgnd , 'Location','best')



plot (time_data,Temp_h_6_BHF_9)
grid on
title('Boundary Temperature Profile - BHF = 9W')
xlabel('Time - s')
ylabel('Temperature - C')
legend(lgnd , 'Location','best')


Distance = (25:10:125);
Distance = [20 Distance 130];
```

```
MaxAveRow = MaxAveOfRow(Tdata4)
%display(MaxAveRow);


scatter(Distance,MaxAveRow(:,1),"black",'LineWidth',1)
%plot(Distance(1:end-1), MaxAveRow(2:end,1))
grid on
title('Max S.D. of Temperature - BHF = 9W')
xlabel('Distance - mm')
ylabel('Standard Deviation')


p =polyfit(Distance,MaxAveRow(:,1),4)
f_1 = fit(Distance',MaxAveRow(:,1), 'exp2')
y2 = polyval(p,Distance');
y3 =f_1(Distance');
plot(Distance,MaxAveRow(:,1),'b-o')
hold on
plot(Distance',y2,'r-*')
plot(Distance,y3,'g-o')
hold off
title('Plot of Data (Points) and Model (Line)')
%plot(Distance(1:end), MaxAveRow(1:end,1))
grid on
title('Exponential and 4th Order Polynomial Curve Fitting')
xlabel('Distance - mm')
ylabel('Maximum \DeltaT/\Deltat')
legend('data', 'poly', 'exp')
```

Heat source size = 10mm

Plate Length = 150mm

BHF = 9W h = 6 W/m^2.C

```
load ('Temp_h_6_HS_10')
load ('time_data')
tRange = (0:10:1500)';
[dataNum, scenarioNum] = size(Temp_h_6_HS_10);
Tdata5 = zeros(scenarioNum, 151);
lgnd = {};
for scenario = 1: scenarioNum
    STemperature3 = reshape(Temp_h_6_HS_10(2:end,scenario), [10 150]);
    T_change1 = arrayfun(@(x) (STemperature3(end,x)-STemperature3(1,x))/10,
1:size(STemperature3,2));
    T_change1 = [0 T_change1];
    Tdata5(scenario, :) = T_change1;
    lgnd{end+1} = sprintf('s_{%d}', scenario);
end
```

```
plot(tRange,Tdata5)
grid on
title('Rate of Change of Temperature, HSL = 10mm - BHF = 9W')
xlabel('Time - s')
ylabel('\DeltaT/\Deltat')
legend(lgnd , 'Location','best')


plot (time_data,Temp_h_6_HS_10)
grid on
title('Boundary Temperature Profile - HSL = 10mm')
xlabel('Time - s')
ylabel('Temperature - C')
legend(lgnd , 'Location','best')


Distance = (25:10:125);
Distance = [20 Distance 130];


MaxAveRow = MaxAveOfRow(Tdata5);
display(MaxAveRow);


scatter(Distance,MaxAveRow(:,1),"red",'LineWidth',1)
%plot(Distance(1:end-1), MaxAveRow(2:end,1))
grid on
title('Max S.D. of Temperature - HSL = 10mm')
xlabel('Distance - mm')
ylabel('Standard Deviation')


p = polyfit(Distance,MaxAveRow(:,1),2)
Distance1 = (20:1:130);
y2 = polyval(p,Distance1);
plot(Distance,MaxAveRow(:,1),'o',Distance1,y2)
title('Plot of Data (Points) and Model (Line)')
%plot(Distance(1:end), MaxAveRow(1:end,1))
grid on
title('Polynomial Fitting - 2nd Order')
xlabel('Distance - mm')
ylabel('Standard Deviation')
```

BHF = 6W

Plate Length = 150mm

Heat source size = 10mm h = 6 W/m^2.C

```
load ('Temp_h_6_BHF_6')
load ('time_data')
tRange = (0:10:1500)';
[dataNum, scenarioNum] = size(Temp_h_6_BHF_6);
Tdata6 = zeros(scenarioNum, 151);
lgnd = {};
for scenario = 1: scenarioNum
    STemperature4 = reshape(Temp_h_6_BHF_6(2:end,scenario), [10 150]);
    T_change1 = arrayfun(@(x) (STemperature4(end,x)-STemperature4(1,x))/10,
1:size(STemperature4,2));
    T_change1 = [0 T_change1];
    Tdata6(scenario, :) = T_change1;
    lgnd{end+1} = sprintf('s_{%d}', scenario);
end


plot(tRange,Tdata6)
grid on
title('Rate of Change of Temperature, HSL = 10mm - BHF = 6W')
xlabel('Time - s')
ylabel('\DeltaT/\Deltat')
legend(lgnd , 'Location','best')


plot (time_data,Temp_h_6_BHF_6)
grid on
title('Boundary Temperature Profile - BHF = 6W')
xlabel('Time - s')
ylabel('Temperature - C')
legend(lgnd , 'Location','best')


Distance = (25:10:125);
Distance = [20 Distance 130];


MaxAveRow = MaxAveOfRow(Tdata6)
%display(MaxAveRow);


scatter(Distance,MaxAveRow(:,1),"black",'LineWidth',1)
%plot(Distance(1:end-1), MaxAveRow(2:end,1))
grid on
title('Max S.D. of Temperature - BHF = 6W')
xlabel('Distance - mm')
ylabel('Standard Deviation')
```

```
p = polyfit(Distance,MaxAveRow(:,1),2)
Distance1 = (20:1:130);
y2 = polyval(p,Distance1);
plot(Distance,MaxAveRow(:,1),'o',Distance1,y2)
title('Plot of Data (Points) and Model (Line)')
%plot(Distance(1:end), MaxAveRow(1:end,1))
grid on
title('Polynomial Fitting - 2nd Order')
xlabel('Distance - mm')
ylabel('Standard Deviation')
```

```
function MaxAveRow= MaxAveOfRow(SDdata6)
n=length(SDdata6);
maxRow=zeros(13,1);
aveRow=zeros(13,1);
sum=0;
for i=1:13
    maxRow(i)=sum+max(SDdata6(i,:));% max of row
    aveRow(i)=sum+mean(SDdata6(i,:));% average of row
end
MaxAveRow=[ maxRow, aveRow ];


end
```